UNIVERSITÉ DU QUÉBEC À CHICOUTIMI

THESIS SUBMITTED TO THE
UNIVERSITÉ DU QUÉBEC À CHICOUTIMI
IN PARTIAL FULFILLMENT OF THE
REQUIREMENT FOR THE DEGREE OF
MASTER IN ENGINEERING

BY

GUILLERMO HERNÁN GARZA ELIZONDO

# MACHINABILITY OF Al-(7-11%)Si CASTING ALLOYS: ROLE OF FREE-CUTTING ELEMENTS

AUGUST 2010

UNIVERSITÉ DU QUÉBEC À CHICOUTIMI

MÉMOIRE PRÉSENTÉ À

L'UNIVERSITÉ DU QUÉBEC À CHICOUTIMI

COMME EXIGENCE PARTIELLE

DE LA MAÎTRISE EN INGÉNIERIE

PAR

GUILLERMO HERNÁN GARZA ELIZONDO

# ASPECTS DE L'USINABILITÉ DES ALLIAGES DE FONDERIE Al-(7-11)%Si : RÔLE DES ÉLÉMENTS DE DÉCOLLETAGE

AOÛT 2010

*Dedicated to the memory of my grandmother,*

*Emilia Elizondo de Elizondo.*

# ACKNOWLEDGEMENTS

I would like to express sincere thanks to my supervisors, Professors F.H. Samuel and A.M. Samuel, Research Professor at Université du Québec à Chicoutimi, PQ (Canada), for motivating me to complete my Master's degree; without their continuous guidance and support it would have been impossible to do so.

Financial support in the form of scholarships received from the Natural Sciences and Engineering Research Council of Canada (NSERC), from the Fondation de l'Université du Québec à Chicoutimi (FUQAC), from General Motors Powertrain Group (U.S.A), and from Corporativo Nemak (Mexico) is gratefully acknowledged.

I would also like to express my appreciation to several colleagues, particularly Mr. Alain Bérubé and. Dr Mathieu Paradis of the TAMLA group, UQAC, for their invaluable assistance during the various stages of this work, and for fostering an enjoyable working atmosphere.

Thanks are also due to Madame Marion Sinclair for her patience and painstaking efforts in proofreading my thesis.

I would like to record my deep gratitude to the members of my family, especially my parents, my brothers, my sister, and my girlfriend Stéphanie. Without their encouragement and support, I would not have been able to fulfill my goal of completing my Master's degree successfully.

Finally, it is a great pleasure to have the opportunity of conveying my thanks to all those who were involved, directly or indirectly, in making this work a success.

# RÉSUMÉ

Deux des alliages d'aluminium les plus utilisés dans les industries de l'automobile et de l'aéronautique sont le 396 et le 319, ce qui s'explique par leur facilité à les mettre en forme et de leur habileté à rencontrer les standards de performances mécaniques du fait que la majorité de la matière première provient du recyclage. Ces alliages, 396 et 319, qui appartiennent au système Al-Si-Cu sont généralement traités thermiquement de façon à obtenir une combinaison optimale de résistance et de ductilité. L'excellente coulabilité et les bonnes propriétés mécaniques des alliages Al-Si-Cu-Mg ont fait d'eux des choix populaires pour les applications industrielles. L'usinage est un procédé courant connu pour l'enlèvement de matière sous forme de copeaux à partir d'une pièce, et il est aussi l'un des plus importants de la fabrication. La réduction du temps d'usinage et l'augmentation de la durée de vie des outils de coupe ont une importance économique. Les essais d'usinage réels sont indispensables pour déterminer les caractéristiques d'usinabilité des alliages et, par conséquent, les essais d'usinage sont devenus une activité essentielle.

La présente étude a été entreprise pour étudier les effets de la composition et le type d'outils de forage sur l'usinabilité des alliages de fonderie Al-Si, à savoir 396 et B319.2 dans l'état traité thermiquement, contenant 10,8% de Si et de 7,5% Si, respectivement, en utilisant quatre différentes forets. Ainsi, un traitement thermique spécifique T6 a été choisi pour établir le niveau de dureté des alliages étudiés dans la plage de 110 ± 10 BHF, conforme à la plupart des niveaux de dureté des applications commerciales des alliages d'aluminium. Les opérations d'usinage de forage ont été conçus pour être effectués dans des conditions fixées en vue d'examiner les éléments suivants: (i) les effets des intermétalliques de fer à savoir α-Fe, β-Fe, et « sludge », ainsi que ceux des éléments de décolletage , tels que Sn, sur l'usinabilité des alliages sélectionnés; (ii) la force de forage, le moment et l'accumulation de chaleur (BUE), ainsi que les caractéristiques des copeaux, (iii) les effets de la composition des outils sur la durée de vie et sur l'usure des outils, et (iv) une évaluation des quatre forets pour savoir lequel fournit une meilleure performance en ce qui concerne les forces de forage et de moments, de manière à obtenir des combinaisons d'usinage optimale.

Les essais de forage ont été effectués sur un Huron K2X 8 Five centre d'usinage vertical à des conditions d'usinage fixes, qui comprennent la vitesse de coupe, la vitesse de pénétration, la profondeur du trou, la géométrie de l'outil, la composition de l'outils et le lubrifiant pour étudier les effets du forage sur l'usinabilité des alliages de fonderie Al- Si à savoir G2: 396 + 0,15%Sn, G3: 396 + 0,25%Fe + 0,25%Mn, et G12: B319.2 + 0,15%Sn dans l'état traité thermiquement. Les quatre forets employés sont de type : « Solid Carbide », « Special Solid Carbide », « Cobalt Grade » et « High Precision Solide Carbide ». Il convient de mentionner ici que les critères pertinents usinabilité se rapportent aux forces et moments de coupe ainsi qu'à la durée de vie des outils, la configuration des copeaux et l'arête rapportée (BUE) évolution.

Les résultats obtenus à partir des essais de forage indiquent que le foret « High Precision Solid Carbide » a obtenu les plus faibles forces et moments de forage pour les essais avec les alliages G2 et G3; alors que pour l'alliage G12 le foret « Cobalt Grade » a obtenu les plus faibles forces et moments de forage. Le foret « High Precision Solid Carbide » affiche un comportement stable lors du perçage et il est recommandé pour les alliages G2 et G3. Également, le foret au cobalt est recommandé pour l'alliage G12.

Les résultats révèlent que les alliages G2 et G3 présentent une augmentation rapide des forces et moments de forage à mesure que le nombre de trous percés augment. Cela peut s'expliquer par leur teneur plus élevée en Si (10,8%). Les différences de comportement d'usinage des alliages 396 et B319.2 peuvent être attribuées principalement aux différences de dureté de la matrice, de composition des alliages obtenus au moyen d'ajouts et de niveau de silicium qui est de 10,8% pour les alliages G2 et G3 et de 7.5% pour G12.

L'addition de 0,15% de Sn aux alliages 396 et B319.2 a un effet bénéfique sur la durée de vie des quatre foret en carbure, ce qui peut être attribuée à la précipitation des particules de la phase β-Sn ayant un faible point de fusion. La présence de « sludge » dans l'alliage G3 avec des ajouts de 0,25%Fe et 0,25%Mn, conduit à une augmentation extrêmement rapide des forces et moments de forage, et a également un effet défavorable sur la durée de vie des outils laquelle diminue avec le nombre de trous percés et présente plus de variations dans l'ensemble des résultats obtenus.

L'examen des photographies de l'arête rapportée indique qu'il y a un minimum de changements dans la largeur de la BUE pour différents nombres de trous dans le cadre du processus de forage pour chaque alliage et foret. Ceci peut être attribué au fait que les dépôts de BUE va progressivement augmenter en taille et qui, si elle excède une taille critique, se sépare de la face de coupe et d'adhérer à la surface inférieure des copeaux. Un examen visuel des copeaux révèle que la forme d'éventail est de loin la forme prédominante au cours du forage des alliages étudiés, aussi, la forme d'éventail est idéale pour la plupart des applications de forage en raison de sa taille compacte. La fragmentation de copeaux provenant du foret au cobalt a été supérieure à celle des forets « Special Solid Carbide » et « High Precision Solid Carbide » pour les alliages G2, G3 et G12.

# ABSTRACT

Two of the most widely used aluminum alloys in the aerospace and automotive industries are the 396 and 319 alloys; this may be attributed to ease of casting and their satisfactory ability to meet the requirements imposed by mechanical properties given the fact that the raw material for processing comes mostly from recycled material. These alloys, 396 and 319, belonging to the Al-Si-Cu system are usually heat treated in order to obtain an optimum combination of strength and ductility. The excellent castability and mechanical properties of such Al-Si-Cu-Mg alloys has made them commercially popular for industrial applications. Machining is a common procedure used for the removal of material from a workpiece or casting in the form of chips, and it is also one of the most important of the manufacturing processes. Reducing the machining time and extending cutting tool life both have great economic significance. Actual machining tests are indispensable for determining the machinability characteristics of the workpiece material and, as a result, machinability testing has become an essential activity.

The present study was undertaken to investigate the effects of drilling tool type and material on the machinability of heat-treated 396 and B319.2 Al-Si casting alloys, containing 10.8%Si and 7.5%Si, respectively, using four different drills. Thus, a specific T6 heat treatment was selected to establish the hardness level for the alloys investigated within the range of 110±10 BHN, conforming to most of the required hardness levels in the commercial application of aluminum alloys. Drilling machining operations were designed to be carried out under fixed conditions in order to examine the following: (i) the effects of Fe-intermetallics namely $\alpha$-Fe, $\beta$-Fe, and sludge; as well as those of free-cutting elements, such as Sn, on the machinability of the selected alloys; (ii) the drilling force, moment, and heat build-up, as well as chip characteristics; (iii) the effects of tool material on tool life and on tool wear behavior; and (iv) an evaluation as to which of the four drills provides a better performance with respect to drilling forces and moments, so as to obtain optimum machining combinations.

Drilling experiments were performed on a Huron K2X 8 Five vertical machining center at fixed machining conditions which included cutting speed, feed rate, length of cut, tool geometry, tool material, and coolant to investigate the effects of drilling on the machinability of Al-Si casting alloys, namely G2: 396 + 0.15%Sn, G3: 396 + 0.25%Fe + 0.25%Mn, and G12: B319.2 + 0.15%Sn alloys, in the heat-treated condition. The four drills employed were Solid Carbide, Special Solid Carbide, Cobalt Grade and High Precision Solid Carbide drills. It should be mentioned here that the pertinent machinability criteria relate to forces and moments as well as to tool life, chip configuration, and built-up edge (BUE) evolution.

The results obtained from the drilling tests reveal that, for the alloys G2 and G3, the lowest total average drilling force and moment are obtained with the high precision solid

carbide drill; whereas for G12 alloy, the cobalt grade drill provides the lowest total average drilling force and moment. The high precision solid carbide drill displays stable behavior when in operation, and is recommended for alloys G2 and G3. Likewise, the cobalt grade drill is recommended for the G12 alloy.

The results also reveal that the G2 and G3 alloys display a rapid increase in the total drilling force and moment with the increase in the number of holes drilled. This can be explained by their higher Si content of 10.8%. The differences in machining behavior of the 396 and B319.2 alloys may be attributed mainly to the difference in matrix hardness and alloy chemistry as obtained through additions, and the difference in the silicon contents 10.8%Si in G2 and G3 alloys versus 7.5%Si in G12 alloy.

The addition of 0.15% Sn to the 396 and B319.2 alloys has a beneficial effect on the tool life of the four carbide drills, this may be attributed to the precipitation of $\beta$-Sn particles which have a low melting point. The presence of sludge in the G3 alloy resulting from the additions of 0.25%Fe and 0.25%Mn to 396 alloy, leads to an extremely rapid increase in the total drilling force and moment, and also has an unfavorable effect on tool life in that the drill life decreases with the progress of the drilled holes of the test and presents more fluctuations in all the results obtained.

An examination of the photographs of the edge build-up (BUE) on the tools indicates that there are minimal changes in the width of the BUE with the number of holes drilled in the course of the drilling process for each alloy and drill. This may be explained by the fact that as the BUE gradually increases in size and exceeds a critical size, it will separate from the cutting face and adhere to the lower surface of the chip, and thus be is removed along with the chip. A visual examination of the chips reveals that the fan shape is by far the predominant form during the drilling of the alloys studied, also, that the fan shape, due to its compact size and shape, is the ideal chip for most drilling applications. The chip breakability of the cobalt grade drill was found to be superior to that of the special solid carbide drill and the high precision solid carbide drill for the alloys G2, G3, and G12.

# TABLE OF CONTENTS

# LIST OF FIGURES

# LIST OF TABLES

# CHAPTER 1

# DEFINING THE PROBLEM

# CHAPTER 1

# DEFINING THE PROBLEM

## 1.1 INTRODUCTION

Aluminum is of importance in such industrial applications as the production of automobiles and aerospace equipment, the packaging of food and beverages, in construction, the transmission of electric power, the transportation industry, the manufacturing of machinery and tools, and in numerous other domains. The fact that aluminum is non-ferromagnetic adds to its importance in the electrical and electronics industries. This element is also observably nontoxic and is routinely used in the manufacture of containers for food and beverages. The use of aluminum and its alloys has increased significantly over the last number of years, successfully replacing iron and steel in a number of different applications. Furthermore, aluminum becomes highly resistant after undergoing heat treatment and is noticeably simple to mold as a result of its high ductility.

The principal industries where aluminum has increased in importance include the automotive and aerospace domains; this was effectuated through the smelting of the metal

and the carrying out of suitable heat treatments for manufacturing cylinder heads, engine blocks, and other crucial parts.[1, 2] The benefits derived from using aluminum for these parts include:

- reduction in car weight;
- reduction in engine noise;
- reduction in vibrations; and
- absence of oxidation, unlike steel.

The use of silicon as the major alloying element in aluminum offers excellent properties such as:

- castability;
- good weldability;
- good thermal conductivity;
- excellent corrosion resistance; and
- satisfactory retention of physical and mechanical properties at elevated temperatures.

Increasing the mechanical properties of Al-Si alloys depends on the complex interaction between (a) chemical composition and the microstructural features developed during solidification, (b) heat treatment methods, and (c) deformation processes.[3, 4]

Two of the most widely used aluminum alloys in the aerospace and automotive industries are the 396 and 319 alloys containing 10.8% and 6.5% Si, respectively; this may

be attributed to ease of casting and their satisfactory ability to meet the requirements imposed by mechanical properties such as the fact that the raw material for processing comes mostly from recycled material. This study will be undertaken to investigate the machinability of Al-Si casting alloys: 396 + 0.15%Sn, 396 + 0.25%Fe + 0.25%Mn, and B319.2 + 0.15%Sn, with the emphasis on the effects of free-cutting elements such as Sn, and Fe-intermetallics on the machinability of these alloys.

Machining is one of the most common yet significant manufacturing processes known for the removal of material in the form of chips from a workpiece, and it is also one of the most important of the manufacturing processes. Actual machining tests are indispensable for determining machinability and, as a result, machinability testing has become an essential activity in the field. Moreover, machining is necessary where tight tolerance on dimensions and finishes is required.[5] It is normal that the machining is affected by several variables namely: workpiece material, cutting tool material, and machining parameters such as cutting speed, feed rate, and depth of cut.[6, 7] The most common types of machining are traditional machining such as turning, milling, and drilling, as well as non-traditional machining such as chemical machining, electrical discharge machining (EDM), and electrochemical machining (ECM). With regard to the machinability of aluminum alloys and castings, it is necessary to take into account several factors which govern the condition of the work material and are determined by: [3]

- alloy chemistry, microstructure, and properties;
- metallic and non-metallic impurities;

- casting method employed;
- heat treatment;
- porosity; and
- physical and mechanical properties.

In this study, drilling will be the primary machining process. Drilling is one of the oldest and most common machining operations; it can be defined as applying a rotating tool having one or more cutting edges and one or more helical or straight flutes for the passage of chips and the admission of a cutting fluid.[2, 8] In this thesis, the drilling force, moment, chips, and heat built-up edge (BUE), will be obtained so as to verify which of the drills (*i.e.* tool material) used demonstrates greater performance with respect to these characteristics. Moreover, the effects of tool material on tool life and tool wear will also be studied. Measuring the thrust force (which is the force component in the cutting direction) and torque (which is the moment about the axis of rotation of the tool) is known to be one of the most commonly used techniques for monitoring conditions of tool wear.[9, 10]

In fact, the workpiece material is the most significant factor dictating which type of cutting tool will be employed. The use of high speed machining (HSM) techniques permits high rates of material removal, which in turn reduces machining cycle times.[11] One of the advantages of using high speeds in machining aluminum alloys is the fact that the melting points fall well below the temperature at which modern tool materials experience thermal softening. A drastic increase in cutting speeds would result in significant productivity gains in the automotive and aerospace industries.[12]

The principal mechanical properties involved are hardness or strength of the material, while in the case of aluminum there exists the problem of built-up edge, which causes poor machinability. As mentioned in the literature, [12, 13, 14, 15, 26] most aluminum alloys can be machined at high speeds without sacrificing tool life. Manganese and chromium are heavy elements which to tend to combine with Al, Fe, Si, and sometimes Cu to form hard complex intermetallic phases, such as sludge or fall-out, causing hard spots and having a dramatic effect on the problems of tool edge build-up. Built-up edge (BUE) occurs during the machining process for Si contents of up to 12%. All automotive and aerospace casting alloys contain Si, Cu, and Mg as major alloying elements. Silicon, like the heavy-element intermetallic phases of iron, manganese, and chromium, is an abrasive material in an otherwise soft matrix, and it is the element which singularly has the greatest tendency to decrease cutting tool life.[5] Certain elements are known to enhance the wet machinability of aluminum and steel; these elements are referred to as free-machining elements and include bismuth (Bi), tin (Sn), lead (Pb), and cadmium (Cd).

Heat treatment improves the mechanical properties, increases the hardness, reduces the built-up edge (BUE) on the cutting tool, and improves the surface finish of the machined part. This treatment improves the strength and hardness values by reducing the built-up edge on the cutting tool and improving the surface finish of the machined part. A minimum hardness of 80 BHN for the alloy casting is desirable to avoid difficulties associated with built-up-edge (BUE) on the cutting tool.[4, 5]

In a collective sense, the more important terms as related to the subject of machinability are: tool wear, characteristics of chip formation, burring tendency, and finish

of machined surface. Wear is a loss of material at the cutting lips of the drill bit because of physical interaction between the cutting tool and workpiece material. Abrasion, adhesion, diffusion, and fatigue are the basic mechanisms which are liable to cause wear in the cutting tool. Tool wear in drilling is a progressive procedure, although it occurs at an accelerated rate once a drill becomes dull.[9] Chips, with their length and curl, as well as the ease or difficulty associated with their removal and handling influence the surface finish.[3] The importance of the type of chip depends on several variables such as the drilling speed, the feed rate, and the mechanical and thermo-physical properties of the workpiece itself. Chip control, involving chip breaking and removal, is of great importance in drilling, since the allowable penetration rate is often limited by chip-breaking characteristics.

Porosity is a defect most commonly found in cast products, and is thus a critical factor to be examined with regard to the quality of the casting. The occurrence of porosity is detrimental not only to the surface quality after machining, but also to the mechanical properties and corrosion resistance of the cast material; this has the potential for causing problems during machining and the life of the cutting tool.

## 1.2 OBJECTIVES

The present study was undertaken to investigate the effects of drilling on the machinability of Al-(6.5-11%)Si casting alloys, namely 396 + 0.15%Sn; 396 + 0.25%Fe + 0.25%Mn; and B319.2 + 0.15%Sn in the heat-treated condition, using four different drills. Drilling machining operations were carried out under fixed conditions in order to examine the following:

1. The effects of Fe-intermetallics as well as free-cutting elements, such as Sn, on the machinability of the selected alloys;
2. The drilling force, moment, and heat build-up (BUE), as well as chip characteristics;
3. The effects of tool material on tool life and on tool wear behavior; and
4. An evaluation of the four drills to determine which of them provides a better performance with respect to drilling forces and moments, so as to obtain optimum machining combinations.

# CHAPTER 2

# SURVEY OF THE LITERATURE

# CHAPTER 2

# SURVEY OF THE LITERATURE

## 2.1 INTRODUCTION

Aluminum is the second most abundant metallic element on Earth, after iron, and thus has become an increasingly strong competitor for engineering applications since the 19th Century. With a density of 2.7 g/cm$^3$, or one third that of steel which is 7.83 g/cm$^3$, aluminum is lightweight, easy to manufacture, has favorable mechanical strength, a high resistance to corrosion, and excellent thermal and electrical conductivity.[17, 18, 19, 20, 21, 22, 23, 24] Aluminum casting alloys are the most versatile of all common foundry alloys. For large productions, the three main casting processes are sand casting, permanent mold casting and high pressure die casting. Figure 2.1 shows a picture of molten aluminum being poured into a mold.

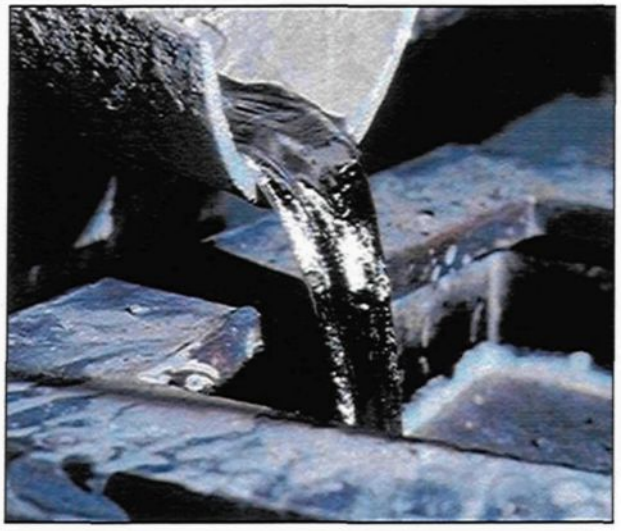

**Figure 2.1** Aluminum smelting.

Aluminum-silicon casting alloys are used in the automobile industry, where there is an increased demand for improved properties. The use of silicon as the major alloying element in aluminum alloys introduces excellent properties such as castability, good weldability, satisfactory thermal conductivity, excellent corrosion resistance, and excellent retention of physical and mechanical properties at elevated temperatures.

Depending on the percentage of the silicon content, Al-Si alloys are divided into three groups: (a) hypoeutectic alloys containing 5-10% Si, (b) eutectic alloys containing 11-13% Si, and (c) hypereutectic alloys containing 14-17% Si.[1, 25, 26, 27, 28] It is necessary to consider the casting process, heat treatment methods, and the chemical composition of the alloys,[3, 4] in order to determine the microstructures of Al-Si casting alloys.

The 319 and 396 cast alloys are typically used for the production of aircraft pump parts, automotive transmission cases, aircraft fittings and controls, water-cooled cylinder

blocks, and numerous other applications. Figure 2.2 and 2.3 show examples of parts manufactured out of such alloys. Improvements to these alloys in terms of their mechanical properties are carried out through melt treatments such as grain refining and modification, and through the addition of certain alloying elements, where modification, in particular is used to modify the morphology and size of the eutectic Si particles from their brittle acicular form to a fibrous form, through the addition of modifiers such as strontium.

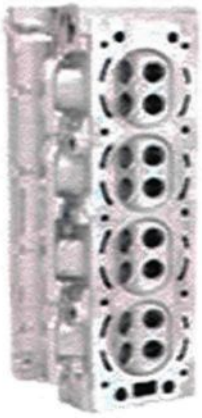

**Figure 2.2** Motor Head.[22]

**Figure 2.3** Monoblock.[22]

### 2.1.1 Properties and Applications of Aluminum

The combination of favorable mechanical properties such as high strength, low weight, and good corrosion resistance has made aluminum an ideal material for use in a number of applications.[16] A summary of these properties is provided in Table 2.1.

**Table 2.1** Summary of the properties of aluminum [17, 18, 19, 20]

| | |
|---|---|
| Chemical symbol | Al |
| Atomic number | 13 |
| Atomic weight | 26.9815 |
| Atomic radius | 0.143 nm |
| Crystalline structure | face-centred cubic |
| Density | 2.7 g/cm$^3$ |
| Melting point | 660°C |
| Boiling point | 2480°C |
| Modulus of elasticity | 72.4 GPa |
| Cutting modulus | 27.5 GPa |
| Poisson's ratio | 0.31 |
| Average specific heat (0–100°C) | 917 J kg$^{-1}$ K$^{-1}$ |
| Thermal conductivity (20–100°C) | 238 W m$^{-1}$ K$^{-1}$ |
| Coefficient of thermal expansion (0–100°C) | 23.5x10$^{-6}$ K$^{-1}$ |
| Electrical resistivity (20°C) | 2.67x10$^{-8}$ Ω·m |

Like all metals, aluminum in its pure form has low mechanical strength and cannot be used in this condition for applications where resistance to deformation and fracture is essential. It thus becomes necessary to add other elements to aluminum primarily to increase its strength.[29] Increasing the mechanical properties of Al-Si alloys depends on a complex interaction between: (a) the chemical composition and the microstructural features developed during solidification, (b) the heat treatment methods applied, and (c) the deformation processes to which the alloy is subjected.[3, 4]

Some aluminum alloys are known to exceed structural steel in strength, although pure aluminum and certain aluminum alloys display low strength and hardness values. In spite of the fact that most metals can be alloyed with aluminum, few have sufficient solubility in the solid to act as major alloying elements. Of the more commonly used alloying elements, only zinc, magnesium, copper, and silicon have any significant solubility in this respect.[17]

It should be remembered that aluminum is non-pyrophoric, which is a significant factor in applications involving the handling of inflammable or explosive-materials as well as exposure to them.[30]

### 2.1.2 Wrought and Casting Alloys

Aluminum alloys can be divided into two groups: aluminum wrought alloys and aluminum casting alloys, depending on their method of fabrication.[31, 32] Aluminum wrought alloys are manufactured into different shapes by hot deformation; the composition and microstructure are different from that of casting alloys, because they display less segregation and structural inhomogeneities. Aluminum casting alloys are specially designed to flow relatively easily into a mold for casting. The casting alloys can be prepared in several ways, although the main casting processes used involve green sand mold, dry sand mold, composite sand mold, plaster mold, investment mold, permanent mold and pressure-die casting. Both aluminum cast and wrought alloys may be separated into heat-treatable and non-heat-treatable alloys, where the alloys are strengthened using heat treatment in the first case and work hardening in the second.

### 2.1.3 Designation System for Aluminum Casting Alloys

The composition of aluminum alloys is regulated by an international classification system for each wrought and casting alloy; this system has been established by the Aluminum Association.[33] The designation system used for aluminum casting alloys is provided in Table 2.2.

**Table 2.2** Nomenclature of aluminum alloys for foundry use [33]

| Nomenclature | Description |
|---|---|
| 1xx.x | pure aluminum (99.00% minimum purity) |
| 2xx.x | aluminum-copper alloys |
| 3xx.x | aluminum-silicon + copper and/or manganese alloys |
| 4xx.x | aluminum-silicon alloys |
| 5xx.x | aluminum-magnesium alloys |
| 6xx.x | aluminum-magnesium and silicon alloys |
| 7xx.x | aluminum-zinc and magnesium alloys |
| 8xx.x | aluminum-tin alloys |
| 9xx.x | unused series |

The first digit in the designation nomenclature indicates the series the alloy belongs to. The second and third digits serve to identify alloys in the same series or in the case of the series 1xx.x, they indicate the minimum percentage of aluminum. The digit to the right of the decimal point indicates the type of product, with 0 when the casting piece is the final product and 1 or 2 when it is an ingot. There are no commercial alloys currently established in the 6xx.x and 9xx.x series. Aluminum-silicon base alloys belong to the 3xx.x and 4xx.x series of aluminum casting alloys. The Al-Si-Mg, Al-Si-Cu, and Al-Si-Cu-Mg alloy

systems are the three major alloy systems in the 3xx.x series, where Mg and Cu are two important alloying elements which act as effective strengtheners.[17, 18, 33]

### 2.1.4 Temper Designation System

The Temper Designation System, established by the Aluminum Association, describes the thermal or mechanical treatments which may have been applied to an alloy. This designation system is used in alloys for casting and mechanical work. When written, the treatment designation is placed after the alloy designation. The designation used for the basic treatments consists of letters, as shown in Table 2.3, and their subdivisions, as shown in Table 2.4; when required, they are indicated by one or more digits following the corresponding letter.[33]

**Table 2.3** Designation system for basic treatment of aluminum alloys [33]

| | |
|---|---|
| **F** | as fabricated |
| **O** | annealed wrought products only |
| **H** | strain-hardened |
| **W** | solution heat-treated |
| **T** | thermally treated to produce tempers other than F, O, or H |

**Table 2.4** Subdivisions of treatments H and T [33]

| | |
|---|---|
| **H1** | strain-hardened only |
| **H2** | strain-hardened and partially annealed |
| **H3** | strain-hardened and stabilized |
| **T1** | cooled from an elevated temperature shaping process and naturally aged |
| **T2** | cooled from an elevated temperature shaping process, cold worked, and naturally aged |
| **T3** | solution heat-treated, cold worked, and naturally aged |
| **T4** | solution heat-treated and naturally aged |
| **T5** | cooled from an elevated temperature shaping process and artificially aged |
| **T6** | solution heat-treated and artificially aged |
| **T7** | solution heat-treated and overaged/stabilized |
| **T8** | solution heat-treated, cold worked, and artificially aged |
| **T9** | solution heat-treated, artificially aged, and cold worked |
| **T10** | cooled from an elevated temperature shaping process, cold worked, and artificially aged |

### 2.1.5 Al-Si Alloys

Aluminum alloys with silicon as the main alloying element are the most important in the casting process as the presence of silicon imparts high casting fluidity to the alloy. These alloys also possess high corrosion resistance and satisfactory weldability.[17] Aluminum-silicon alloys experience an increase in mechanical resistance with the addition of copper, magnesium, or nickel. These alloys account for 85-90% of the total of cast aluminum pieces produced.[28] Commercial alloys of this type represent the full range of compositions, including eutectic, hypoeutectic, and, in some cases, hypereutectic alloys. The eutectic composition contains approximately 12% silicon, as shown in Figure 2.4.

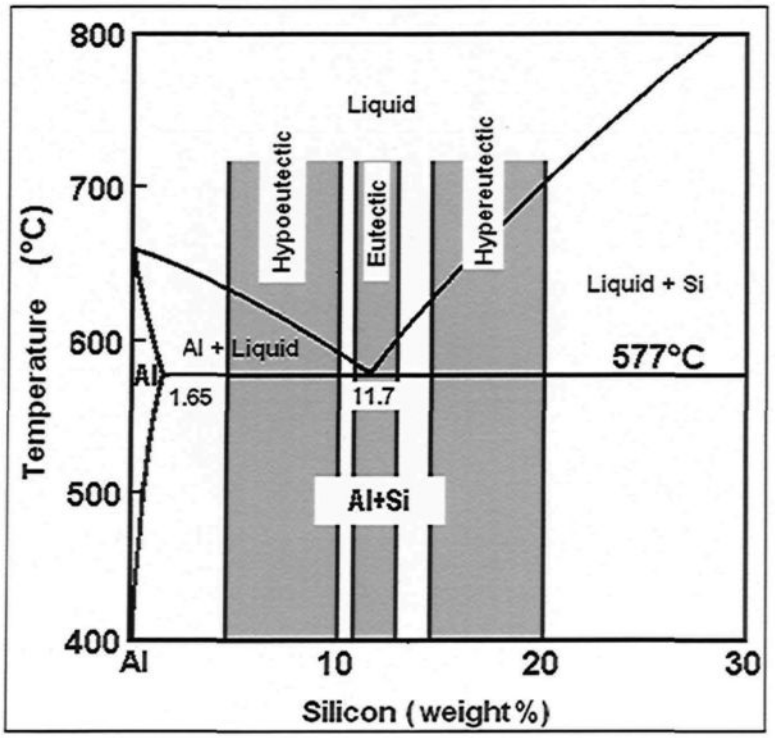


**Figure 2.4** Al-Si phase diagram.[20]

With regard to this type of alloy, it is necessary to regulate a series of parameters which have a direct effect on alloy properties. These variables are related to the microstructure and depend as much on the alloy composition as on the casting process used. These include: (a) dendrite arm spacing (DAS), (b) level of modification of the eutectic silicon, (c) grain size, and (d) porosity resulting from hydrogen dissolved in the liquid metal and shrinkage.

### 2.1.6 Alloying Elements

The various alloying elements used in aluminum alloys are provided in Table 2.5 together with a description of their respective roles in alloying.

**Table 2.5** Alloying elements added to aluminum and their respective roles [21]

| | |
|---|---|
| **Zinc (Zn)** | Zinc is occasionally added to certain alloys since it presents an excellent response to aging heat treatment. |
| **Copper (Cu)** | Copper is used to increase the tensile strength and hardness through heat treatment; it also reduces the resistance to corrosion and hot cracking, or hot tearing, and also facilitates casting. |
| **Tin (Sn)** | Tin is effective in reducing friction; it is also useful in applications where load support is required. |
| **Iron (Fe)** | Iron helps to improve resistance to hot cracking and reduces the tendency towards adhesion, or die sticking, in permanent molds; it also tends to form insoluble compounds which affect alloy properties. |
| **Manganese (Mn)** | Manganese is considered as an impurity and is therefore maintained at a minimum level. When combined with iron, it forms insoluble phases thereby reducing the detrimental effects which iron is known to have on alloy ductility. |
| **Silicon (Si)** | Silicon reinforces the casting characteristics of aluminum, improves its fluidity, and increases resistance to hot cracking. The optimal amount of silicon depends on the casting process involved. In processes involving low cooling rates (*e.g.* sand molds), this amount lies between 5 and 7%. For processes where high cooling rates prevail (*e.g.* permanent molds), it varies between 8 and 12%. |

## 2.2 ROLE OF IRON AND MANGANESE IN Al-Si ALLOYS

Iron is considered to be an impurity when found in aluminum; this impurity is present in those alloys which are made out of commercially pure base material. An Al-Si-Fe eutectic composition containing any amount of Fe over 0.5% will be present as Al-Fe-Si in the form of large platelets (or needles as they appear in an optical micrograph) which will, up to about 0.8%Fe, increase strength and hardness but reduce ductility slightly. If, however, more than 0.8%Fe is used, the strength and elongation will be seen to deteriorate rapidly, while at the same time there is also a deleterious effect on the machinability to be observed. It should be noted that the addition of iron to Al-Si alloys is, in general, detrimental to the mechanical properties; even a small addition of Fe to any of the Al-Si alloys will seriously diminish tensile strength and elongation.[5]

Iron can enter the melt during further downstream melt activity through two basic mechanisms: [32]

1. Liquid aluminum is capable of dissolving iron from unprotected steel tools and furnace equipment. Iron levels can reach 2 wt% at a normal melt temperature of ~700°C; it should be noted that an Al-Fe eutectic exists at 1.7%Fe at 655°C, as shown in Figure 2.5. For a melt maintained at 800°C, the Fe level may reach up to 5%.
2. Iron may also enter an aluminum melt through the addition of such low-purity alloying materials as Si, or *via* the addition of scrap metal containing higher background iron than the primary metal itself.

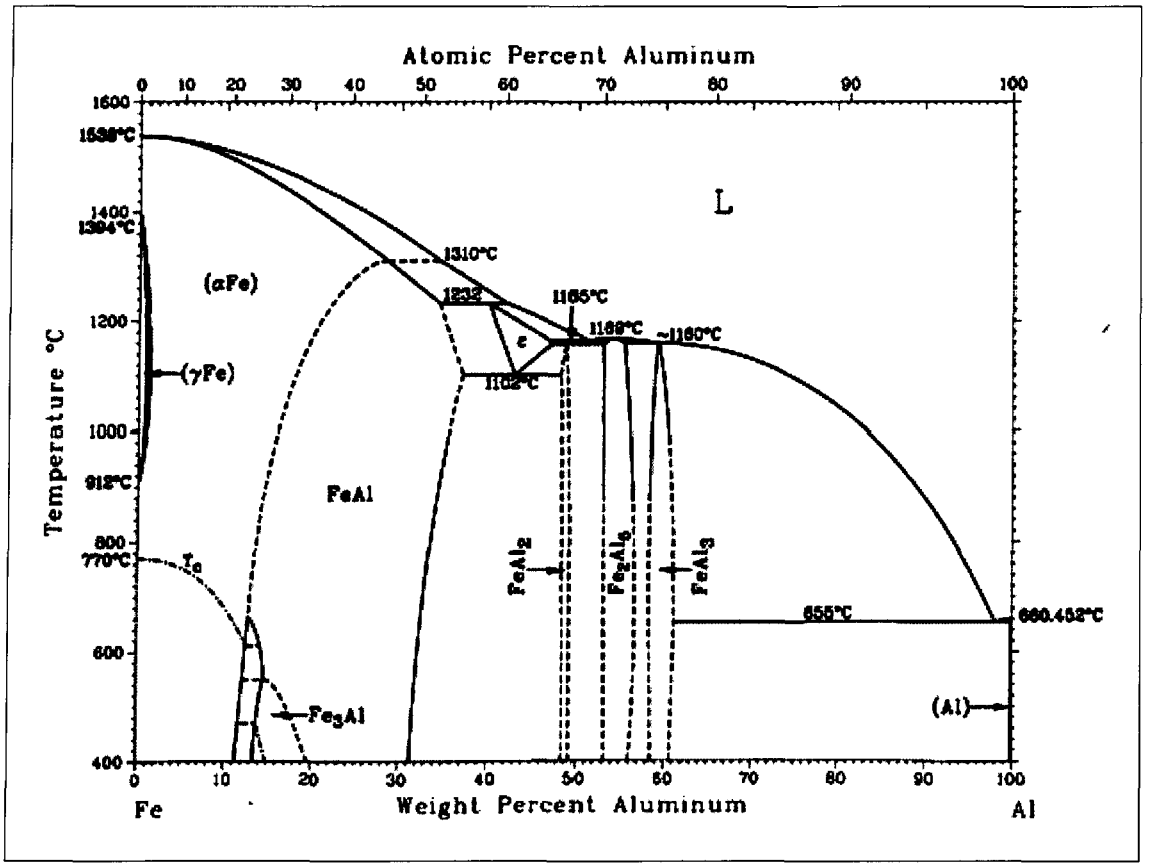


**Figure 2.5** Binary Al-Fe equilibrium phase diagram.[34]

Manganese is the most common alloying additive which is used to neutralize the effects of iron as well as to modify the morphology and type of the intermetallic phases formed.[35, 36] This element is capable of changing the morphology of the iron-rich phase from platelets to a more compact form or to globules, thereby improving tensile strength, elongation, and ductility.[35, 37, 38] Manganese may be added to many of the alloys being investigated for the following two reasons: (i) to increase high temperature strength and creep resistance through the formation of the high melting compounds $Cu_2Mn_3Al_{20}$, $Mn_3NiAl_{16}$, $MnCrAl_{12}$,

and $(FeMn)_3Si_2Al_{15}$, while more complex compounds containing chromium and nickel may also be involved; (ii) to compensate for the embrittlement effects of iron.

The negative effects of iron in aluminum-silicon alloys can be minimized or overcome by applying any of the following techniques:

- rapid solidification;
- addition of neutralizing elements such as Mn, Cr, Be, and Ca;
- melt superheating;
- strontium modification; and
- non-equilibrium solution heat treatment.

These techniques convert the crystallization of the platelet-like $\beta$-AlFeSi phase to the less harmful *Chinese-script* form ($\alpha$-AlFeSi), otherwise they dissolve the $\beta$-AlFeSi phase in the matrix, either partially or completely, thereby improving the mechanical properties and alloy machinability.[32]

A wide range of AlFeSi particle types has been reported in the literature.[5] These can generally be divided into three different categories by morphology:

1. polyhedral crystals (primary $\alpha$-phase),
2. *Chinese script* ($\alpha$-phase), and
3. thin platelets ($\beta$-phase).

The solidification rate of any given casting is perhaps the most important of the various parameters influencing its microstructure, since this directly or indirectly affects almost all the microstructural parameters including:

- dendrite arm spacing (DAS);
- degree of eutectic silicon modification and grain refinement;
- amount of microporosity; and
- intermetallics and inclusions observed in the microstructure.

The crystallization and volume fraction of the three different AlFeSi particle morphologies mentioned above depend on the Fe:Mn ratio, the cooling rate, and the melt holding temperature.

### 2.2.1 Effects of $\alpha$-AlFeSi and $\beta$-AlFeSi Intermetallics

The two main intermetallics generally observed in Al-Si alloys are the $\alpha$-Fe and $\beta$-Fe intermetallic phases. The composition of the $\alpha$-Fe phase is $Al_8Fe_2Si$ (31.6%Fe, 7.8%Si) and $Al_{12}Fe_3Si_2$ (30.7%Fe, 10.2%Si), with a probable composition range of 30-33% Fe and 6-12%Si. These phases are dominant in slowly-cooled castings, whereas the metastable phases $Al_6Fe$ (orthorhombic) and $\alpha$-$Al_{20}Fe_5Si_2$ (cubic) only occur in rapidly quenched material.[35, 39] The $\alpha$ phase is reported as having a hexagonal structure with the parameters a=12.3 Å, c=26.3 Å, a density of 3.58 g/cm$^3$, and it appears in the form *Chinese-script* particles. The $\alpha$-AlFeSi phase presents certain characteristics and may be described as showing irregular curved crystal growth conforming to the complicated shape of the interdendritic spaces during solidification. This type of growth occurs at high driving forces

of solidification or rapid cooling.[32] Manganese is the most common alloying addition and is highly soluble in aluminum; it is used to neutralize the effects of iron and to modify the morphology and type of the intermetallic phase formed. Small amounts of manganese play a positive role in combining with iron to form the *Chinese-script* structure instead of a platelike structure. The $\alpha$-phase is much more compact and far less detrimental to the mechanical properties; it also improves feeding into interdendritic channels slightly. [32] With regard to $\beta$-AlFeSi platelets, there are two types, (i) pre-eutectic particles characterized by their large size, and (ii) co- or post-eutectic particles which are relatively thin. The difference in their size is directly related to the rates of diffusion of the iron atoms with respect to the temperatures at which the two particle types precipitate.[5]

The composition of the $\beta$-Fe phase is $Al_5FeSi$ (25.6%Fe, 12.8%Si), with a range of 25-30% Fe and 12-15% Si. This phase has a monoclinic structure with parameters a=b=6.12 Å, and $\alpha$=91°, a density of 3.30-3.35% g/cm$^3$, and it appears in the form of thin platelets in the microstructure. The temperature at which $\beta$-Fe can form prior to the Al-Si eutectic decreases with increasing Si content for a given Fe content. The morphology of the phase allows it to act as a stress raiser, which serves to explain the lower mechanical properties of the cast part. The threshold amount of iron leading to the formation of primary $Al_5FeSi$ capable of undermining the properties is >0.7%. The percentage of iron required to form primary or secondary $Al_5FeSi$ depends on the cooling rate and silicon content. The effects of increasing Fe may be seen in the gradual reduction of the elongation, impact strength, and tensile strength of aluminum-silicon alloys, while BHN hardness and yield strength are reported to increase gradually. The increase in content from 0.5-1.2% in an Al-

Si casting alloy reduces the mechanical properties, mainly ductility, due to the formation of such $\beta$-Fe platelets.[32] Iron content of up to 0.2% improves the tensile strength, while higher levels reduce the tensile strength and elongation but increase hardness.

At higher Mn:Fe ratios and in the presence of chromium, however, the iron, manganese, and chromium tend to segregate towards the bottom of melting and holding furnaces for aluminum, thereby forming solid particles of the $\alpha$-iron phase which may precipitate in the form of the *Chinese script-like* $Al_{15}(Fe,Mn,Cr)_3Si_2$, termed *sludge*. An empirical formula called the "*sludge factor*" was proposed by Gobrecht.[40] The sludge factor for Al-Si type alloys is used to determine how much Fe, Mn, and Cr can cause sludge to form; it also serves as a rough guide to avoid sludging in casting operations such as die casting. This factor is calculated as: [40, 41]

$$\text{Sludge Factor (S.F.)} = 1 \times \text{wt\% Fe} + 2 \times \text{wt\% Mn} + 3 \times \text{wt\% Cr} \qquad (2.1)$$

The above formula is useful for predicting susceptibility to sludge formation, although metal temperature and the agitation of the molten metal, to some extent, also influence susceptibility to sludge formation. The critical sludge factor beyond which sludge is formed equals 1.8 if a casting temperature of 650°C or more is maintained. For holding temperatures lower than this value, however, a critical sludge factor of 1.4 is recommended, since sludge formation is a temperature-dependent process in combination with the Fe, Mn, and Cr concentrations. Excessive tool wear can come from occluded oxides in the metal casting. Tool breakage may be caused by non-metallic inclusions such as aluminum oxide,

corundum, and intermetallic complexes or sludge. Sludge can cause excessive tool wear, while hard spots may cause tool breakage.[5]

## 2.3 ROLE OF FREE-CUTTING ELEMENTS IN Al-Si ALLOYS

Typical aluminum alloys for drilling, milling, and turning contain elements with low melting points, such as lead (Pb), bismuth (Bi), tin (Sn), indium (In) or cadmium (Cd), to minimize chip size and hence increase machinability. The free-cutting elements have a limited solubility in the aluminum solid solution and form soft, low-melting phases which support chip breakage and lubricate the tool. Generally, alloying elements which cause chip breaking should display the following properties:

i. be insoluble in both liquid and solid aluminum;
ii. show a low-melting point with regard to aluminum;
iii. not form intermetallic compounds with aluminum or other alloying elements; and
iv. have lower hardness value compared to the aluminum matrix.

These conditions may be fulfilled by using lead (Pb), bismuth (Bi), tin (Sn), cadmium (Cd), indium (In), antimony (Sb), or a number of other elements which are, however, not suitable from a practical point of view.[44, 45]

One of the approaches for improving machinability has been to develop free-cutting alloys from standard heat-treatable alloys to which elements such as Pb, Bi, Sn, *etc.* have been added to form additional phases in the aluminum matrix. These phases improve the machinability of any given material because they provide a smooth surface, cause less tool wear, and produce chips which are more easily breakable.[44, 45] The minimum required

amount of free-cutting additives depends on the casting composition and its microstructure, as well as on the selected additive itself and the stringency of the machining operations involved. Preferably, the total addition of one or more of these soft lubricity-imparting elements should not exceed about 2 wt% of the casting, in such a way as not to alter the other properties of the same casting to any significant degree. According to the inventor Young, bismuth and/or tin are the additives preferred by most researchers.[46] The lower strength values of the alloys containing added Sn results from the distribution of fine soft particles of $\beta$-Sn, mainly at the grain boundaries, as well as from the formation of other intermetallic compounds such as $Mg_2Sn$. Smolej *et al.*[43] demonstrated that tin, together with phases based on aluminum and copper, formed nets enveloping the crystal grains of the matrix, although tin was not found in the crystal grains themselves. The size and distribution of free-cutting constituents in the matrix are important factors in the machinability of alloys. Tin constituents were observed to be smaller and more densely distributed compared to the free-cutting constituents in $AlCu_5PbBi$.

## 2.4 HEAT TREATMENT

There are two ways of increasing the mechanical strength of aluminum alloys once they are in solid form; these are mechanical work and heat treatment. Both methods may be applied to alloys prepared for mechanical work, although the response to hardening by heat treatment will depend on the individual alloying elements present in each alloy. Heat treatment provides as-cast aluminum samples and/or castings with many advantages, such as:

- homogenization of the microstructure in the alloys;
- releasing the residual stresses caused during solidification;
- improving the dimensional stability and machinability of parts; and
- optimizing the hardness, toughness, ductility, and corrosion resistance of the cast piece.

The term *heat treatment* refers to any of the heating and cooling operations which are performed with the purpose of changing the mechanical properties, metallurgical structure, and residual stress state of a metal product. In aluminum alloys, the use of heat treatment is restricted to frequently used operations intended to increase the tensile strength and hardness of alloys responding to precipitation hardening.[47, 48] The process for increasing the mechanical strength of aluminum alloys through heat treatment consists of three stages:

(i) solution heat treatment;

(ii) quenching; and

(iii) aging.

### 2.4.1 Solution Heat Treatment

Solution heat treatment is carried out by heating the alloy to a suitable temperature, followed by maintaining this temperature long enough to allow the constituents to become supersaturated in the solid solution, and then cooling rapidly enough to allow the excess solute to precipitate. The purpose of solution heat treatment is to put the maximum amount

of hardening solutes such as Cu and Mg into solid solution in the aluminum matrix. A schematic of the solution heat treatment and aging regimes is shown in Figure 2.6.

In Al-Si-Cu-Mg alloys, solution heat treatment is applied to homogenize the alloy, to change the morphology of the interdendritic phases, and to dissolve precipitation-hardening constituents such as $CuAl_2$, AlMgCu, and $Mg_2Si$. During this treatment, the morphology of the eutectic Si particles changes with time, through the fragmentation, spheroidization, and coarsening of the particles. It should be noted that the spheroidization rate increases with the degree of strontium concentration in the alloy.

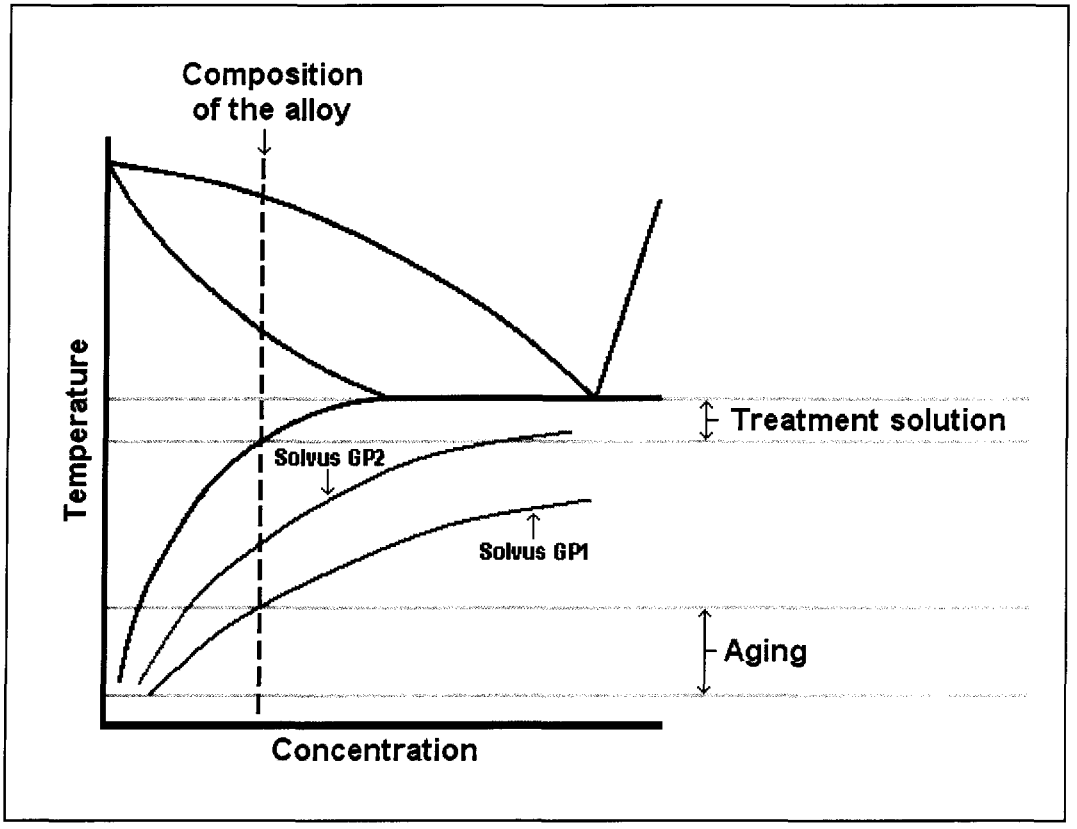


**Figure 2.6** Temperature intervals for solution heat treatment and aging of binary aluminum alloys.[49]

### 2.4.2 Quenching

Quenching is the critical stage of the heat treatment process, following upon solution heat treatment. The main objective of quenching is to retain the solute atoms in solid solution formed during solution heat treatment, through rapid cooling to a temperature close to the ambient temperature. This stage, however, not only seeks to obtain a supersaturated solid solution, but also attempts to preserve a certain density of vacancies favoring the diffusion which will be required during the aging stage.[48]

During quenching, precipitation of a certain amount of solute may occur, which will cause the amount of hardening to decrease. To prevent this type of precipitation, two requirements must be met. The first is to regulate the time span during which the cast part is to be heat-treated, causing it to take place between the solution stage and the quenching stage. This lapse of time should be short enough to prevent the temperature from reaching the critical range where precipitation accelerates. The second requirement is to apply a heat extraction rate which is high enough to curtail the period of time during which the temperature crosses the critical range, thereby causing the precipitation to be practically negligible or even zero.[48] This last requirement may be met by applying a cold water process for the extraction of heat, in view of the fact that this is one of the most commonly used means to obtain cooling. It should be kept in mind, however, that such an abrupt form of cooling can, in some cases, generate problems of distortion and residual cracks. It is necessary to apply a lower speed to allow the type of cooling which will create a balance between the residual stresses generated and the distortions and precipitation mentioned

above. Once these precautions have been taken, it becomes possible to obtain an acceptable dimensional stability and the mechanical properties required with the final heat treatment.[33]

### 2.4.3 Aging

Aging is the final stage of the heat treatment process. It consists of maintaining the alloy at a certain temperature for a sufficient period of time to permit the solute atoms to precipitate in the form of finely dispersed metastable phases. In some alloys, the temperature is suitable enough to promote the precipitation over the course of a few days, a phenomenon known as *natural aging*. In other alloys, however, a longer time might be needed and thus, it is necessary to promote precipitation by using higher temperatures. This is known as *artificial aging* or precipitation treatment.[48] The stages in this type of precipitation are shown as a function of aging time in Figure 2.7.

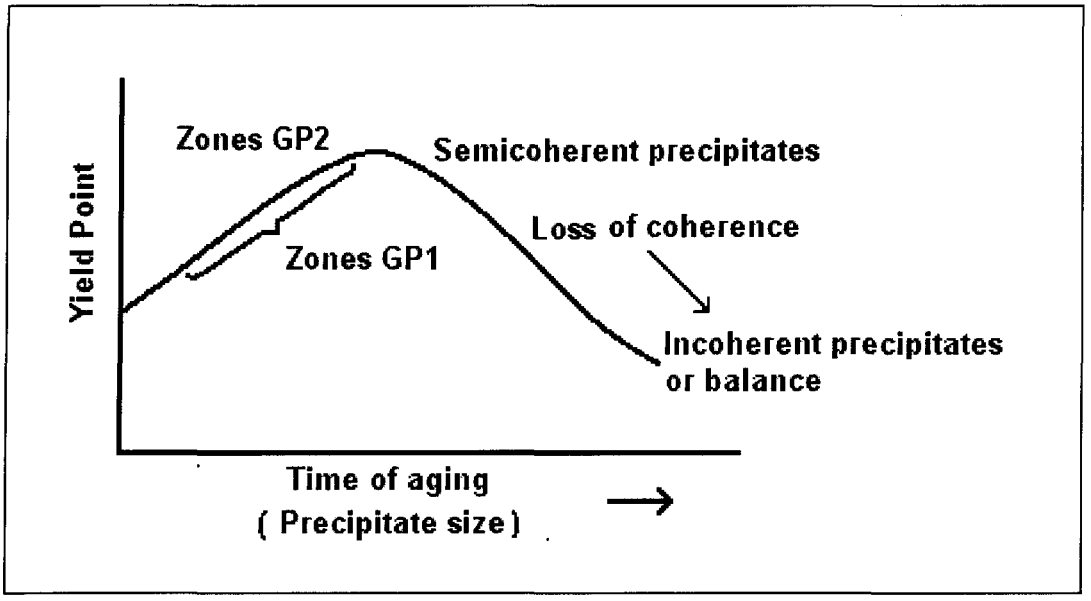


**Figure 2.7** Diagram representing precipitation stages with progress of aging time.[20]

Precipitation occurs in the sequential appearance of metastable phases which differ in size and other parameters with respect to the matrix, as may be seen in Figure 2.7. Guinier-Preston (GP) zones may be classified as either GP1 or GP2 zones according to the order and area in which they fall. The main difference between them is that GP2 zones are larger in size. In fact, GP zones are not a single phase which differs from the matrix, but rather they are made up of regions consisting of a rich concentration of solute atoms. The temperatures required to effectuate the aging process vary for each alloy, and are determined by the *solvus line* of the metastable phases, as shown in Figure 2.7. Each metastable phase formed during aging has its own solvus line below which the phase can be formed and above which it dissolves. It is necessary for the aging temperature to be below the solvus line of the GP zones.[20, 48] In some cases, however, higher temperatures are used without going beyond the solvus line of the GP2 zones, in order to improve certain properties such as resistance to corrosion cracking, while sacrificing the tensile strength to some extent.[18]

Throughout the aging process, in addition to the abovementioned precipitation sequence, the precipitates present tend to increase in size with the duration of the aging time; both events cause changes in the properties of the alloy. Initially, there is an increase in tensile strength and hardness up to a maximum value as produced by a T6 temper and shown in Table 2.4; this may be ascribed to an optimum distribution of precipitates as well as to their size and to the presence of coherent and semi-coherent precipitates. After reaching this maximum value, the tensile strength and hardness values begin to decrease once again. This phenomenon is known as over-aging or stabilization as produced by a T7

temper and shown in Table 2.4; it appears to be the result of the formation of incoherent precipitates or an equilibrium phase.[2]

## 2.5 POROSITY

Porosity is a defect most commonly found in cast products; it is thus a factor of primary importance to be examined with regard to the quality of the casting. The occurrence of porosity is detrimental not only to the surface quality after machining, but also to the mechanical properties and corrosion resistance of the cast material. Porosity can be classified as two types: (a) shrinkage porosity, and (b) gas porosity. Shrinkage porosity results from the volume decrease accompanying solidification. This type of porosity can also occur as "microshrinkage" or "microporosity" dispersed in the interstices of dendritic regions, and is typically found in alloys with a large difference between their solidus and liquidus temperatures. Limited or inadequate liquid metal feeding in the interdendritic regions gives rise to this type of shrinkage. Gas porosity results from the decrease in the solubility of hydrogen in aluminum on going from the liquid to the solid state during solidification.

The presence of porosity is undesirable since it weakens the alloy strength and ductility. There are occasions, however, when porosity may be beneficial because it reduces the tendency to hot-tearing. By using high cooling rates and grain refinement techniques, it is possible to reduce the total amount of porosity, in that the pores which do form will be more evenly distributed and smaller in size. Porosity can cause problems particularly in those workpiece areas where holes are to be drilled. Excess porosity due to improper

gating, venting, and injection can result in poor machining characteristics. Porosity due to entrapped air can be minimized by proper gating and venting while porosity resulting from excess lubricant in the die can be reduced by use of minimum and suitable lubricants.[5]

## 2.6 MICROSTRUCTURAL FEATURES

The fact that Al-Si alloys are being used increasingly in the automotive and aerospace industries has led to a concomitant increase in microstructural investigations with a view to acquiring a better understanding of the effects of machinability. As mentioned previously, the microstructure of Al-Si casting alloys is determined by: (a) the chemical composition of the alloys, (b) the casting process, and (c) the heat treatment methods applied to the alloys.[3, 4]

The overall condition of the work material can influence the machinability outcome considerably, which is why certain metallurgical factors must be taken into account; these include alloying elements, microstructural features and porosity, casting methods, heat treatment, grain refinement and modification, as well as the physical properties of the work material itself.[49] Aluminum-Silicon alloys may thus have radically different machining characteristics under similar cutting conditions, as a result of differences in the microstructure, which in turn generate variations in composition or in manufacture. As an example, variations in the microstructure of the workpiece material can affect chip formation in high speed machining for continuous and interrupted cutting.

## 2.7 MACHINABILITY OF ALUMINUM ALLOYS

Machining may be defined as the process of removing material from a workpiece in the form of chips and is an important manufacturing process. Moreover, machining is necessary where maintaining a tight tolerance of dimensions and finishes is required. [5] The most common types of machining are traditional, such as turning, milling, and drilling, as well as non-traditional, such as chemical machining, electrical discharge machining (EDM), and electrochemical machining (ECM). The term machinability includes all those properties which are relevant to the machining and cutting process, namely, the wear on tools, the necessary cutting force, the resulting form of the chips, and the quality of the surface produced.

### 2.7.1 Machinability Criteria

Machinability is a phenomenon of the interaction between the workpiece (material type and form), the cutting tool (material type and geometry), and the cutting medium (air or liquid) in a number of different removal sequences (turning, drilling, tapping, milling, sawing, *etc.*) and cutting conditions (speed, feed, and depth of cut). Drill performance is influenced by a considerable number of factors, most of which are listed in Figure 2.8. Since the machinability response is known to be different for different operations and operating conditions, machinability should probably be viewed as an interaction rather than as a property. In a collective sense, the terms relating to machinability are:

- tool life, wear level, and fracture probability;
- specific power consumed, forces, and temperature increase;

- chip control (chip breakability, chip shape, and built-up edge);
- dimensional tolerances in terms of surface roughness, microstructure, and burr formation;
- work requirement (machining rate); and
- overall cost.

The two factors known to affect machinability are hardness and ductility. Increasing hardness makes penetration by the tool more difficult, thereby decreasing machinability. Generally speaking, lower ductility is beneficial to machinability, since it promotes the production of discontinuous chips.

The following list includes the factors determining the condition of the work material and which are capable of influencing the outcome of machinability:

- alloy chemistry and additions;
- morphology, size, and volume fraction of the constituent phases;
- microstructure (grain refining and modification);
- porosity;
- heat treatment; and
- physical and mechanical properties.

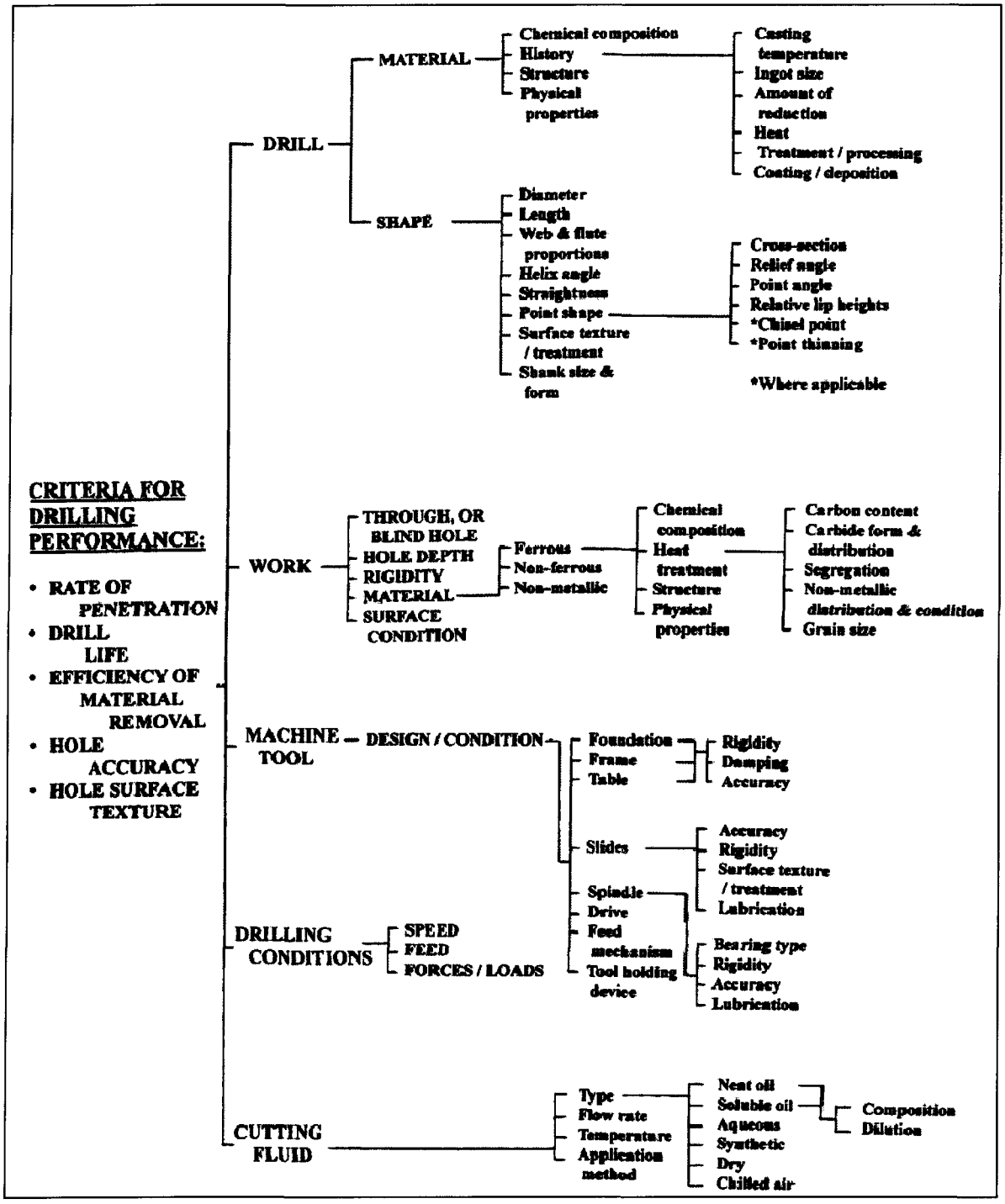


**Figure 2.8** Principal technical drill performance criteria and factors associated with drilling operations/castings.[50]

### 2.7.2 Tool Materials

There are various types of tool materials, ranging from high carbon steel to ceramics and diamonds which may be used in the metalworking industry. A good cutting tool must have the following properties:

- high strength, or hardness values, at elevated temperatures;
- high increased impact toughness and thermal shock resistance;
- higher hardness values than the workpiece itself;
- low adhesion to prevent wear and/or diffusion;
- low coefficient of friction; and
- low diffusivity to workpiece material.

The main materials used in a cutting tool are: [5]

- high speed steels (HSS);
- ceramic-metallic composites (cermets), ceramics, cast carbides, and cemented carbides;
- polycrystalline cubic boron nitride (PCBN); and
- polycrystalline diamonds (PCD).

### 2.7.3 Machining Aluminum Using Solid Carbide Drills

Casting alloys which have a relatively high abrasive action are mostly machined using solid carbide drills. This type of drill may be used on twist drills to make the edges more wear-resistant at higher speeds.[51] The production of smaller helix angles and thicker

webs is a convenient measure which is often used to improve the rigidity of these drills, and which also ultimately helps to preserve the carbide. For economic reasons, solid carbide drills are being increasingly used for machining the less abrasive wrought alloys. An extremely long tool operating life of one week or more, as well as the high cutting speeds attainable, more than compensate for the higher price of solid carbide drills.[52]

### 2.7.4 Heat Build-Up on the Cutting Tool Edge (BUE)

Under most cutting conditions, some of the cut material will attach to the cutting point or tip. This tends to cause the cut to be deeper than the tip of the cutting tool itself and to degrade the surface finish. Also, periodically the built-up edge will break off and remove some of the cutting tool with it; tool life is thus reduced. In general, built-up edge may be reduced by taking the following steps:

- increasing cutting speed;
- decreasing feed rate;
- increasing ambient workpiece temperature;
- increasing rake angle; and
- reducing friction by using a cutting fluid.

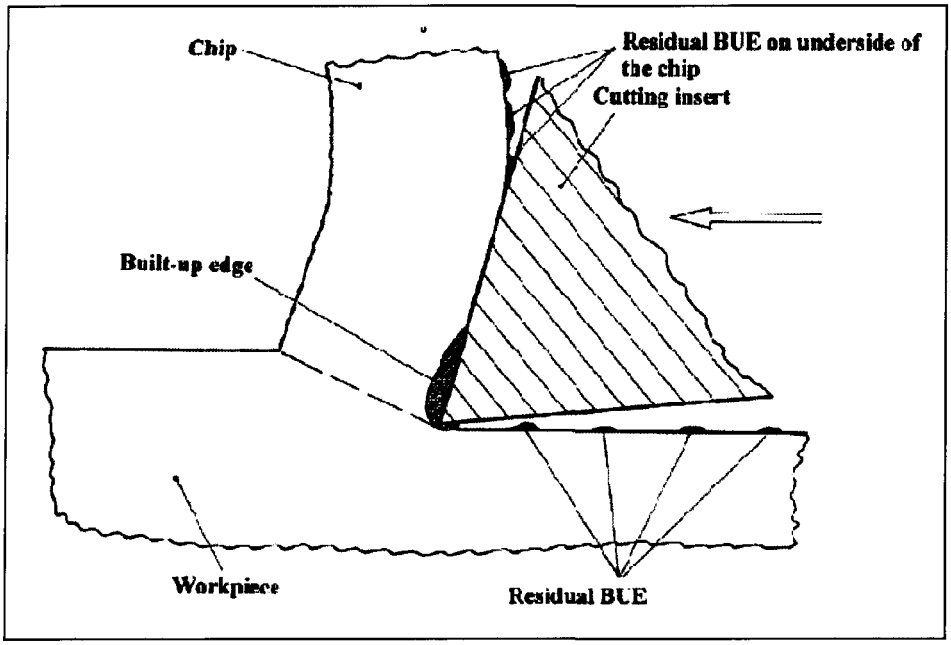


**Figure 2.9** Edge build-up on the tool, and residual effects on the workpiece and chip.[50]

The built-up edge consists of aluminum particles which have become welded to the tool edge because they melted from the heat generated by the cutting. Essentially, what happens is that the aluminum begins to be cut by the aluminum welded to the cutting edge, resulting in the deterioration of several parameters including chip size, tool life, surface finish, the dimensional control of the part, and the effectiveness of the coolant. Built-up edge occurs during the machining process of Si up to 12% in Al-Si alloys. As the Si% increases, the abrasive wear mechanisms dominate and result in shorter tool life.[5]

This BUE is one of the major sources of surface roughness and it also plays an important role in tool wear. The workpiece material adheres to the rake face of the tool in two forms namely, built-up edge (BUE) and built-up layer (BUL). Tool damage is engendered mainly by the formation of this type of layer. Studies carried out on built-up

edge have shown that the chip material is welded, deformed, and then deposited, layer by layer, onto the rake face of the tool. It is thus possible to observe the presence of built-up edge by studying the back face of the chip during the machining process.[50] Built-up edge may be reduced by integrating several steps such as improving the lubrication conditions, using sharp tools as well as better surface-finished tools, and by applying ultrasonic vibration during the machining process. At higher rates of metal removal, *i.e.* at a higher speed or feed, a built-up edge is no longer discernible; a transition from built-up edge to flow zone is strongly influenced by both speed and feed, and occurs in a range of cutting conditions commonly encountered in industrial machining operations. The flow zone is usually more strongly bonded to the tool than the built-up edge, and is preferably described as the "thermoplastic shear band". The behavior of work material in the thermoplastic shear bands is probably the most significant parameter governing its "machinability" in high speed machining.[5]

### 2.7.5 Chip Formation

The chip formation process is influenced by a number of factors including cutting conditions, cutting fluids, tool geometry, chip control devices, machine tool dynamics, and tool and work material properties. In drilling, the specific type of the chip depends on a number of parameters, in particular, the drilling speed, the feed rate, and the mechanical and thermo-physical properties of the workpiece.

During the machining process, three basic types of chips may be formed. These types are discontinuous chips, continuous chips, and continuous chips with built-up edge, as shown in Figure 2.10.[53]

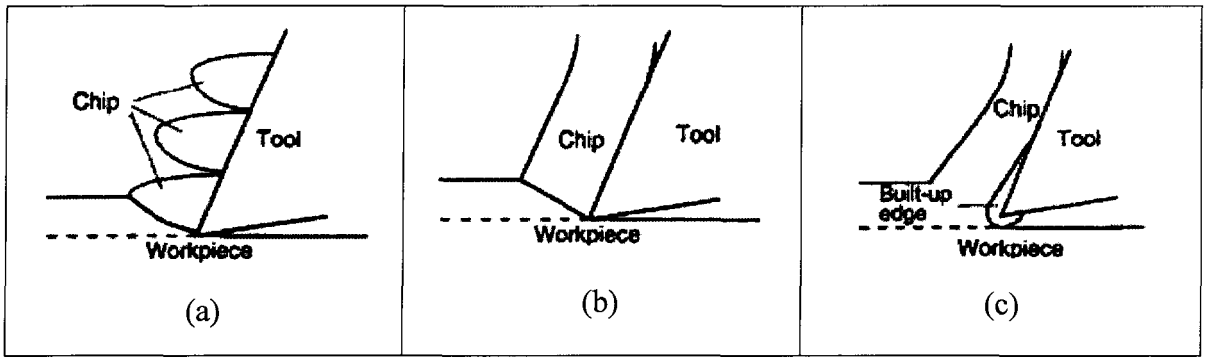


**Figure 2.10** Three types of chips: (a) discontinuous; (b) continuous; and (c) continuous with built-up edge (BUE).[53]

Discontinuous chip formation usually occurs when cutting hard, brittle materials, partly since these materials cannot withstand high shear forces which would otherwise cause the chips formed to shear cleanly away. This type of chip also occurs in machining operations with small rake angles on cutting tools, coarse machining feeds, and low cutting speeds. There is a greater possibility of tool chatter or breakage when discontinuous chips

are formed, unless the tool, tool-holder and workpiece are held extremely rigidly; this phenomenon results from an increase of pressure at the tool tip during chip formation followed by its sudden release as the chip shears thereby causing the unstable behavior. Continuous chips are observed during the machining of ductile metals, such as low-carbon steel, aluminum, and copper. There is less likelihood of chatter, and the surface finish is usually better than when discontinuous chips are formed. A disadvantage of continuous chips is the fact that they can become very long and thus become entangled with the machine or pose a safety hazard. This problem can be overcome by using a chip-breaker, which is a device clamped to the top of the tool encouraging the chip to curl more tightly, then hit the workpiece and break off. A continuous chip with built-up edge (BUE) formation is basically the same process as continuous chip formation, except that as the metal flows up the chip-tool zone, small particles of the metal begin to adhere or weld themselves to the edge of the cutting tool. As the particles continue to weld to the tool, the cutting action of the tool itself is affected. This type of chip formation is common in the machining of the softer non-ferrous metals and low carbon steels. Built-up edge is formed when particles of the workpiece material weld to the rake face of the tool during cutting. Large built-up edges can be extremely detrimental to surface finish and integrity, since they effectively change the geometry of the cutting edge and consequently the shear plane angle as well, leading to residual stresses in the material below the depth of cut. As a large BUE becomes dislodged, it can deposit work-hardened particles, which will ultimately be embedded in the finished surface. Built-up edge formation can be minimized by using a

more positive rake angle, higher cutting speeds, and a coolant with increased lubricity to reduce tool-chip friction.

In the drilling process, chip size is governed by its formation geometry at the cutting edge, namely thickness and curl, and the characteristic length, determined by the point at which the chip breaks in the generation cycle. Chip formation in the drilling processes is governed by the following three points and is depicted in Figure 2.11: [54]

1. The rake faces of the first part of the cutting lip in the straight drill are not flat and the rake angle varies along the cutting edges. The twisted rake face gives the chip a rotation, $\omega_c$, about the drill axis.

2. The cutting speed varies proportionally with the distance from the drill center, which causes a strong side curling, or large $\omega_z$.

3. The side-curled chip is forced to curl in another direction by the obstruction of the web and flutes of the drill, this is thus a chip with a large $\omega_x$.

Given the three components of angular velocity $\omega_c$, $\omega_z$, and $\omega_x$, the chip experiences a helical motion with the angular velocity $\omega_h$, which is the resultant of these three components. As the drilling process progresses, the weight of the chip increases constantly and the center of gravity moves away from the root of the chip. The chip-flow gradually becomes impeded by the web and flutes, which impose a resistance force on the chip. This force develops a bending moment, or non-uniform stress distribution, at the root of the chip, producing unstable or fragmented chips, which decrease the bending and the

resistance force. In other words, the chip changes its form to meet the external forces and constraints governing its flow. The resistance force acting on the chip contributes to the total thrust and torque on the drill.

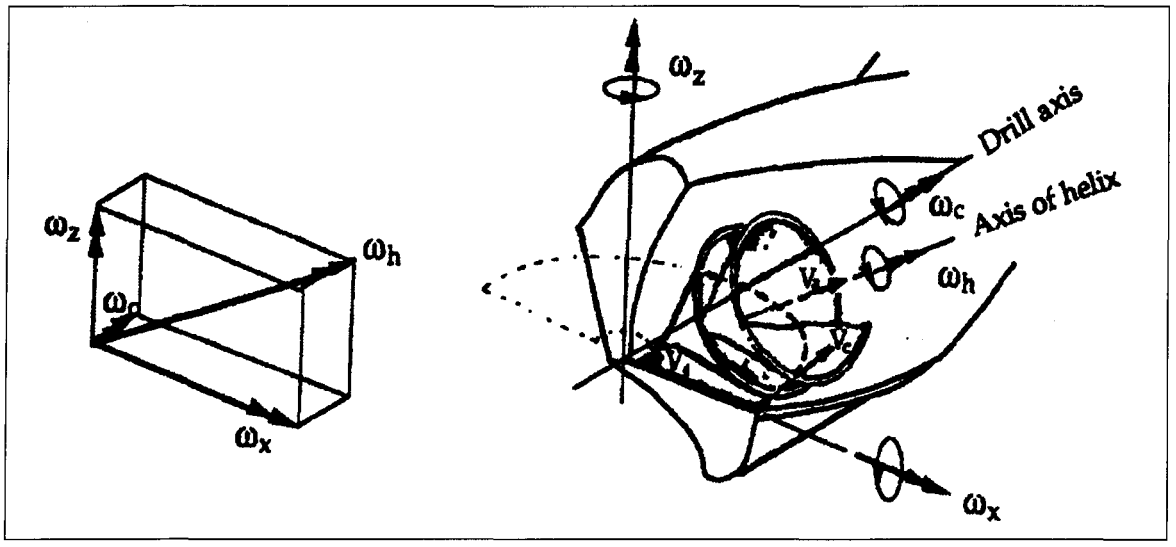


**Figure 2.11** Drilling chip-curl components.[54, 55]

The chip forms which may be generated during the drilling experiments are shown in Figure 2.12; these include: [55]

1) Conical Chip: The diameter of this chip must be small enough to allow it to move through the flute/hole wall cavity without breaking.[56] The conical chip begins with a spiral form when the drill contacts the workpiece and grows as the entire lip becomes engaged. After several rotations, the chip fractures and all the newly-developed chips display the fan shape.

2) Fan-Shaped Chip: These are formed when conical chips cannot curl sufficiently to follow the flute; they tend to fracture prior to a complete revolution. The fan shape

is by far the predominant chip form and can be considered the ideal chip for most drilling applications.

3) Chisel-Edge Chip: This chip forms as a result of the extrusion of metal from the drill chisel edge.[57] The chip is long and narrow, streaming out of the drill along the interior of the flute at the web. When this chip forms, there is also a second chip type forming along the cutting edge. To eliminate the chisel-edge chip, it may be necessary to decrease the feed and thereby the amount of metal extruded.
4) Amorphous Chip: This chip has a rather wrinkled, uncurled appearance. It does not have enough consistent curl to take a fan shape and is observed to be guided unbroken up the flutes. The amorphous chip form is the heaviest chip form and the least desirable.
5) Needle Chip: This type of chip is caused by severe upcurling.[54] There is no clear demarcation between needle and fan-shaped chips. It is the marked change in the radius of the chip about the lip axis which results in the needle shape. This change in radius occurs when the BUE alters the drill cutting surface geometry. Built-up-edge is caused by the strain-hardened workpiece material welding itself to the rake face and becoming a new cutting surface.
6) Impacted Chip: This chip is the aggregation of primary smaller chips which have amalgamated while moving up the flute. It is thus heavier than the primary chip and takes on the shape of the flute. The impacted chip is undesirable since its formation results in the clogging of the flute. To eliminate this type of chip, it may be

necessary to reduce the feed, or the cutting speed or both, or otherwise to use a drill with larger flute cavity.

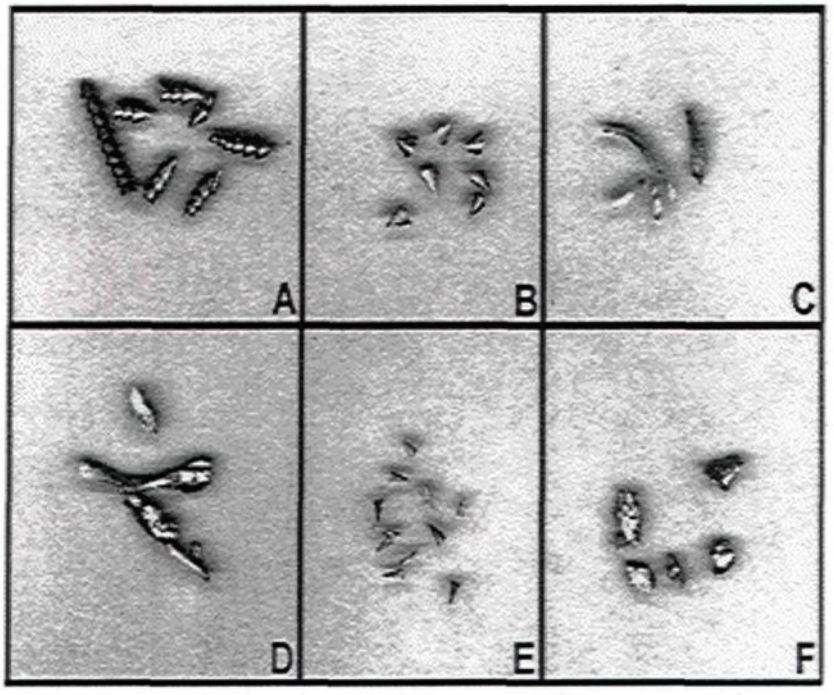


**Figure 2.12** Generated chip forms: (A) conical; (B) fan-shaped; (C) chisel-edge; (D) amorphous; (E) needle; and (F) impacted.[55]

### 2.7.6 Cutting Fluids

Cutting fluids are essential to machining processes. They are used to reduce the effects of friction, that is to say, to carry away heat in machining operations since excessive heat can damage the microstructure of metals. The proper use of coolants can make higher metal removal rates possible; they can also help improve the quality and dimensional accuracy of the cast part. The goal of machining operations must be to improve productivity and reduce costs. This is accomplished by machining at the highest speeds achievable while still maintaining a practical form of tool life, reducing the quantity of scrap, and producing parts having the desired surface quality.

The proper selection and use of cutting fluids can help achieve all of these goals. In machining, almost all of the energy expended in cutting is transformed into heat. The deformation of the metal to create chips and the friction of the chip sliding across the cutting tool produce heat. The primary function of cutting fluids is to cool the tool, work piece, and chip; to reduce friction at the sliding contacts; and to prevent or reduce the welding or adhesion on the contact edges which cause a built-up edge on the cutting tool or insert. Cutting fluids also help to prevent rust and corrosion, while also flushing chips away. Machining operations create heat, which must be removed from the process.

Chips help to carry away heat from the tool and workpiece. The coolant then absorbs heat from the chip, the tool, and the work piece; [58] to be effective the fluid must be able to transfer heat extremely rapidly by absorbing it and subsequently carrying it away. In a typical machining operation, two-thirds of the heat is created by the resistance of the

workpiece atoms to being sheared. The friction of the chip sliding over the cutting tool face creates the other one-third of the heat. The lubrication actually changes the shear angle, which reduces the shear path and produces a thinner chip. Good lubrication also reduces internal friction and heat as a result of diminished molecular disturbance. Cutting fluids may be divided into four main categories: straight cutting oils, water-miscible fluids, gases, and paste or solid lubricants. Water quality has a considerable effect on the efficacy of the coolant. Very hard water having a high mineral content can cause rust, stains, and corrosion of the machines and workpieces; such water can, however, be deionized to remove the impurities and minerals. The benefits of using coolants are that they improve part quality, reduce tooling costs, increase cutting speeds and feeds, improve surface finishes, reduce bacterial growth, and provide rust and corrosion prevention.

### 2.7.7 Drilling

Drilling is the manufacturing process by which a round hole is created within a workpiece or enlarged by the rotating end of a cutting tool, namely, a drill; it is the simplest, quickest and most economical method of hole production. The chief characteristic which distinguishes it from other machining operations is the combined cutting and extrusion of metal at the chisel edge in the center of the drill. Although many other processes contribute to the production of holes, including boring, reaming, broaching, and internal grinding, it is the drilling which accounts for the majority of holes produced in the machine shop.[5] Reaming is a similar process where a hole feature is enlarged to a noticeably specific or accurate size by introducing a rotating-end and side-cutting tool called a reamer. Drilling and reaming machines vary from the tiny bench machine used for high quality jeweler's operations to the heavy duty machines which are capable of boring large holes. Some of the most commonly used drilling machines are drill presses, milling machines, and lathes.

#### 2.7.7.1 Drill Nomenclature

A drill may be defined as a rotary end-cutting tool having one or more cutting lips, and having one or more helical or straight flutes for the passage of chips and the admission of a cutting fluid.[59] There are many different types of drills. Examples are twist drills for general machining, rock drills for mining minerals, laser drills for extremely small holes, spade drills for large holes, and gun drills for deep holes. The type of drill illustrated in Figure 2.13 is the twist drill.

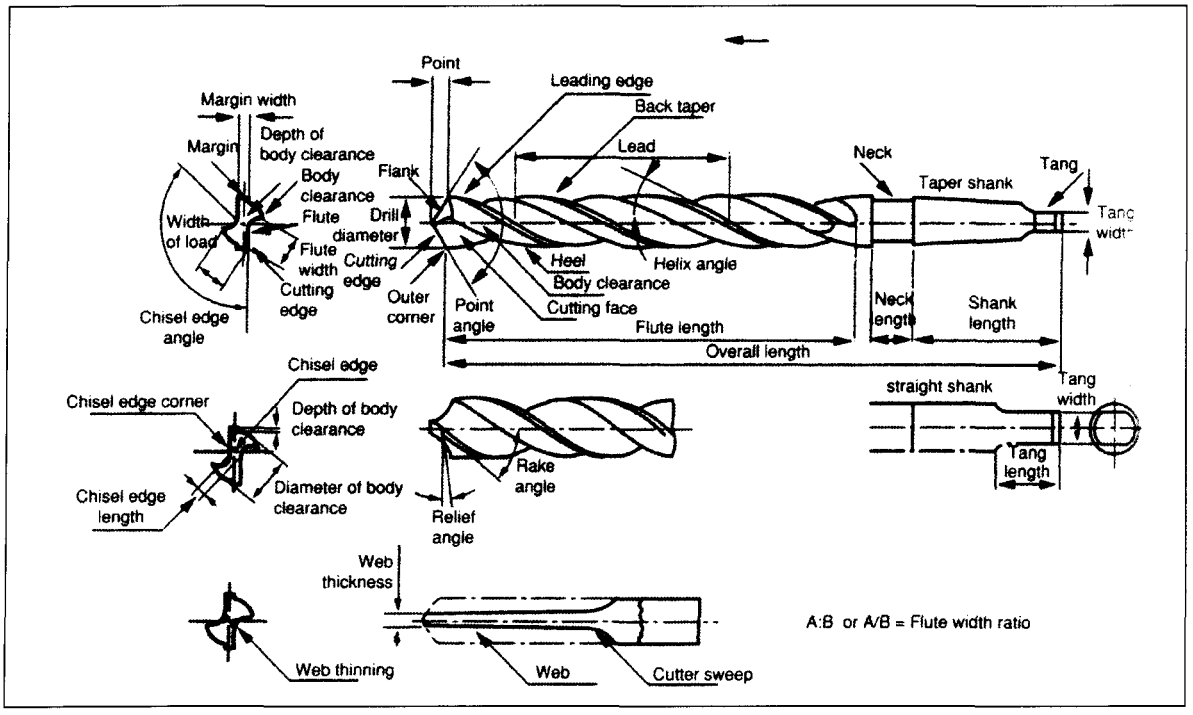


**Figure 2.13** Twist drill nomenclature.[53]

In the United States, three different systems for designating twist drill sizes are used:

- fractional inches and millimeters;
- letters, or Morse gauge;
- numbers, with higher numbers representing smaller drills.

The lengths provided in the Table 2.6 are jobber's lengths.[60] For certain purposes these may be too short, whereas unusually long twist drills, often called aircraft drills, sometimes electrician's drills, are available in 6, 12, and even 24-inch lengths. The ideal point should be suited to the materials to be drilled; bits usually come with a 135° split point, although several proprietary designs are also offered.

**Table 2.6** Nomenclature for Jobber's Lengths [60]

| Material | Point Angle | Chisel Angle |
|---|---|---|
| **Aluminum** | 118°–130° | 125°–130° |
| **Brass** | 118°–125° | 125°–135° |
| **Bronze (hard)** | 118° | 115°–125° |
| **Copper** | 100°–130° | 125°–135° |
| **Plastic** | 60°–118° | 125°–135° |
| **Stainless Steel** | 118°–140° | 115°–125° |
| **Cast Iron** | 90°–118° | 115°–125° |

A drill is composed of a shank, body, and point: (i) the shank is the part of the drill which is held and driven, and it may be straight or tapered; (ii) the body of the drill extends from the shank to the point, and contains the flutes; (iii) flutes are grooves which are cut or formed in the body of the drill to provide cutting lips for the removal of chips and to allow cutting fluid to reach the cutting lips, (it should be noted that although straight flutes are used in some cases, they are normally helical); (iv) the land is the peripheral portion of the body between adjacent flutes, the land width being the distance between the leading edge and the heel of the land measured at right angles to the leading edge; (v) the margin is the cylindrical portion of the land which is not cut away to provide clearance; (vi) the web is the central portion of the body that joins the lands, (the extreme end of the web forms the chisel edge on a two-flute drill); (vii) the edge ground on the tool point along the web is called the chisel edge and connects the cutting lips; (viii) the point is the cutting end of a drill made up of the ends of the lands and the web, resembling a cone but departing from a true cone to furnish clearance behind the cutting lips.[5, 51, 59]

### 2.7.7.2 Operating Conditions

Drill manufacturers and a variety of reference texts provide recommendations for proper speeds and feeds for drilling a variety of materials. Cutting speed may be referred to as the rate at which a point on the circumference of a drill will travel in one minute, expressed in surface feet per minute (SFPM). At low speeds, the drill might chip or break, whereas high speeds dull the cutting lips.[5, 51] Cutting speeds are known to depend on the following seven variables:

- type of workpiece material;
- the harder the material, the slower the cutting speed;
- cutting tool material and diameter;
- type and use of cutting fluids;
- rigidity of the drill press;
- rigidity of the drill;
- rigidity of the work setup; and
- quality of the hole required.

Work material and cutting speed are the most significant variables and should be considered prior to initiating the drilling process. Hard cutting tool material can be used at high speeds. Large drill diameters must revolve at low cutting speeds and a short drill has better rigidity. To calculate the revolution per minute (RPM) rate of a drill, the diameter of the drill and the cutting speed of the material must be taken into consideration. The formula normally used to calculate cutting speed is as follows: [51]

$$SFPM = (Drill\ Circumference) \times (RPM) \qquad \text{(Eq. 2.2)}$$

where *SFPM* represents surface feet per minute, or the distance in feet traveled by a point on the drill periphery each minute; *Drill Circumference* is equal to the distance around the drill periphery in feet; and *RPM* is equal to the number of revolutions per minute. In the case of a drill, the circumference is:

$$Drill\ Circumference = \pi/12 \times (d) = 0.262 \times d \qquad \text{(Eq. 2.3)}$$

where *Drill Circumference* = the distance around the drill periphery in feet; *Pi* is the constant 3.1416; and *d* is the drill diameter in inches. By substituting the *SFPM* for the drill circumference, the cutting speed can be written as:

$$SFPM = 0.262\ x\ d\ x\ RPM \qquad \text{(Eq. 2.4)}$$

Feed in drilling operations is expressed in inches per revolution, or IPR, which is the distance the drill moves in inches for each revolution of the drill. The feed may also be expressed as the distance traveled by the drill in a single minute or IPM (inches per minute), which is the product of the RPM and IPR of the drill; this can be calculated as follows:

$$IPM\ x\ IPR \qquad \text{(Eq. 2.5)}$$

where the terms *IPM*, *IPR*, and *RPM* represent inches per minute; inches per revolution; and revolutions per minute, respectively.[5, 51]

# CHAPTER 3

# EXPERIMENTAL PROCEDURES

# CHAPTER 3

# EXPERIMENTAL PROCEDURES

## 3.1 INTRODUCTION

This chapter will provide all the details relevant to the 396 and B319.2 type alloys with regard to general melting, casting procedures, heat treatment, and machining regimens. The alloy codes for the various alloys which were prepared for the purpose have been collectively listed in Table 3.1. Drilling machining tests were carried out using a Huron K2X 8 Five high-speed high-precision vertical machining center under fixed machining conditions which include cutting speed, feed rate, length of cut, tool geometry, tool material, and coolant. The operations described in this study were carried out with the intention of investigating and viewing the effects on the machining performance of the 396 and B319.2 type alloys, involving cutting force and moment, chip configuration, and built-up edge (BUE) formation.

## 3.2 ALLOY PREPARATION AND CASTING PROCEDURES

The 396 and B319.2 base alloys used in this project were supplied in the form of 12.5 kg ingots which were cut into smaller pieces, then dried and melted in charges of 100 kg each for alloy preparation. The alloys selected for the project may be identified as follows: (a) alloy G2: 396 + 0.15%Sn; (b) alloy G3: 396 + 0.25%Fe + 0.25%Mn; and (c) alloy G12: 319 + 0.15%Sn. Table 3.1 shows the composition for each, representing the average of five spectrometric analyses.

Melting was carried out in a 120-kg capacity SiC crucible using an electrical resistance furnace in which the melting temperature was maintained at 750 ± 5°C. All alloys were grain-refined by adding 0.15%Ti in the form of rods of Al-5%Ti-1% B; they were then Sr-modified using Al-10%Sr master alloy to achieve a Sr level of 90 ppm in the melt. Iron and manganese were added in the form of Al-25%Fe and Al-25%Mn master alloys, respectively, whereas Sn was added as pure metal. The melts were degassed for ~15-20 min with a rotary graphite impeller rotating at ~130 rpm, using pure dry argon at a gas flow rate of 0.4$m^3$/hr. The melt was poured at ~740°C into a waffle-plate graphite-coated metallic mould originally preheated to 450°C, as shown in Figure 3.1, to prepare the castings for machinability studies. Prior to pouring, surface oxides and inclusions were skimmed off thoroughly.

**Table 3.1** Chemical composition of the alloys investigated in the current work (average of five spectrometric analyses)

| Element (wt%) | | | | | | | | | | | | | |
|---|---|---|---|---|---|---|---|---|---|---|---|---|---|
| **Alloy Code** | **Si** | **Fe** | **Cu** | **Mn** | **Mg** | **Zn** | **Sn** | **Ti** | **Bi** | **Sr** | **Al** | **Mn/Fe** | **S.F.** |
| **G2** | 10.812 | 0.533 | 2.228 | 0.550 | 0.260 | 0.035 | 0.196 | 0.221 | 0.01 | 0.009 | 84.4 | 1.04 | 1.653 |
| **G3** | 10.841 | 0.880 | 2.417 | 0.703 | 0.291 | 0.130 | 0.064 | 0.262 | 0.03 | 0.009 | 82.6 | 0.82 | 2.353 |
| **G12** | 7.533 | 0.346 | 3.597 | 0.286 | 0.240 | 0.040 | 0.178 | 0.241 | 0.00 | 0.009 | 87.3 | 0.83 | 0.934 |

Specimens were cut from the waffle-plate casting having overall dimensions of 300 mm in length by 175 mm in width by 30 mm in thickness, with ribs ~25 mm wide, separated by 16 mm gaps, as shown in Figure 3.2(a) and (b), respectively.

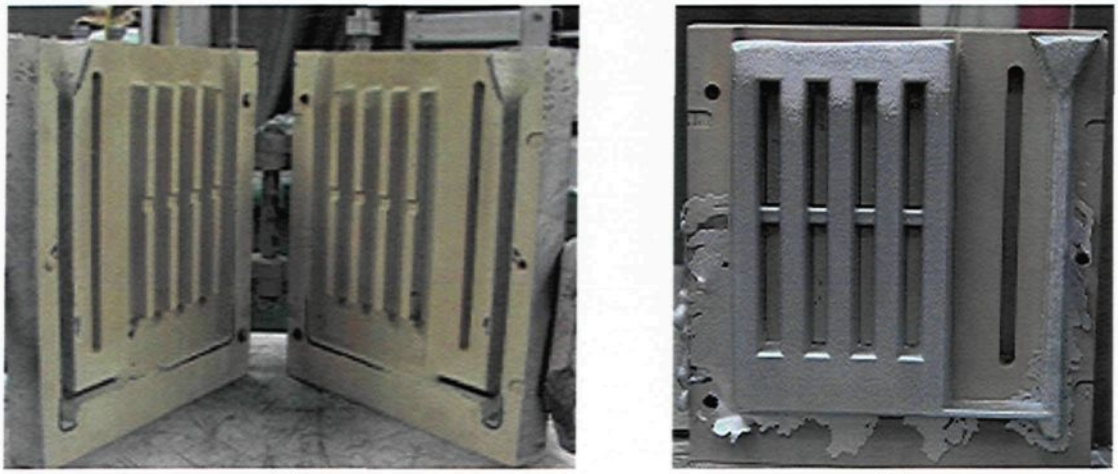

(a) (b)

**Figure 3.1** (a) Graphite-coated metallic mold; and (b) waffle-plate casting.

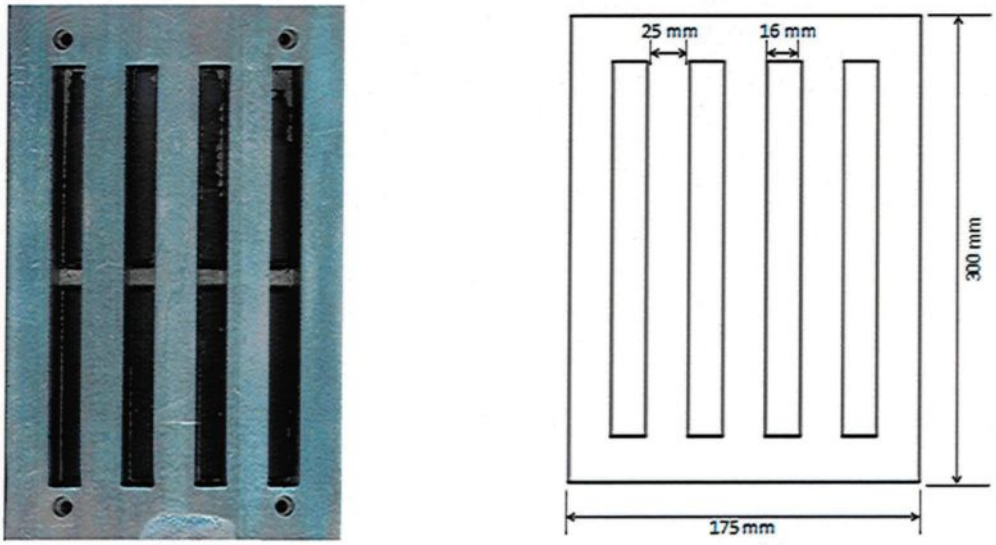


(a) (b)

**Figure 3.2** (a) Specimen block ready for drilling test; (b) diagram showing dimensions of the test block.

## 3.3 HEAT TREATMENT

The heat treatments were carried out in a Blue M forced-air electric furnace equipped with a programmable temperature controller accurate to ± 2°C for both solution and aging treatments, as shown in Figure 3.3. The solution heat treatments were carried out at 490°C/8hrs for the 396 and B319.2 alloys, followed by quenching in 65°C water and subsequent artificial aging at 180°C/5hrs, *i.e.* the machinability test blocks were subjected to a T6 temper.

**Figure 3.3** Blue M forced-air electric furnace for alloy heat treatment.

## 3.4 MACHINING PROCEDURES

From the point of view of machinability, it is expected that heat treatment, which increases the hardness values, will also reduce the built-up edge on the cutting tool and improve the surface finish of the machined part. Drilling experiments were carried out on a

Huron K2K 8 Five high-speed high-precision vertical machining center on the shop floor at the Aeronautical Technology Centre (CTA), in St-Hubert, Montreal. The Huron, illustrated in Figure 3.4, operates at 24 kW power and a maximum rotation speed of 24,000 rpm, such a set-up is used mainly for complex workpieces such as injection moulds or aeronautic workpieces. This type of vertical milling centre provides simple yet satisfactory control over the workstation. Highly finished surfacing qualities are possible thanks to the working speed and the accuracy involved. The experimental set-up consists of a dynamometer with fours sensors, charge amplifiers, and an A/D converter; designed for use in the online measurement of drilling forces. The optimum drilling conditions are listed in Table 3.2.

| Properties | |
|---|---|
| **Spindle Motor Power (Con./30 min Rating)** | 18/24 kW (kilowatt) |
| **Max. Torque on Spindle (Con./30 min Rating)** | 29/38 Nm |
| **Spindle Speed** | 100-24000 rpm |
| **Number of Tools** | 20 |

**Figure 3.4** Huron K2X 8 Five vertical machining center with table of properties.

**Table 3.2** Optimum drilling conditions

| Parameters | Drilling |
|---|---|
| **Cutting Speed** | 234.458 m/min or 11000 rpm. |
| **Cutting Depth** | 31.75 mm |
| **Cutting Feed Rate** | 44 IPM (0.1016 mm/rev) |

### 3.4.1 Cutting Tools

Throughout this project, four special drills were put to use when working with aluminum alloys. The information and data presented for the Gühring 768-Bright drill was also used as a basis for drawing better comparisons between the results obtained in the machinability tests and this drill.[61] From the data obtained, it is possible to calculate the moment and force by using MatLab software to determine which of the three drills is optimal for convenient application. The drills chosen for use were:

- Solid Carbide Drill (Gühring 768-Bright);
- Special Solid Carbide Drill (Gühring 5512-Firex);
- Cobalt Grade Drill (Kennametal B411A06500);
- Solid Carbide High Precision Drill (Mapal Giga-Drill M2195-0650);

Details of these drills and the coolant used in this study, as well as their respective specifications, are described in the following subsections.

### 3.4.1.1 Solid Carbide Drill (Gühring 768 – Bright)

Type K-quality cemented carbides are used, as a rule, for the short-chipping of Al-Si alloys; these have satisfactory qualities such as the required rigidity, a straight flute design allowing for aggressive feed rates while at the same time maintaining excellent hole concentricity and straightness. This type of drill is shown in Figure 3.5 with its specifications provided in Table 3.3.

**Figure 3.5** Solid Carbide Drill.

**Table 3.3** Solid Carbide Drill Specifications

| Grade | High Performance |
|---|---|
| **Material** | Solid Carbide |
| **Point Type** | Standard |
| **Drill Point (Deg.)** | 120° |
| **Metric Size (mm)** | 6.5 |
| **Flute Length (mm)** | 53 |
| **Shank length (mm)** | 36 |
| **Overall Length (mm)** | 90 |

### 3.4.1.2 Special Solid Carbide Drill (Gühring 5512 – Firex)

Gühring's range of solid carbide drills are the largest in the cutting tool industry. This type of drill, as shown in Figure 3.6 with its specifications given in Table 3.4, is most commonly used on materials for aerospace applications.

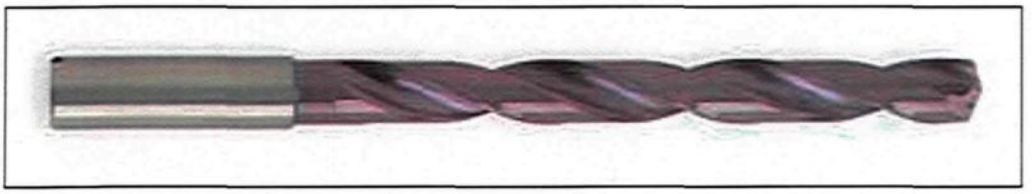

**Figure 3.6** Special Solid Carbide Drill.

**Table 3.4** Special Solid Carbide Drill Specifications

| Grade | High Performance |
|---|---|
| **Material** | Solid Carbide |
| **Point Type** | Self-Centering Point |
| **Drill Point (Deg.)** | 140° |
| **Metric Size (mm)** | 6.5 |
| **Flute Length (mm)** | 66 |
| **Overall Length (mm)** | 106 |
| **Application** | High penetration rate for alloy and tool steel, aluminum, cast iron, general steel, heat-treated steel, stainless steel, nickel alloys, and titanium. |

### 3.4.1.3 Cobalt Grade Drill (Kennametal B411)

This carbide drill, shown in Figure 3.7, is excellent for gray cast iron, nodular iron, aluminum, and aluminum alloy applications; it also performs well with respect to non-ferrous materials and is best suited for high quality, close tolerance holes requiring a good surface finish. Specifications of this drill type are provided in Table 3.5.

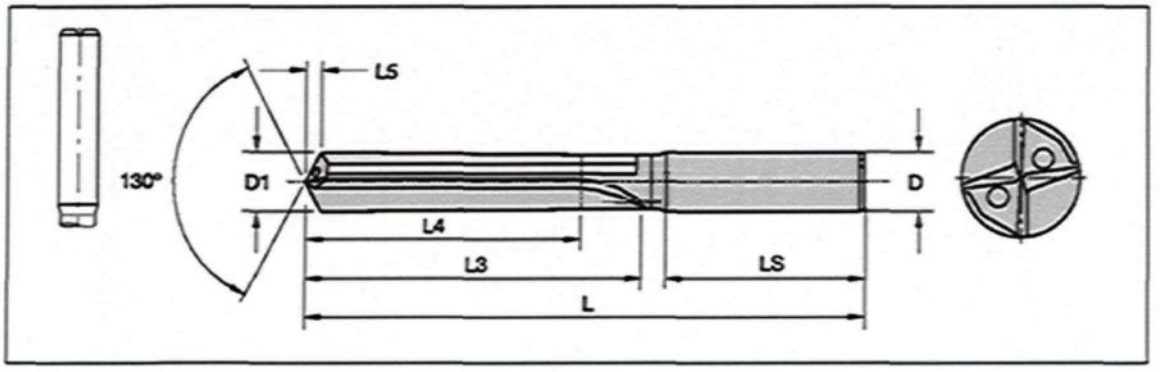


**Figure 3.7** Cobalt Grade Drill.

**Table 3.5** Cobalt Grade Drill Specifications

| Grade | High Performance |
|---|---|
| **Material** | Solid Carbide |
| **Point Type** | Self-Centering Point |
| **Drill Point (Deg.)** | 130° |
| **Drill Diameter (D1)** | 6.5 mm |
| **Shank Diameter (D)** | 8 mm |
| **Overall Length (L)** | 91 mm |
| **Flute Length (L3)** | 53 mm |
| **Drilling depth max (L4)** | 43 mm |

| | |
|---|---|
| **Shank length (LS)** | 36 mm |
| **Point length (L5)** | 1.52 mm |
| **Application** | For use on gray iron, nodular iron, aluminum, and non-ferrous workpiece materials. |

### 3.4.1.4 Solid Carbide High Precision Drill (Mapal Giga M2195-0650)

The Giga-drill, shown in Figure 3.8 with specifications listed in Table 3.6, can be used both for solid drilling and for gun boring, where two solid drilling flutes and two gun boring flutes are used to cut the material. Cutting and guiding the tool in the machined bore are the principal features of tools used for machining bores. Moreover, this drill is endowed with high dimensional stability.

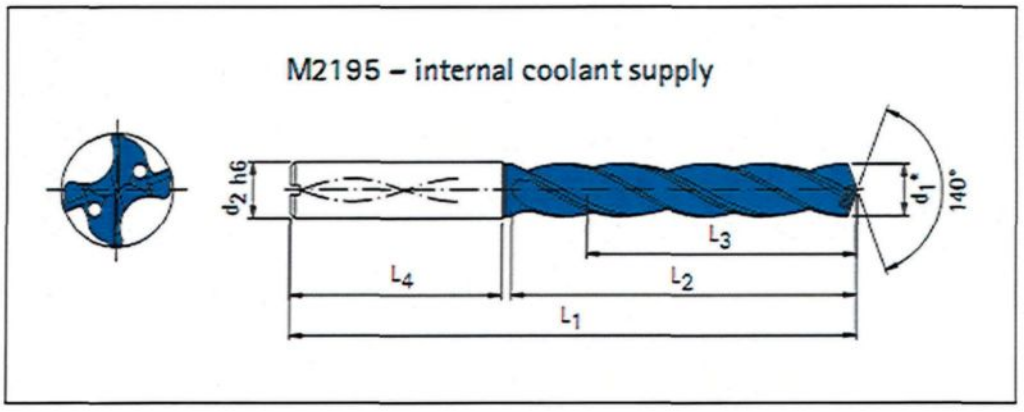


**Figure 3.8** Special Carbide High Precision Drill.

**Table 3.6** Special Carbide High Precision Drill Specifications

| Grade | High Performance |
|---|---|
| **Grade** | High Performance |
| **Material** | Solid Carbide High Precision |
| **Point Type** | Self-Centering Point |
| **Drill Point (Deg.)** | 140° |
| **Drill Diameter ($d_1$)** | 6.5 mm |
| **Shank Diameter ($d_2h_6$)** | 8 mm |
| **Total length ($L_1$)** | 91 mm |
| **Margin length ($L_2$)** | 53 mm |
| **Drilling depth max. ($L_3$)** | 43 mm |

### 3.4.2 Coolant

A synthetic metalworking fluid concentrate known as CIMTECH® 310 (5% cutting fluid + 95% liquid) was applied to avoid the effects of the heat generated during machining; this low-pH fluid is recommended for aerospace and automotive machining and grinding operations, including the creep feed grinding of ferrous or non-ferrous metals. More specifically, the metals which can be used with this coolant include wrought and cast aluminum alloys, cast and nodular iron, carbon steels, stainless steels, and titanium, among others. Figure 3.9 illustrates this coolant being used in a machining application.

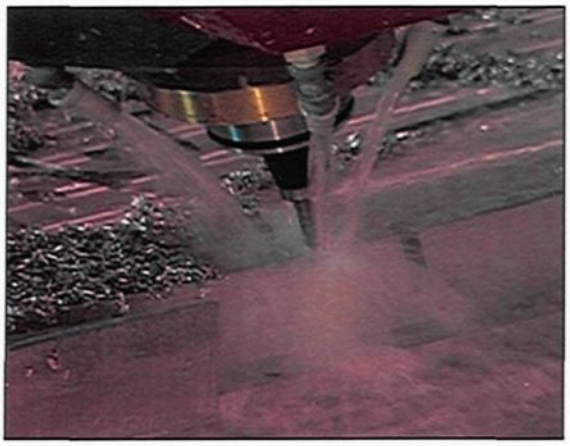

**Figure 3.9** Coolant used for machining.

### 3.4.3 Methodology for Data-Processing of Drilling

#### 3.4.3.1 Cutting Force and Moment

The following is an introduction to the force and moment calculations which are used for the evaluation of drilling and machining processes. Evaluating machinability based on the cutting forces requires adequate piezoelectric sensor technology. The piezoelectric force measuring system differs considerably from other methods of measurement. A Kistler 6-component piezoelectric quartz crystal dynamometer (model 9255B) was used for 6-component force and moment: Fx, Fy, Fz, Mx, My, and Mz measurement during drilling tests. The forces acting on the quartz crystal element are converted to a proportional electric charge. The charger amplifier converts this charge into standardized voltage and current signals, which can then be evaluated by signal processing. A Kistler multi-channel charge amplifier, type 5017B18, with 8 independent measuring channels was used in combined force and moment measurement using piezoelectric multi-component dynamometers.

Figure 3.10(a), (b), and (c) illustrate the Kistler dynamometer with four sensors as used in this study, while the schematic shows the measuring chains for the 6-component forces and moment measurements. The four sensors of the dynamometer, thus, provide eight electric charges corresponding to the values of the eight components of the cutting forces in the x, y, and z directions, namely $Fx_{1+2}$, $Fx_{3+4}$, $Fy_{1+4}$, $Fy_{2+3}$, $Fz_1$, $Fz_2$, $Fz_3$, and $Fz_4$, as shown in Figure 3.10(a). The eight output signals were fed directly to the eight charge amplifiers by the eight-core connecting cable, type 1677A5/1679A5. All signals were independently monitored and digitized, then recorded for each test block in the LabVIEW program where DynoWare software was used for force measurements and the data processing of cutting forces and moments.

The drilling moment (Mz) and feed force (Fz) are of particular interest in analyzing the drilling process and were taken into account for evaluating the effects of different alloying element additives on drilling tests. The deflective forces Fx and Fy perpendicular to the rotary axis provide additional information on the machining process. The three forces Fx, Fy, Fz and the three moments Mx, My, Mz were calculated from the 8-channel force components using the set of equations, as shown in Table 3.7.

**Table 3.7** Cable diagram and calculation equations

| **Cable types A10 Pin. N°.1677A5/1679A5/1678A5/** | **Output signals** | **Cable types A10 Pin. N°.1677A5/1679A5/1678A5/** | **Output signals** |
|---|---|---|---|
| 1 | Grounds | 6 | Z1 |
| 2 | X1 + 2 | 7 | Z2 |
| 3 | X3 + 4 | 8 | Z3 |
| 4 | Y1 + 4 | 9 | Z4 |
| 5 | Y2 + 3 | | |
| $\mathbf{Fx = Fx_{1+2} + Fx_{3+4}}$ | | $\mathbf{Mx = b\,(Fz_1 + Fz_2 - Fz_3 - Fz_4)}$ | |
| $\mathbf{Fy = Fy_{1+4} + Fy_{2+3}}$ | | $\mathbf{My = a\,(-Fz_1 + Fz_2 + Fz_3 - Fz_4)}$ | |
| $\mathbf{Fz = Fz_1 + Fz_2 + Fz_3 + Fz_4}$ | | $\mathbf{Mz = b\,(-Fx_{1+2} + Fx_{3+4}) + a\,(Fy_{1+4} + Fy_{2+3})}$ | |

where a = 80mm is the distance of the sensor axes from the X-axis; and b = 80mm is the distance of the sensor axes from the Y-axis, as shown in the Figure 3.10 (a). In general, a 6-component measuring system provides the following results:

- The 3 components of the resultants of all applied forces, including their direction but not their location in space;
- The 3 components of the resulting moment vector related to the coordinate origin.

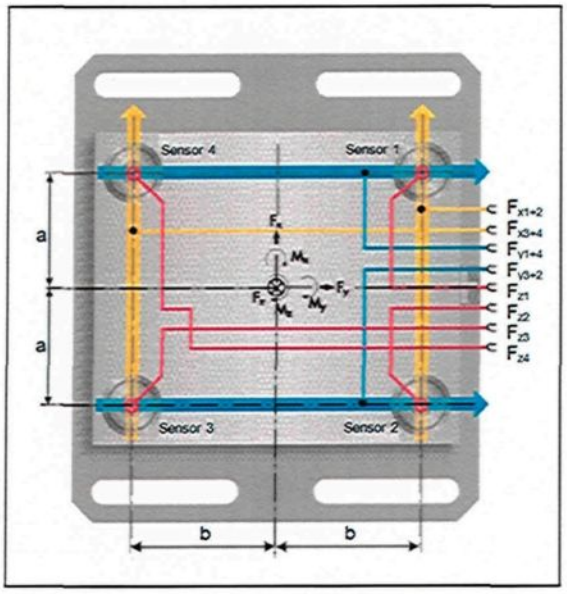


a)

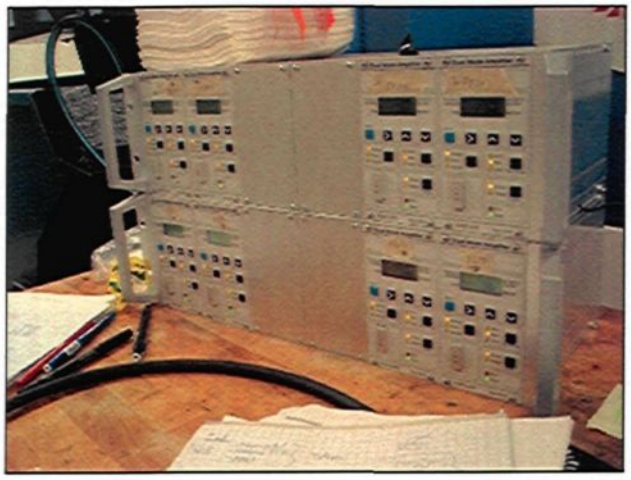

b)

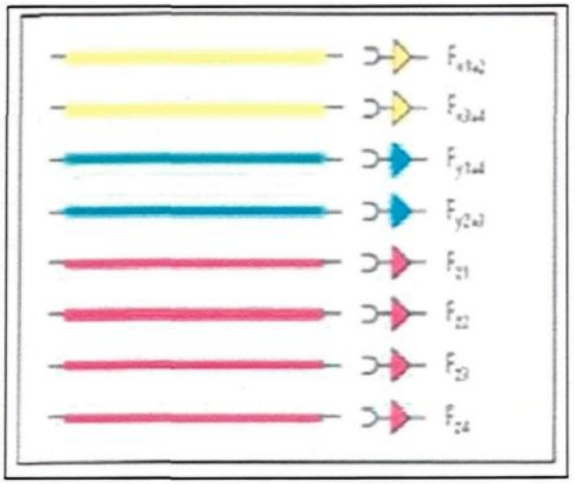

c)

**Figure 3.10** Kistler 6-component electronic dynamometer: (a) dynamometer with the four sensors as well as the measuring chains for the 6-component force and moment measurements, (b) 8-core connecting cables as well as 8 charge amplifier channels, and (c) 8-component channels.

MatLab programs were developed specifically for processing the drilling data related to all the conditions studied in the present work; these programs are similar to those produced in an earlier study on the machining behavior of 356 and 319 alloys carried out by Tash[5] from our research group. Complete details of these programs may be found in Appendix B of his PhD thesis.[5] The data were first separated according to each component of force and moment, followed by the application of a signal processing procedure for calculating the value of force and moment. The sampling rate of these charges or force is 1000Hz which implies that each force component is measured at each 0.001s of the drilling test; 1600 sample points per cycle were acquired for calculating the mean value of the cutting feed force (Fz) and 1200 sample points per cycle for the other five components of force and moment Fx, Fy, Mx, My, and Mz in each signal of 72 cycles or holes per signal.

Any error was taken into consideration and incorporated into the MatLab drilling program for the six-component force and moment by using the following equations:

$$mFx = Fx_{up} - Fx_{down};$$

$$mFy = Fy_{up} - Fy_{down};$$

$$mFz = Fz_{up} - Fz_{down};$$

$$mMx = Mx_{up} - Mx_{down};$$

$$mMy = My_{up} - My_{down};$$

$$mMz = Mz_{up} - Mz_{down}.$$

### 3.4.3.2 Measurement of Total Cutting Force and Moment

The MatLab output results for all components of force and moment for drilling tests were transferred onto an Excel data sheet, followed by calculations to obtain the total cutting force and moment which were used as a means for evaluating the drilling process in this study. The calculations were carried out using the following equations:

$$F_t = (F_x^2 + F_y^2 + F_z^2)^{1/2}$$

$$M_t = (M_x^2 + M_y^2 + M_z^2)^{1/2}$$

### 3.4.3.3 Chip Form, Built-up Edge (BUE), and Hole Size

The chips during the drilling tests were collected for each sample block tested with the purpose of examining their size and shape after drilling. A Go/No-Go gauge test was periodically carried out and was taken as the assessment of dimensional accuracy control for the drilled holes. Holes were checked at the end of the hole-drilling stage in the sample block, *i.e.* after 144 holes. Reference diameters of 6.5024 – 6.5278 mm of the Go/No-Go gauge test were used for the drilling processes, respectively. The built-up edge (BUE), or in other words, the thickness of the aluminum layer accumulated on the cutting tool edge, was measured using a Toolmaker's microscope, TM-505 type, at 30x magnification, as shown in Figure 3.11.

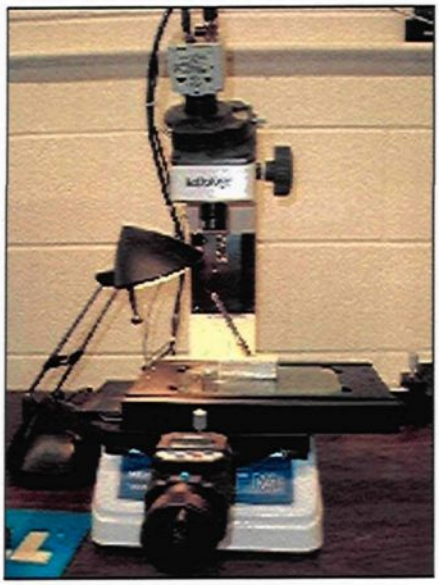

**Figure 3.11** TM-505 Type Toolmaker's Microscope.

# CHAPTER 4

# RESULTS AND DISCUSSION

# CHAPTER 4

# RESULTS AND DISCUSSION

## 4.1 INTRODUCTION

In order to carry out this project, Al-Si-Cu-Mg alloys belonging to the Al-Si alloy system were selected and represented, respectively, by 396 (G2 and G3) and B319.2 (G12) alloys. These alloys contain mainly $\alpha$-Fe, $\beta$-Fe, and sludge, free-cutting elements, such as Sn, and display related hardness levels of 110±10 HB. Owing to the high demand for these alloys in the automobile and aerospace industries, drilling operations were carried out under fixed machining conditions to study the machining performance of these same alloys by investigating the following:

(i) a metallographic study with the intention of identifying the phases contained in the microstructure, such as the eutectic silicon phase and iron-rich intermetallic phases;

(ii) mechanical properties, specifically tensile and hardness properties; and

(iii) machinability as the main focus of the study including:

a. total drilling force and moment,

b. tool life,

c. built-up edge (BUE), and

d. chip characterization.

It should be mentioned here that the iron intermetallic phases and the eutectic silicon particle morphology, size, shape, and distribution, are the main parameters which control the mechanical properties of the 396 and B319.2 alloys. Acquiring an understanding of these parameters would contribute to selecting the conditions necessary to achieve optimum drill and machining conditions for maximum productivity at high speeds. The results obtained will be discussed in the following subsections.

## 4.2 MICROSTRUCTURAL CHARACTERIZATION AND MECHANICAL PROPERTIES

From the point of view of microstructure, Al-Si casting alloys depend on the chemical composition of the alloy, the casting process used, and the heat treatment applied. Alloys 396 and B319.2 are popular Al-Si casting alloys used extensively by the automotive and aerospace industries mainly for their high strength and ductility. In the context of this research study, the main focus has been on the machinability of these alloys (containing 10.8%Si and 7.5%Si) with a view to optimizing their machining characteristics and, hence, productivity. It was also thought worthwhile to show the effects of Fe-intermetallics, namely $\alpha$-Fe, $\beta$-Fe, and sludge together with the effects of free-cutting elements, such as Sn, on the microstructure and mechanical properties in relation to the tensile properties and hardness of these alloys.

A metallographic study was conducted using samples which had been sectioned from the heat-treated machinability test block, with the aim of examining the specific changes resulting from additions of 0.15%Sn to the G2 and G12 alloys, and 0.25%Fe + 0.25%Mn to the G3 alloy. Optical microscopy was used to characterize the effects of Fe-intermetallics and free-machining elements on the microstructure of the alloys investigated. Samples measuring 25mm x 25mm for metallographic examination were sectioned from the machinability test sample and mounted in bakelite using a Struers Labopress-3 Mounting Press. These samples were then ground and polished to the desired fine finish on 9, 6, 3, and 1μm diamond lap wheels. After that, the microstructure was examined using a Leica DMLM optical microscope.

The eutectic silicon-particle characteristics, including particle area, length, roundness (%), aspect ratio, and density (particles/mm$^2$) were measured and quantified using a Clemex image analyzer system in conjunction with the optical microscope. For each sample, 50 fields were examined at a magnification of 200x in such a way as to cover the entire sample surface in a regular and systematic manner. The results obtained were analyzed in detail in order to grasp the influence of the relevant additives on the machinability behavior.

### 4.2.1 Silicon Particle Characteristics

The microstructure of Al-Si alloys, in this case the 396 and B319.2 alloys, is typically composed of an aluminum matrix containing eutectic silicon which may be present in the form of acicular needles and plates, or a refined fibrous structure, depending

upon the level of chemical modification and the cooling rate of the cast section. The machining characteristics of Al-Si cast alloys depend on the chemical composition, in particular, on microstructural features such as the shape, size, and morphology of the eutectic silicon particles, the dendrite morphology of $\alpha$-Al, as well as the morphology and amount of other intermetallics namely $\alpha$-Fe, $\beta$-Fe, and sludge, which are also present in the microstructure.

The percentage of Si in Al-Si alloys together with the shape and distribution of the silicon particles all play an important role in determining the machinability characteristics of cast Al-Si alloys. The microstructure of the modified grain-refined and T6 heat-treated G2 and G12 alloys, containing Al-10.8%Si and Al-7.5%Si, may be observed in Figures 4.1(a) and (b) which show the effects of Sn addition. Table 4.1 summarizes the eutectic Si-particle characteristics obtained from quantitative measurements of the alloys investigated with respect to additions. It will be observed that the addition of 0.15%Sn to the G2 and G12 alloys leads to a slight coarsening of the eutectic Si particles, as may be observed in Figure 4.1(a) and (b), and from the data listed in Table 4.1.

As Figure 4.1(a) and (b) show, the eutectic silicon particles are not uniformly distributed, but tend to be concentrated at the interdendritic boundaries. Both of the Fe-containing phases, *i.e.* $\alpha$-$Al_{15}(Fe,Mn)_3Si_2$ or *Chinese script*, and the needle-like $\beta$-$Al_5FeSi$, as well as the Cu-containing phases, mainly $Al_2Cu$, are seen to nucleate within the matrix or at the interface of such preexisting constituents as Si or intermetallic particles. [31, 32, 61]

**Table 4.1** Summary of eutectic Si-particle measurements for the alloys studied

| Alloy code | Particle Area (μm2) | | Particle Length (μm) | | Roundness Ratio (%) | | Aspect Ratio | | Density (particles/mm2) |
|---|---|---|---|---|---|---|---|---|---|
| | Av | SD | Av | SD | Av | SD | Av | SD | |
| **G2** | 17.07 | 18.60 | 8.16 | 6.68 | 39.97 | 20.83 | 2.76 | 1.65 | 41071 |
| **G3** | 9.10 | 12.10 | 4.87 | 4.12 | 51.60 | 20.90 | 2.02 | 1.06 | 67114 |
| **G12** | 7.44 | 10.60 | 4.33 | 3.73 | 60.00 | 18.90 | 2.07 | 1.05 | 12000 |

The morphology and size of the eutectic Si particles, together with the precipitation-hardening phases during heat treatment, all have an important influence on machining properties. It was found that the addition of Sn elicits similar behavior from both 396 and B319.2 alloys, where the addition of 0.15%Sn has little influence on the eutectic Si particles. The size, shape, and distribution of free-machining particles, in this case Sn, are of major importance in the machining of Al-Si casting alloys. The iron precipitates in the form of a coarse $\alpha$-Fe phase, which is always seen to occur within the $\alpha$-Al dendrites, indicating that it corresponds to a predendritic reaction, and thus tends to nucleate in the liquid alloy prior to solidification.

The copper phase may be seen represented by small pockets of the blocklike $Al_2Cu$ phase nucleating either within the aluminum matrix, or at the interface of pre-existing phases such as Si or intermetallic particles.[26, 61, 62] Concerning the precipitation of Sn in the form of $\beta$-Sn particles, the latter are observed in the form of black phase particles in Figure 4.1(a) and (b).

Figure 4.1 also illustrates how an increase in the level of Mg and Cu hinders the modifying effect of Sr, when these elements are added to the Sr-modified alloys, considering that certain Si areas are fully modified, whereas others are only partially modified. This observation is in satisfactory agreement with reports by Joenoes and Gruzleski *et.al.*,[25, 63] by Moustafa,[64] and by Paray *et al.*[65] who observed that about 1%Mg has a slightly refining effect on the Si phase and a negative effect on strontium modification, that is to say, it changes the microstructure from a well-modified to a partially modified one, due to the presence of both Mg and Cu which react with the Si and Sr present in the alloy to form $Mg_2Sr(Si,Al)$ and Al-Cu-Sr compounds, respectively.

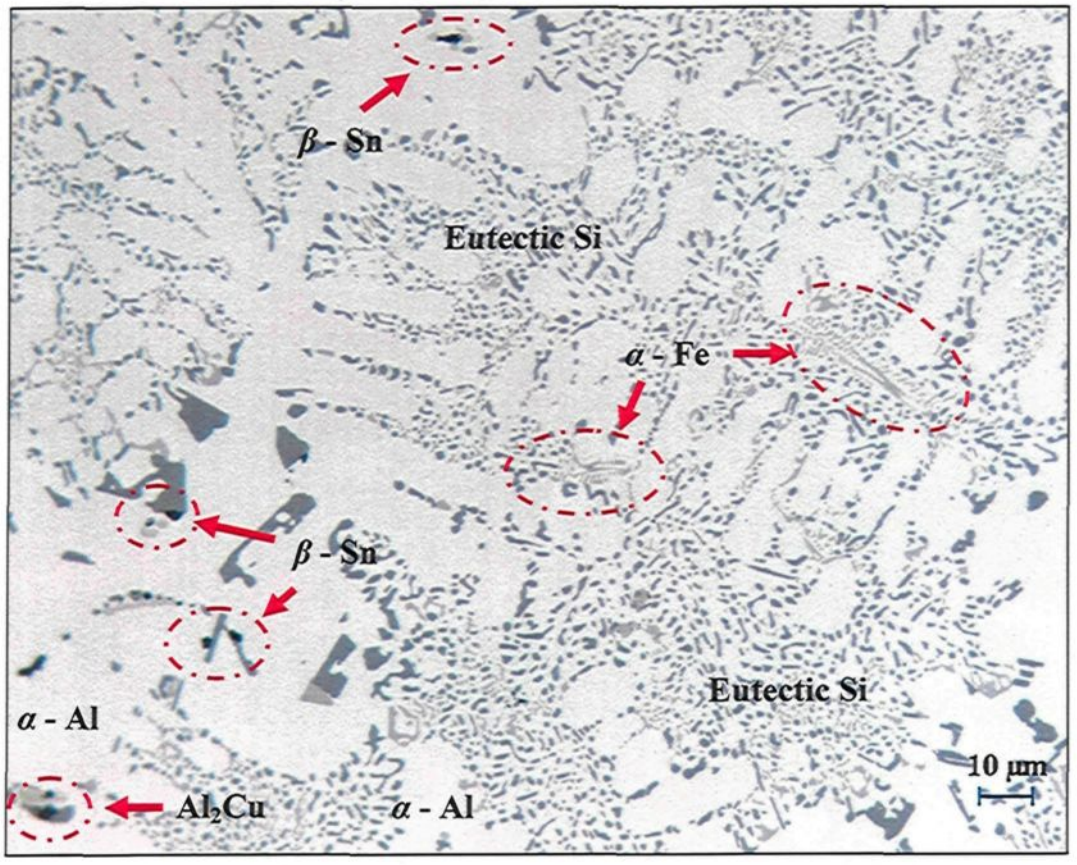


(a)

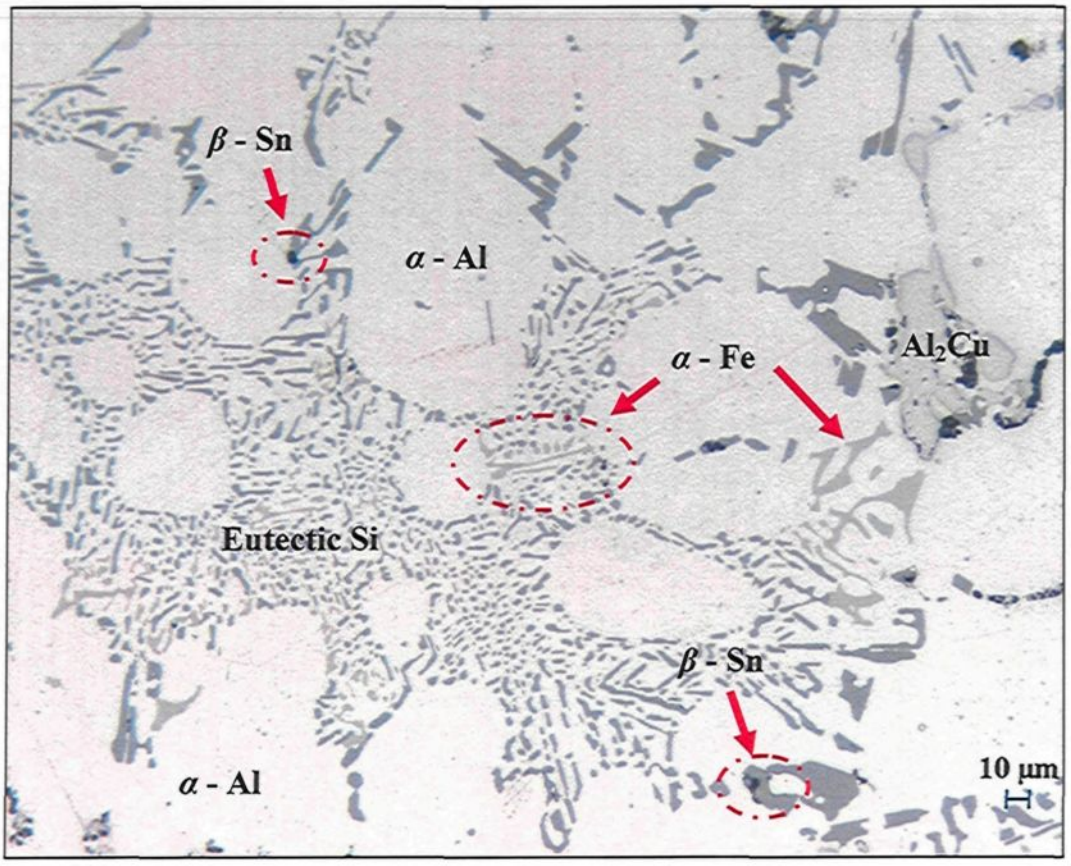


(b)

**Figure 4.1** Optical micrographs showing the effects of Sn on Si morphology in grain-refined and heat-treated (a) G2 alloy, and (b) G12 alloy.

The Fe-content of the alloy is a significant consideration from the point of view of microstructure. The correct identification of the comparatively coarse Fe-rich intermetallic phases generally found in Al-Si casting alloys is also of major importance, since some of these phases are associated with reduced mechanical properties. The most important of the AlFeSi intermetallics are generally considered to be the $\alpha$-Fe phase, the $\beta$-Fe phase, and the sludge intermetallic phase. Figure 4.2 shows the microstructure of the G3 alloy in which

the $\alpha$-Fe phase appears in the form of small *Chinese-script* particles interspersed with Si particles; this observation indicates that the $\alpha$-Fe particles had previously precipitated in co-eutectic or post-eutectic reactions.

The conditions which influence the formation of the $\alpha$-Fe phase, as opposed to the $\beta$-Fe phase, are still not completely understood; moreover the formation of the $\alpha$-Fe phase reduces the possibility of the formation of the $\beta$-Fe phase. The $\alpha$-Fe phase may be precipitated either in the *Chinese-script* form, or else as compact polygonal or star-like particles termed sludge with a composition close to that of the $\alpha$-Fe phase.

Sludge precipitation depends principally on the levels of Fe, Mn, and Cr present in the alloy, as well as on the processing parameters, which include the melt holding temperature, pouring temperature, melt additives, and cooling conditions.[37] The G3 alloy being studied, including the addition of iron and manganese, reveals that the Al(Fe,Mn)Si primary particles which precipitate directly from the liquid display a predominantly polyhedral or star-like form, and appear to be located within the $\alpha$-Al dendrites.

The composition of the $\alpha$-Fe phase is $Al_8Fe_2Si$ (31.6%Fe, 7.8%Si) and $Al_{12}Fe_3Si_2$ (30.7%Fe, 10.2%Si) with a probable composition range of 30-33% Fe and 6-12%Si.[30, 34] The $\alpha$-Fe phase is reported as having a hexagonal structure with the parameters a=12.3 Å, c=26.3 Å, and a density of 3.58 g/cm$^3$. The platelet-like $\beta$-Fe phase was not in evidence because of the higher Mn/Fe ratio in the G2 alloy of ~1.04; this ratio promotes the formation of the $\alpha$-Fe phase at the expense of the $\beta$-Fe phase.[35] The $\alpha$-Fe phase may precipitate either in the form of the *Chinese-script* phase or else as compact polygonal or

star-like particles termed *sludge* with a composition close to that of the $\alpha$-Fe phase. This sludge precipitation depends upon the levels of Fe, Mn, and Cr present in the alloy, and the processing parameters which include melt holding temperature, pouring temperature, melt additives, and cooling conditions.[37] The presence of hard sludge particles within the soft $\alpha$-Al dendrites should lead to a more uniform distribution of the stresses throughout the alloy matrix and, hence, to improved mechanical properties. Thus, the precipitation of sludge particles need not necessarily be harmful to the alloy, as is commonly perceived in the literature, where the sludge particles may usually be observed in the interdendritic regions.

This phenomenon of iron intermetallic precipitation within the $\alpha$-Al dendrites proves extremely useful in the case of such Al-Si die-casting alloys as the 380 alloy, containing 9%Si, where the proportion of $\alpha$-Al dendrites is relatively higher.[66]

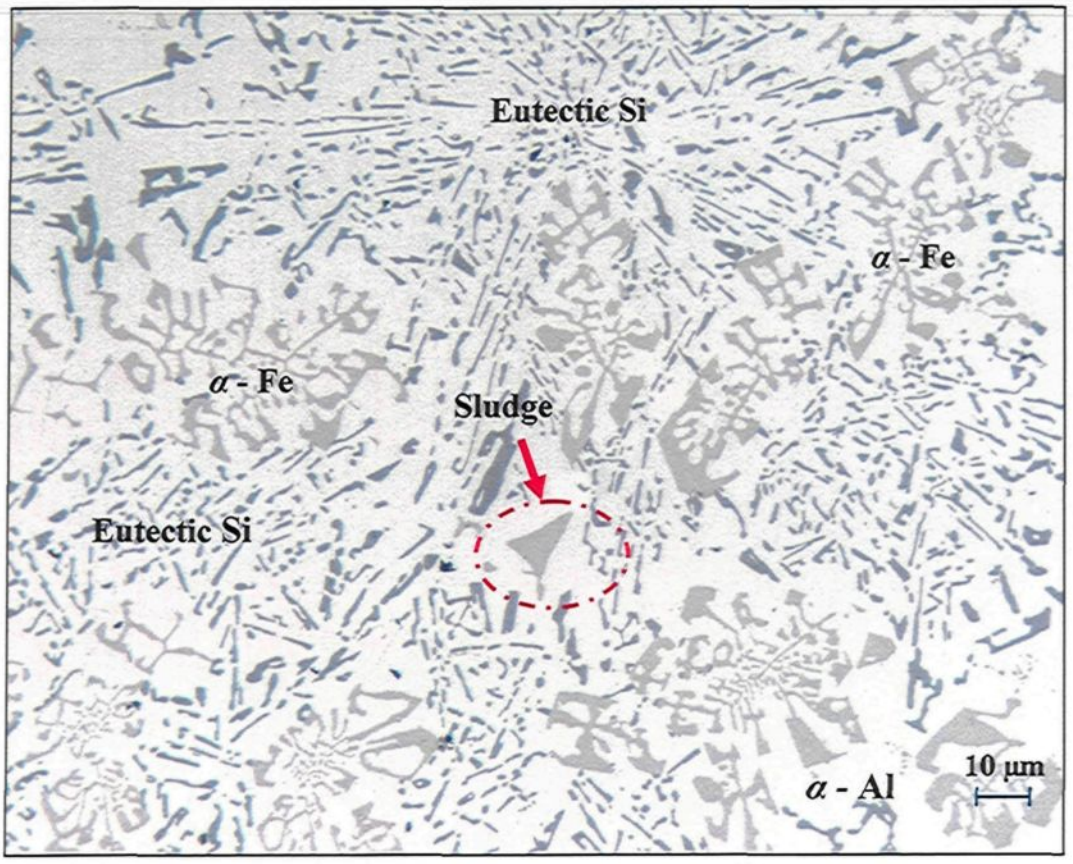


**Figure 4.2** Optical micrograph showing the sludge particles observed in the Sr-modified and grain-refined G3 alloy.

Table 4.2 also provides the volume-fraction measurements of Fe-intermetallics and undissolved $Al_2Cu$ phase in G3 alloy. It was reported in previous works [5, 32, 61] that the volume fraction of Fe-intermetallics increased with the addition of increasing levels of Fe and/or Mn addition to the 396 and B319.2 alloys.

**Table 4.2** Volume fraction of Fe- and Cu-intermetallics for the G3 alloy studied [61]

| Alloy Code | Volume Fraction (%) | |
|---|---|---|
| | **Fe-intermetallics** | **Undissolved Cu-intermetallics** |
| **G3** | 4.98 ± 0.71 | 0.22 ± 0.12 |

### 4.2.2 Hardness and Tensile Property Values

Hardness and tensile properties represent some of the most important metallurgical parameters influencing alloy machinability; furthermore, aluminum alloys differ from many other metals in the context of machinability. Most automotive machine shops agree that a minimum hardness number of 80 BHN is desirable in the case of aluminum castings.

Hardness and tensile property measurements are relevant to the evaluation of the changes occurring in the aluminum matrix and eutectic silicon due to the addition of alloying elements and to use of modification and grain refinement melt treatments. Heat treatment is yet another significant factor used to enhance the mechanical properties and machinability of cast Al-Si alloys. Heat treatment thus tends to increase the hardness values, to reduce the built-up edge (BUE) on the cutting tool, and to improve the surface finish of the machined part. Drilling forces are proportional to the hardness of the alloy and the feed rate. [5]

The T6 heat treatment was selected to establish the hardness level for the alloys investigated within the range of 110 ± 10 BHN. Hardness measurements were carried out

on the heat-treated machinability test blocks to ensure that they possessed the required hardness levels.

Tensile testing is important in the assessment of the changes occurring in the aluminum matrix and eutectic silicon as a result of the addition of alloying elements. Table 4.3 provides the relevant data relating to T6 heat-treated mechanical properties; these include the hardness (BHN), yield strength at 0.2% offset strain (YS), ultimate tensile strength (UTS), and percent elongation (%El) of the 396 and B319.2 alloys.

**Table 4.3** Summary of mechanical properties for the alloys studied [61]

| Alloy Code | BHN (MPa) | YS (MPa) | UTS (MPa) | El (%) |
|---|---|---|---|---|
| **G2** **396 + 0.15%Sn** | 106 ± 3.19 | 351.65 ± 2.57 | 390.54 ± 5.73 | 1.02 ± 0.15 |
| **G3** **396 + 0.25%Fe + 0.25%Mn** | 111 ± 4.39 | 326.84 ± 2.13 | 354.72 ± 4.86 | 0.84 ± 0.04 |
| **G12** **B319.2 + 0.15%Sn** | 108 ± 3.39 | 392.83 ± 3.48 | 404.08 ± 3.75 | 0.77 ± 0.03 |

## 4.3 MACHINABILITY EVALUATIONS

The purpose of the subsequent sections is to present the results obtained from the drilling incurred in the process of this work for the two types of alloys studied, namely, 396 and B319.2, using the solid carbide drill, the special solid carbide, the cobalt grade, and the high precision solid carbide drills. The alloys in question were individually represented by the codes G2: 396 + 0.15%Sn; G3: 396 + 0.25%Fe + 0.25%Mn; and G12: B319.2 +

0.15%Sn; these alloy compositions were selected in order to study the effects of the addition of Sn and those of the Fe-intermetallics, namely $\alpha$-Fe, $\beta$-Fe, and sludge on the machinability characteristics displayed by said alloys. The upcoming sections will discuss the machinability behavior of the alloy conditions investigated in this work with respect to (a) the total cutting force and moment, (b) tool life expressed as the number of holes drilled up to the point of tool breakage, (c) chip configuration, and (d) built-up edge (BUE) evolution.

The drilling process for each test block was accomplished in such a way that the 35 holes, of 6.5 mm diameter each, which were drilled per rib were arranged in two columns of 18 holes per rib, giving a total of 36x4 or 144 holes drilled per test block. An example of a machinability test block, after 144 holes had been drilled, is shown in Figure 4.3(a), while the dimensions of the resulting holes are provided in Figure 4.3(b). For each machinability block tested, the drilling test was carried out in two stages: ribs 1 and 2 covering 72 holes, followed by ribs 3 and 4 covering the remaining 72 holes, as shown in Figure 4.3(a). It should be mentioned here that the middle rib was not included in the drilling tests, since this rib invariably tended to show shrinkage porosity which would affect the validity of the results. In carrying out these tests, it was found that it was possible to obtain two different results for the total drilling force and moment for each set of 72 holes.

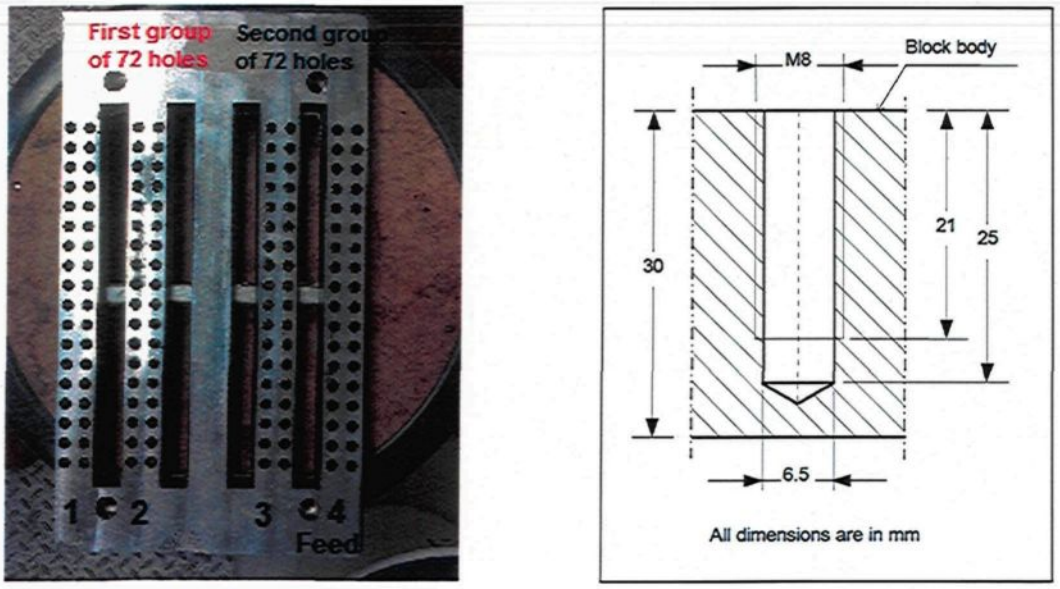


(a) (b)

**Figure 4.3** (a) Machinability test block after drilling; (b) dimensions of the resulting holes.

Machinability is a phenomenon of the interaction between the workpiece (material type and form), the cutting tool (material type and geometry), and the cutting medium (air or liquid) in a number of different removal sequences (turning, drilling, tapping, milling, sawing, *etc.*) and cutting conditions (speed, feed, and depth of cut). Since the machinability response is known to be different for different operations and operating conditions, machinability should probably be viewed as an interaction of the above-mentioned parameters, rather than as a property of the alloy. In a collective sense, the most important terms relating to machinability are:

- tool life, wear level, and fracture probability;
- specific power consumed, forces, and temperature increase;

- chip control (chip breakability, chip shape, and built-up edge);
- dimensional tolerances in terms of surface roughness, microstructure, and burr formation;
- work requirement (machining rate); and
- overall cost.

The machinability criteria relate to forces and moments analysis as well as to tool life, chip configuration, and built-up edge (BUE) evolution. In the present study, the drilling tests were carried out under fixed machining conditions of speed, feed, depth of hole drilled, tool geometry, tool material, and coolant used.

### 4.3.1 Evaluation of Cutting Forces and Moments: Effects of Alloy Material

In this section, it is necessary to stress the relevance of evaluating the total drilling force and moment of the value of 72 holes (36 holes per rib), and 144 holes per test block, as well as the possible impact that the effects of the addition of Sn and the Fe-intermetallics, namely $\alpha$-Fe, $\beta$-Fe, and sludge, may have on the drilling process. The effects of Sn on drilling, as well as on the force and moment of the G2: 396 + 0.15%Sn and the G12: B319.2 + 0.15%Sn alloys are shown in Figure 4.4 (a) and (b), and Figure 4.5 (a) and (b), respectively. Figure 4.6 (a) and (b) shows the results for alloy G2: 396 + 0.25%Fe + 0.25%Mn containing mainly Fe-intermetallics.

With regard to machinability drilling results, it was found that the total drilling force and moment increase with the number of holes drilled. The machining characteristics of the Al-10.8%Si alloy *i.e.* the 396 alloy, depend mainly on the shape, size, and distribution of $\alpha$-

Al dendrites, eutectic Si morphology, and $Al_2Cu$ particles in the interdendritic regions. From the machinability point of view, a material having high yield strength, *i.e.* sufficient force required per unit area to create permanent deformation, necessitates a high level of force to initiate chip formation during machining operations.[61] It should also be noted that a higher number of holes drilled can cause several fluctuations to appear in the total drilling force and moment values.

The addition of Sn to the 396 and B319.2 casting alloys in small amounts of ~0.15%, thereby producing the G2 and G12 alloys, significantly improves the machinability characteristics of these alloys in comparison with the G3 alloy which, with additions of 0.25%Fe and 0.25%Mn, contains $\alpha$-Fe and sludge intermetallic phases. It is necessary to take into account the fact that the rapid increase in the drilling force and moment in conjunction with the progress of the cutting process during the machining of the G2 alloy which contains 10.8%Si and 2.3%Cu may be attributed to the presence of the greater amount of silicon phase present in the alloy, which makes the alloy harder than the G12 alloy which contains 7.5%Si and 3.6%Cu. This difference is reflected in the microstructure which shows much larger regions of Al-Si eutectic in the 396 alloy.

The 396 and B319.2 alloys yield hardness values of 106 and 108 BHN, respectively. During drilling tests, it was found that the G2 alloy, containing 0.15%Sn and 10.8%Si, displayed the same number of holes drilled as did the G12 alloy, which contains the same percentage of Sn but a 7.5%Si content, as both alloys were observed to fulfill the test limit of obtaining 2016 drilled holes over the 14 machinability blocks tested for each alloy. The

lower ductility displayed by both alloys due to the presence of Sn, decreases drill-chip friction which in turn decreases the cutting force and moment, in comparison with G3 alloy which contains $\alpha$-Fe and sludge intermetallic phases, and presents a greater number of fluctuations in the results. These effects may be observed in Figure 4.4 and 4.5 for the G2 and G12 alloys; and in Figure 4.6 for the G3 alloy.

It may be assumed that Sn presents a lubricating effect in the drilling process, in relation to the fact that the addition of Sn as a free-cutting element with its low melting-point allows it to act as a lubricant, thereby decreasing the friction between chip and tool edge which tends to decrease the ductility of the material in the cutting zone, causing, in turn, a reduction in drilling force and moment during the cutting process. These conclusions are in satisfactory agreement with the results obtained by Smolej *et al.*[43, 67] who substituted Pb and Pb + Bi with Sn in the standard AA2030 and AA2011 alloys, respectively. It has been reported that, as a result of the extremely limited solubility of the Sn particles in the Al-matrix, these particles remain as separate entities dispersed in the matrix; during machining operations, the temperature generated in the cutting zone is frequently high enough to soften or even to melt these dispersed entities. Consequently, this melting gives rise to a local loss of material strength and ductility which in turn leads to the formation of broken chips. Preferably, the total addition of one or more of such lubricating elements should not exceed about 2 wt% of the casting in such a way as not to alter the other properties of the casting to any significant degree. Young [46] reported that bismuth and/or tin are the additives preferred by most researchers. Subhasish [68] noted that if the amount of the

additive is not high enough, such low melting point constituents will be too dispersed to have any significant impact on machinability.

It is thus clear that amounts of Mg-content of about 0.3% improve the machinability and tool life, producing the lowest cutting force and moment, and lowering the high number of holes drilled. These observations are in satisfactory agreement with those of Jorstad, [3, 4] who reported that a small addition of Mg, of about 0.3%, in Al-Si-Cu alloys hardens the alloy but does not increase abrasiveness since it does not contribute in any way to the formation of hard intermetallic phases.

The effects of free-machining elements may be interpreted by an examination of the alloy microstructure, as discussed previously in section 4.2.1 together with an analysis of the existing bibliographic data regarding the effects of these elements on the machinability of the alloys. Thus, the factors involved in reducing the drilling force and moment for the free machining alloys may be considered in terms of the free-cutting elements having a limited solubility in the aluminum solid solution, and of their forming soft, low melting-point phases, supporting chip breakage and lubricating the tool. Moreover, the low melting-point elements act as a lubricant during machining, thereby decreasing the friction between chip and tool edge which then results in a reduction of the cutting forces.

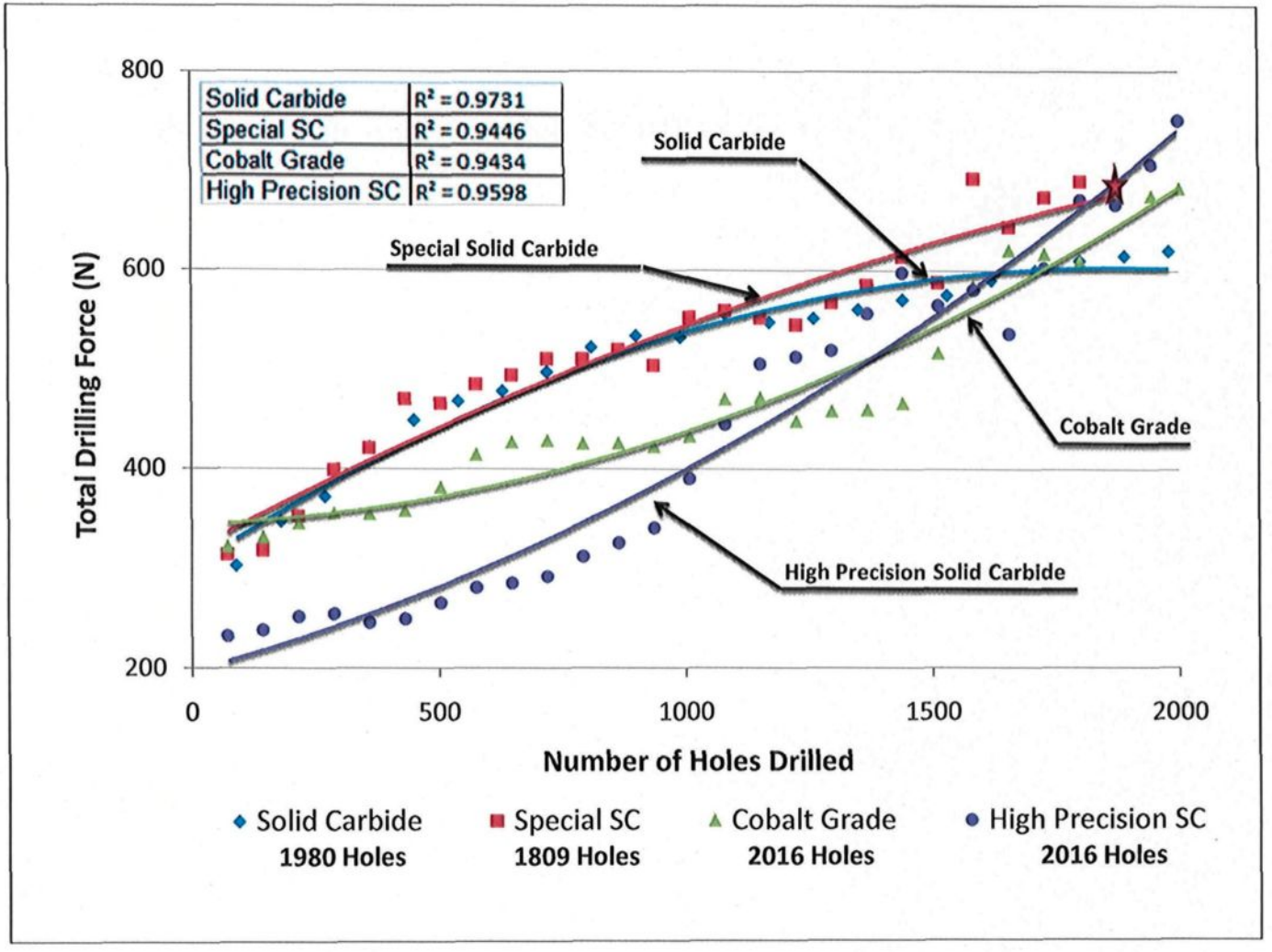
Solid Carbide R² = 0.9731
Special SC R² = 0.9446
Cobalt Grade R² = 0.9434
High Precision SC R² = 0.9598
Solid Carbide
Special Solid Carbide
Cobalt Grade
High Precision Solid Carbide
Total Drilling Force (N)
800
600
400
200
0
500
1000
1500
2000
Number of Holes Drilled
Solid Carbide 1980 Holes
Special SC 1809 Holes
Cobalt Grade 2016 Holes
High Precision SC 2016 Holes

**Figure 4.4 (a)**

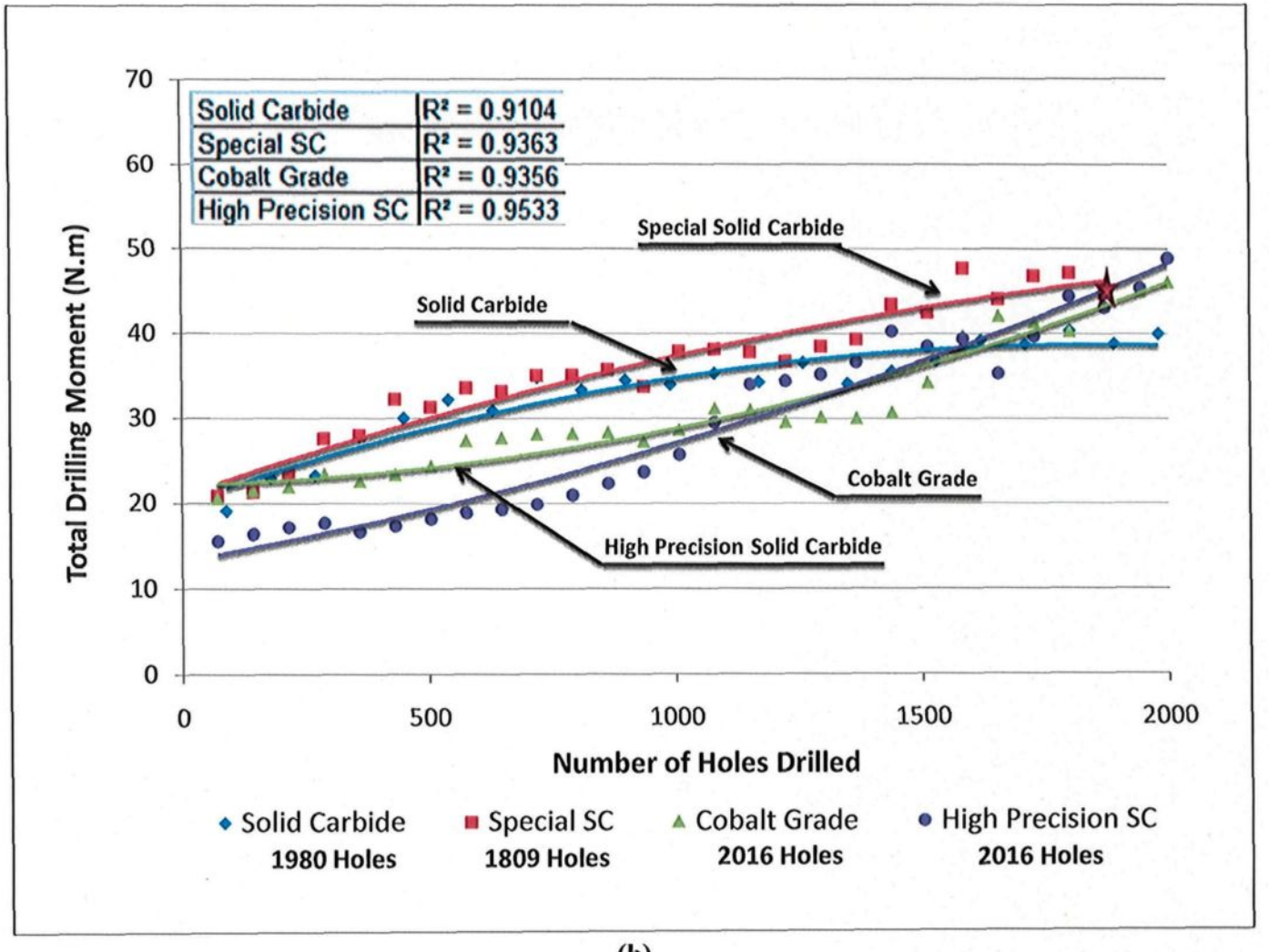


**(b)**

**Figure 4.4** Effects of Sn on the machinability of G2 alloy (396+0.15%Sn) in terms of (a) total drilling force, and (b) total drilling moment required for drilling 72 holes.

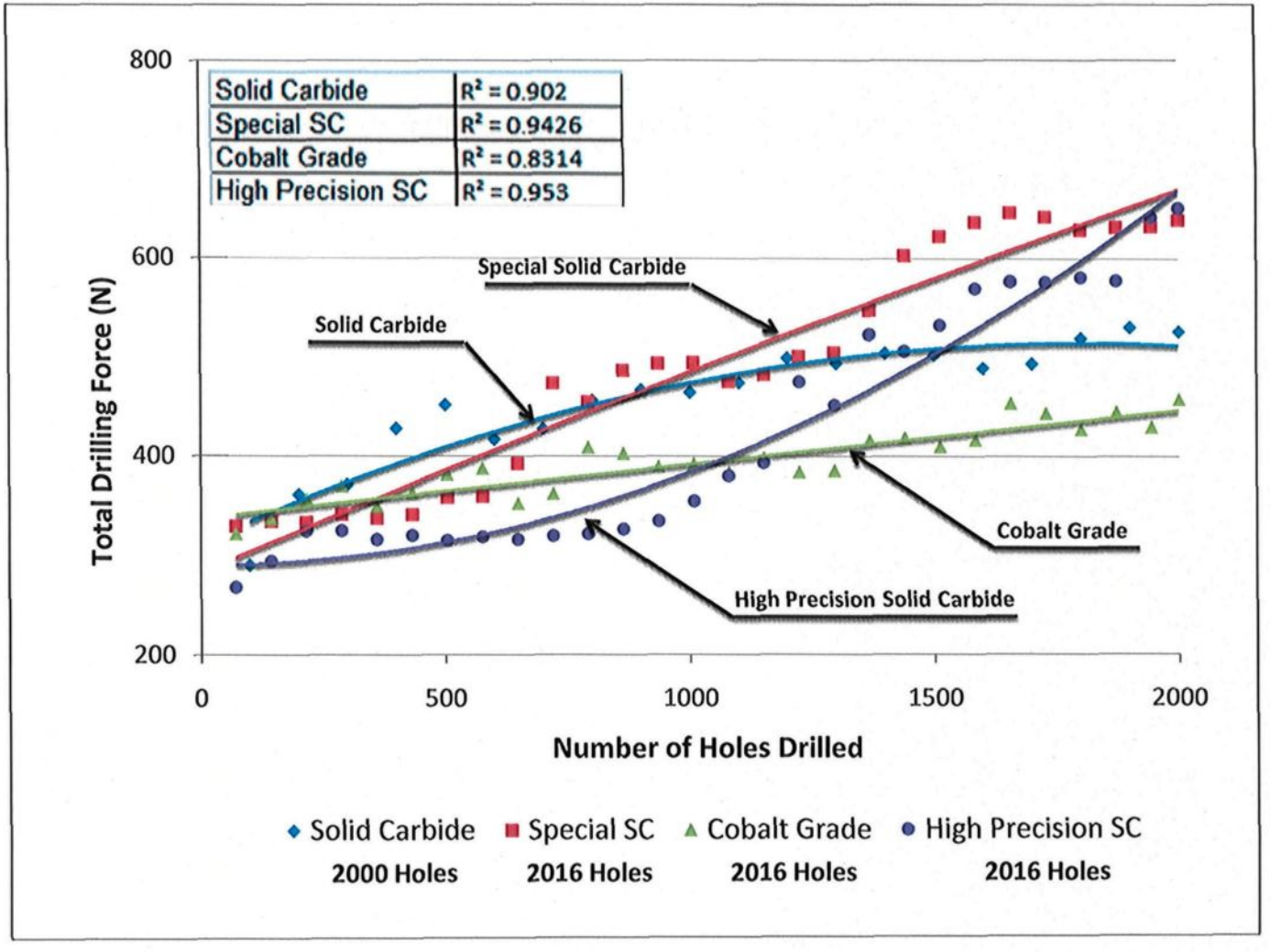
Solid Carbide R² = 0.902
Special SC R² = 0.9426
Cobalt Grade R² = 0.8314
High Precision SC R² = 0.953
Special Solid Carbide
Solid Carbide
Cobalt Grade
High Precision Solid Carbide
Total Drilling Force (N)
800
600
400
200
0
500
1000
1500
2000
Number of Holes Drilled
Solid Carbide 2000 Holes
Special SC 2016 Holes
Cobalt Grade 2016 Holes
High Precision SC 2016 Holes

**Figure 4.5 (a)**

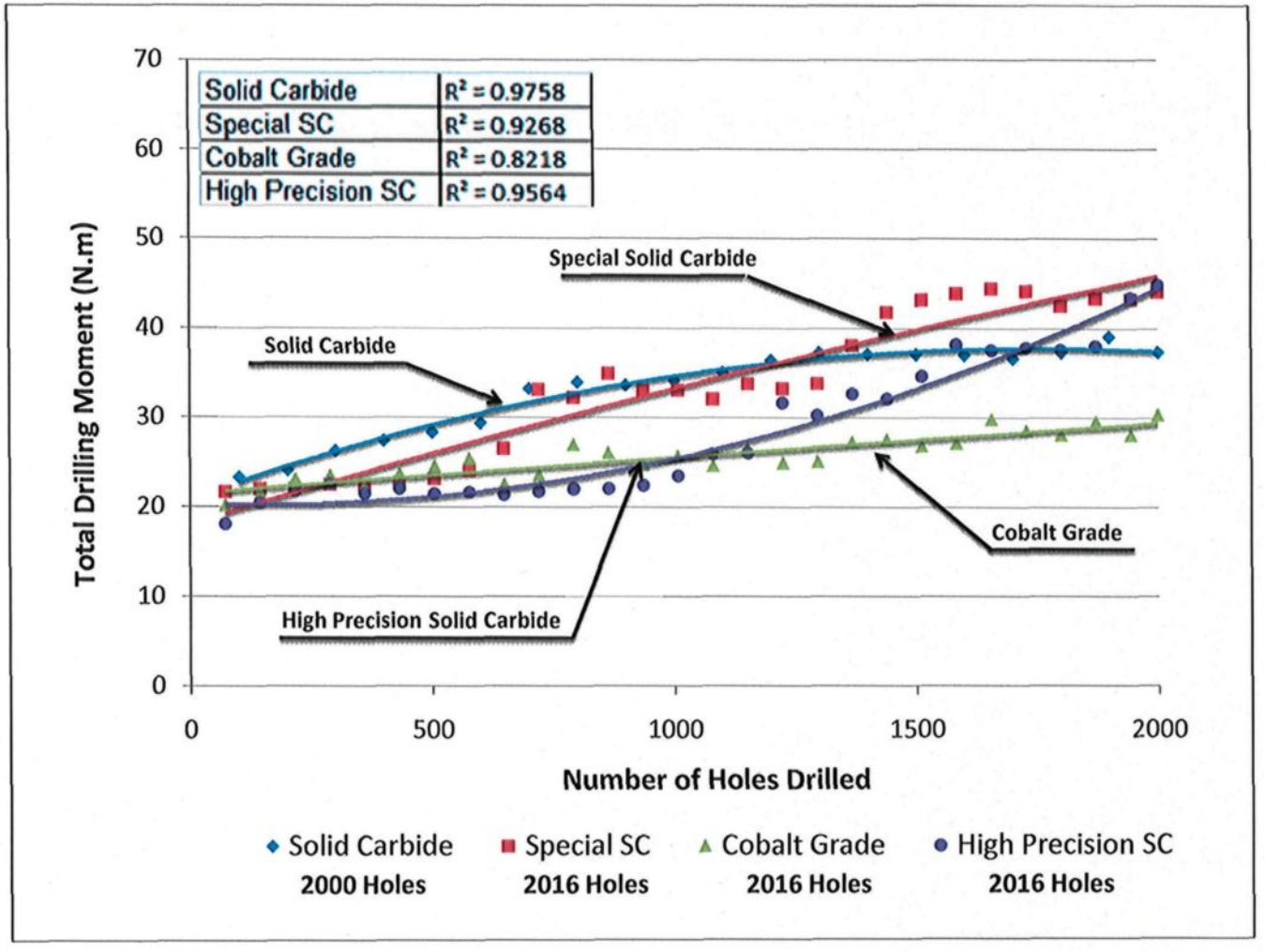


**(b)**

**Figure 4.5** Effects of Sn on the machinability of G12 alloy (396+0.15%Sn) in terms of (a) total drilling force, and (b) total drilling moment required for drilling 72 holes.

The number of insoluble phases present in the microstructure is dependent upon the Fe level in the alloy. Lowering the Fe content is extremely effective in suppressing the formation of the needle-like $\beta$-Fe intermetallic phase and in preventing sludge formation, thereby ultimately improving tool life. The modification of Fe intermetallics, through the addition of such suitable neutralizers as Mn and Cr, converts the $\beta$-Fe platelets into the more compact and less harmful $\alpha$-Fe scriptlike phase. This phase shows an irregular, curved crystal growth which conforms to the complicated shape of the interdendritic spaces during solidification.[61] The addition of 0.25%Fe and 0.25%Mn to the G3 alloy causes this alloy to contain sludge as the predominant phase, thereby leading to an extremely rapid increase in the total drilling force and moment. Figure 4.6 (a) and (b) display several fluctuations in the total drilling force and moment values during the drilling process of the G3 alloy; this may be due to the distribution and the size of the sludge particles within the alloy structure itself.

The results obtained using the G3 alloy show that the total cutting force and moment increase as the number of holes drilled increases. The slopes signaled by these two forces, however, are noticeably different. Tool wear has been shown to have a more significant effect on the thrust than on the torque. This observation is in comparatively good agreement with previous work carried out by Ting.[69] The sludge phase behaves similar to an abrasive in an otherwise relatively soft matrix, thus causing excessive tool wear, and resulting in an increase in the cutting force and moment. This increase may also possibly be explained by the formation of the hard, complex, intermetallic sludge phase in the G3 alloy. These conclusions are in satisfactory agreement with results obtained by Jorstad,[3,4] by Bonsack,[70] and by Colwell and Ticky,[71] who reported that the heavy

elements, manganese and chromium, when present even in moderate quantities in most aluminum casting alloys, tend to combine with aluminum, iron, silicon, and sometimes copper to form hard complex intermetallic phases. It has also been reported that the microhardness of sludge usually lies between 500 and 900 BHN, as compared to a matrix hardness of 111 BHN for the G3 alloy.[3, 4]

The increase in the total drilling force and moment which occurred in the G3 alloy after 500 holes were drilled, is significant, resulting in the presence of several fluctuations, which may be seen in Figure 4.6 (a) and (b). These effects were observed with the solid carbide drill, special solid carbide drill, and cobalt grade drill.

The high precision solid carbide drill displays different behavior compared to the abovementioned drills, for the reason that high precision solid carbide drills present a homogeneous performance from beginning to end of the drilling test, so that for the G3 alloy, the drill produced better results for the total drilling force and moment. Tool breakage may be caused by non-metallic inclusions such as aluminum oxide, corundum, and intermetallic complexes or sludge. Sludge can cause excessive tool wear, while hard spot inclusions cause tool breakage.[5]

Figure 4.6 (a) and (b) show the results for the G3 alloy in which the solid carbide drill broke down during machining. With respect to the number of holes drilled, it was possible to drill 1728 holes with the special solid carbide drill, the cobalt grade drill, and the high precision solid carbide drill as expected, whereas with the solid carbide drill only 971 holes could be drilled before drill breakdown occurred.

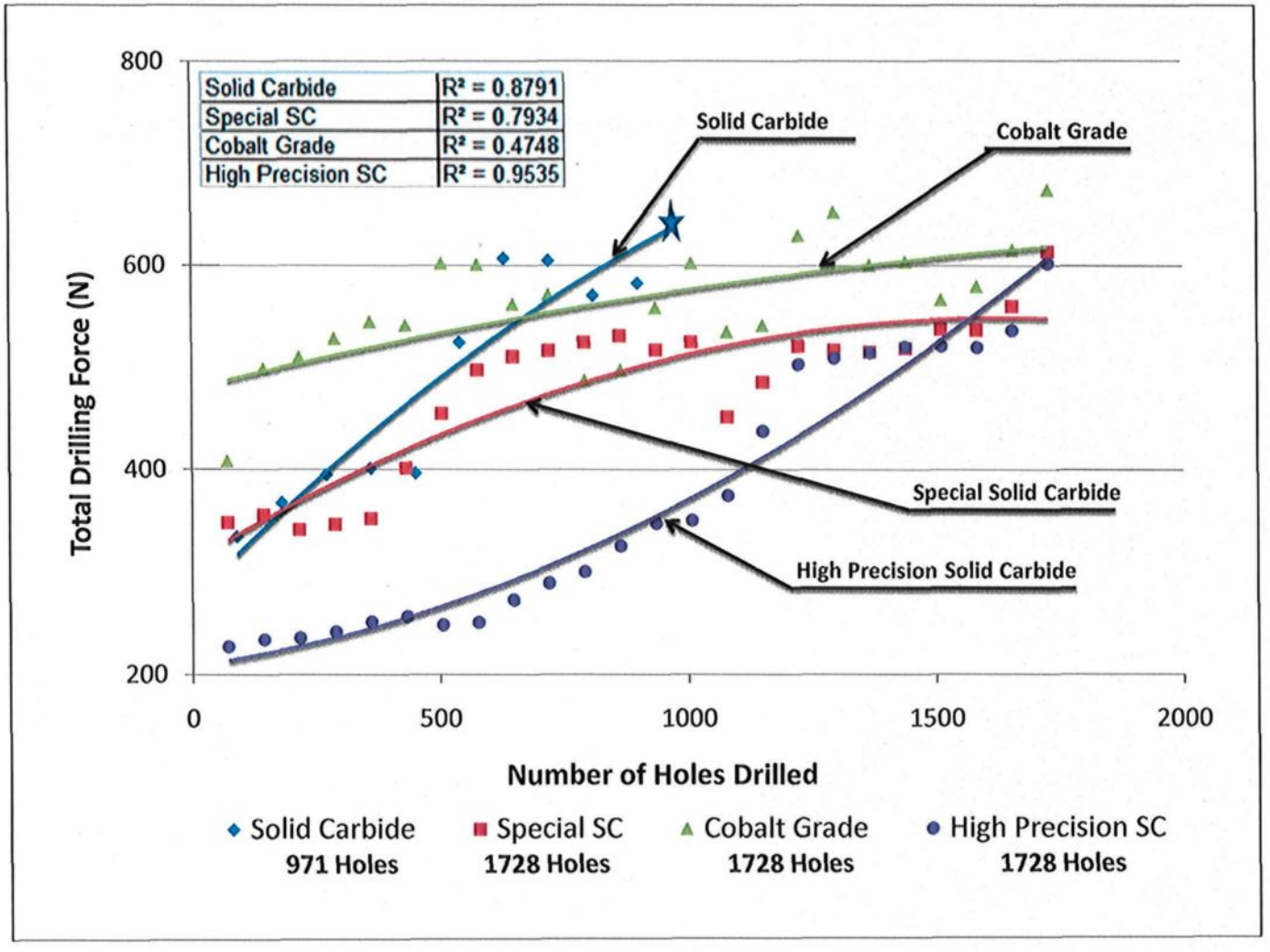
Solid Carbide R² = 0.8791
Special SC R² = 0.7934
Cobalt Grade R² = 0.4748
High Precision SC R² = 0.9535
Solid Carbide
Cobalt Grade
Special Solid Carbide
High Precision Solid Carbide
Total Drilling Force (N)
800
600
400
200
0
500
1000
1500
2000
Number of Holes Drilled
Solid Carbide 971 Holes
Special SC 1728 Holes
Cobalt Grade 1728 Holes
High Precision SC 1728 Holes

**Figure 4.6 (a)**

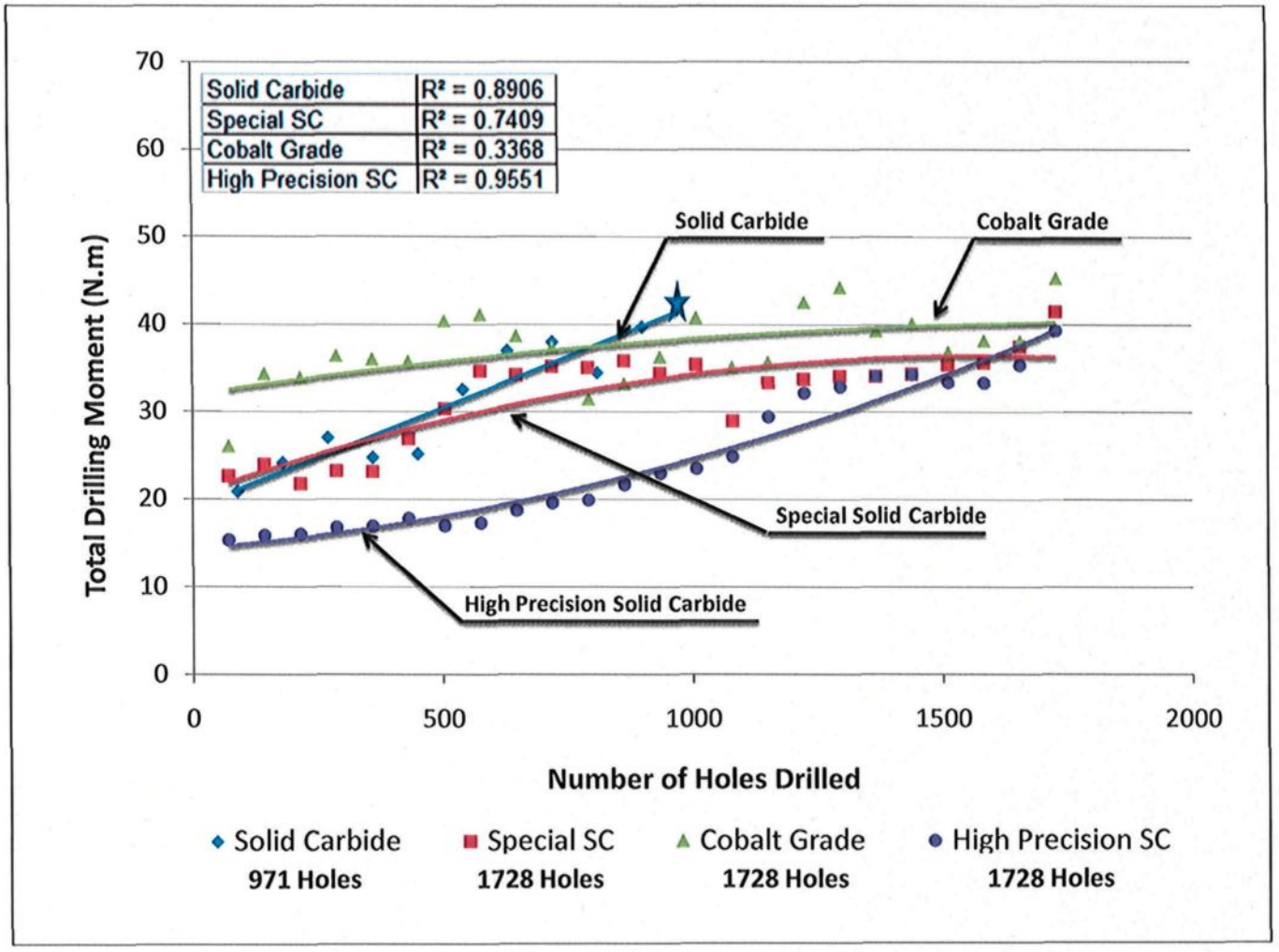


**(b)**

**Figure 4.6** Effects of Fe-intermetallics on the machinability of G3 alloy (396 + 0.25%Fe + 0.25%Mn) in terms of (a) total drilling force, and (b) total drilling moment required for drilling 72 holes.

### 4.3.2 Evaluation of Cutting Forces and Moments: Effects of Drill Type

A drill is an end-cutting tool for producing holes; it has one or more cutting edges as well as flutes to allow fluids to enter and chips to be ejected. A drill is composed of a shank, body, flutes, land, margin, web, edge, and the point. A good cutting tool must have the following properties:

- high strength, or hardness values, at elevated temperatures;
- increased impact toughness and thermal shock resistance;
- higher hardness values than the workpiece itself;
- low adhesion to prevent wear and diffusion, and a low coefficient of friction;
- low diffusivity in relation to workpiece material.

The results obtained from the drilling tests which were carried out reveal that the total drilling force and moment increase as the number of holes drilled increases; these results may be observed in Figure 4.7 (a) and (b), Figure 4.8 (a) and (b), Figure 4.9 (a) and (b), and Figure 4.10 (a) and (b), which show the results for each drill type tested and the three alloys used in this study. The free-machining element Sn was added to the aluminum alloys used, with the intention of cutting down on chip breakage and to minimize friction, thus allowing for higher machining speeds, improved tool life, better surface finish, and greater dimensional control with a concomitant decrease in machining costs.[72]

With respect to the microstructures of the 396 and B319.2 alloys, while both alloys contain Si, Cu, and Mg as the main alloying elements, the main difference lies in their Si content. The 396 alloy has 10.8%Si and 2.3%Cu, while the B319.2 alloy contains 7.5%Si

and 3.6%Cu. This difference is reflected in the microstructure which shows much larger regions of Al-Si eutectic in the 396 alloy.

The 396 and B319.2 alloys have hardness values of 106 and 111 BHN, respectively. In Figure 4.7, the significant increase in cutting force in the case of the G3 alloy may be explained by the formation of the hard, complex intermetallic sludge phase as the predominant phase in this alloy. It has also been reported that the microhardness of sludge usually lies between 500 and 900 BHN, as compared to a matrix hardness of 111 BHN for the G3 alloy.[3, 4] The sludge phase may display behavior which is similar to that of an abrasive in an otherwise relatively soft matrix, whereby it is capable of causing excessive tool wear and resulting in an increase in the cutting force and moment. It should also be noticed that the fluctuations of the total drilling force and moment values during the drilling of the G3 alloy result from the distribution and the size of the sludge particles within the cast alloy structure, *i.e.* the machinability test block itself.

The G12 alloy, which contains 7.5%Si and 0.15%Sn, reveals the lowest values of total drilling force and moment. By contrast, the presence of 0.25%Fe and 0.25%Mn in the G3 alloy causes deterioration in drill life; it should also be noted that this alloy presents a greater number of fluctuation values in the total drilling forces and moment, the drill breaking after only 971 holes were drilled. With regard to this observation, it is probable that the solid carbide drill became encrusted with a number of sludge intermetallic particles after which drill breakdown occurred. The G2 alloy, containing 10.8%Si, displays a behavior similar to that of the G12 alloy, which contains the same amount of Sn addition.

The results of total drilling force and moment obtained with the solid carbide drill and special solid carbide drill show that the G2 and G12 alloys, which both contain 0.15%Sn, present similar behavior with either drill type, as may be seen from Figure 4.7 and 4.8. In comparison, the G3 alloy presents greater fluctuations in drilling force and moment values with the progress of drilling.

It should be noted that, in the case of the special solid carbide drill, the drill broke after drilling 1728 holes in the G2 alloy, without completing the targeted goal of 2016 holes set for this alloy, and which had been met by the other three drills in the drilling process.

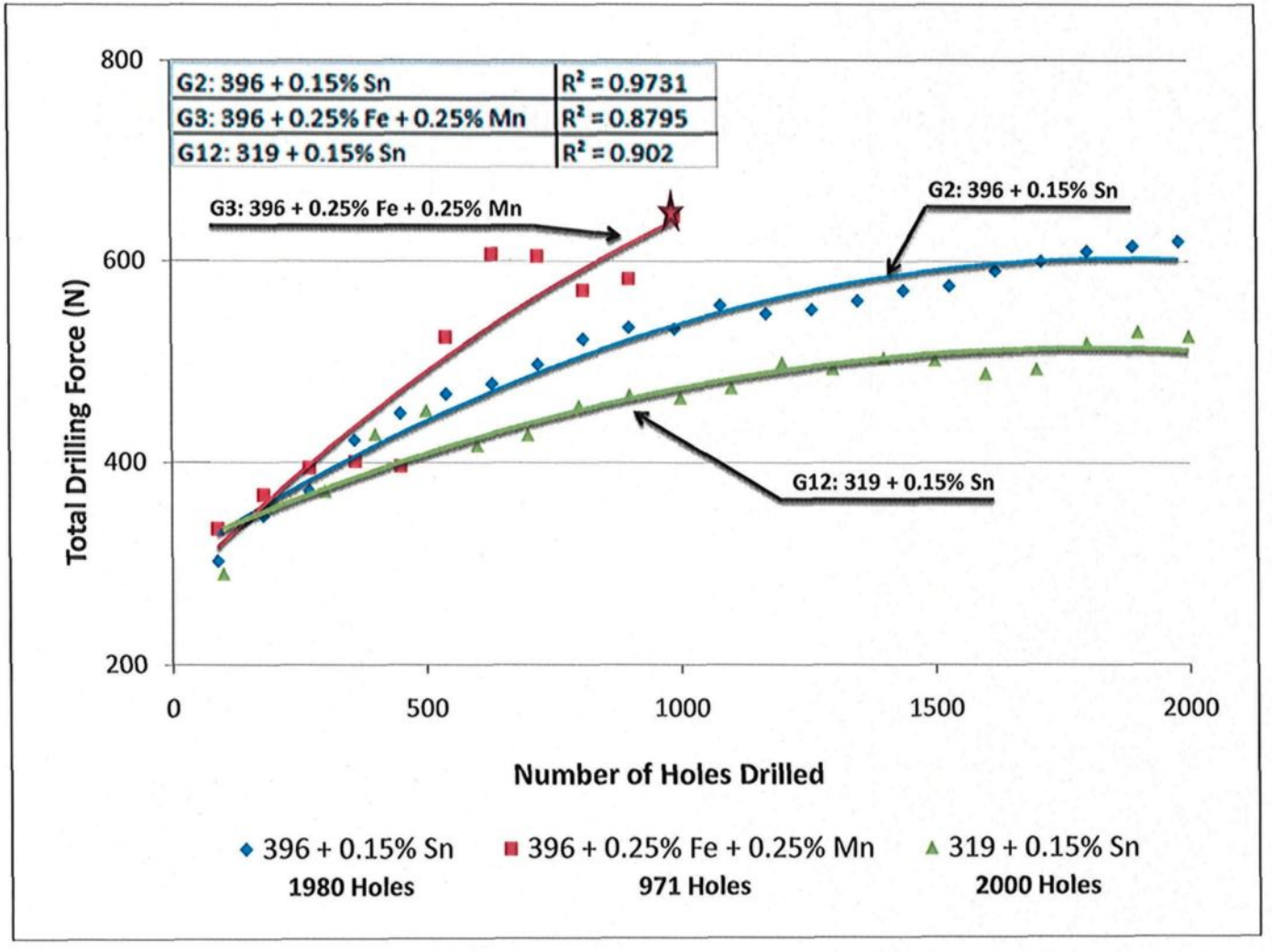
G2: 396 + 0.15% Sn
R² = 0.9731
G3: 396 + 0.25% Fe + 0.25% Mn
R² = 0.8795
G12: 319 + 0.15% Sn
R² = 0.902
G3: 396 + 0.25% Fe + 0.25% Mn
G2: 396 + 0.15% Sn
G12: 319 + 0.15% Sn
Total Drilling Force (N)
800
600
400
200
0
500
1000
1500
2000
Number of Holes Drilled
396 + 0.15% Sn
1980 Holes
396 + 0.25% Fe + 0.25% Mn
971 Holes
319 + 0.15% Sn
2000 Holes

**Figure 4.7(a)**

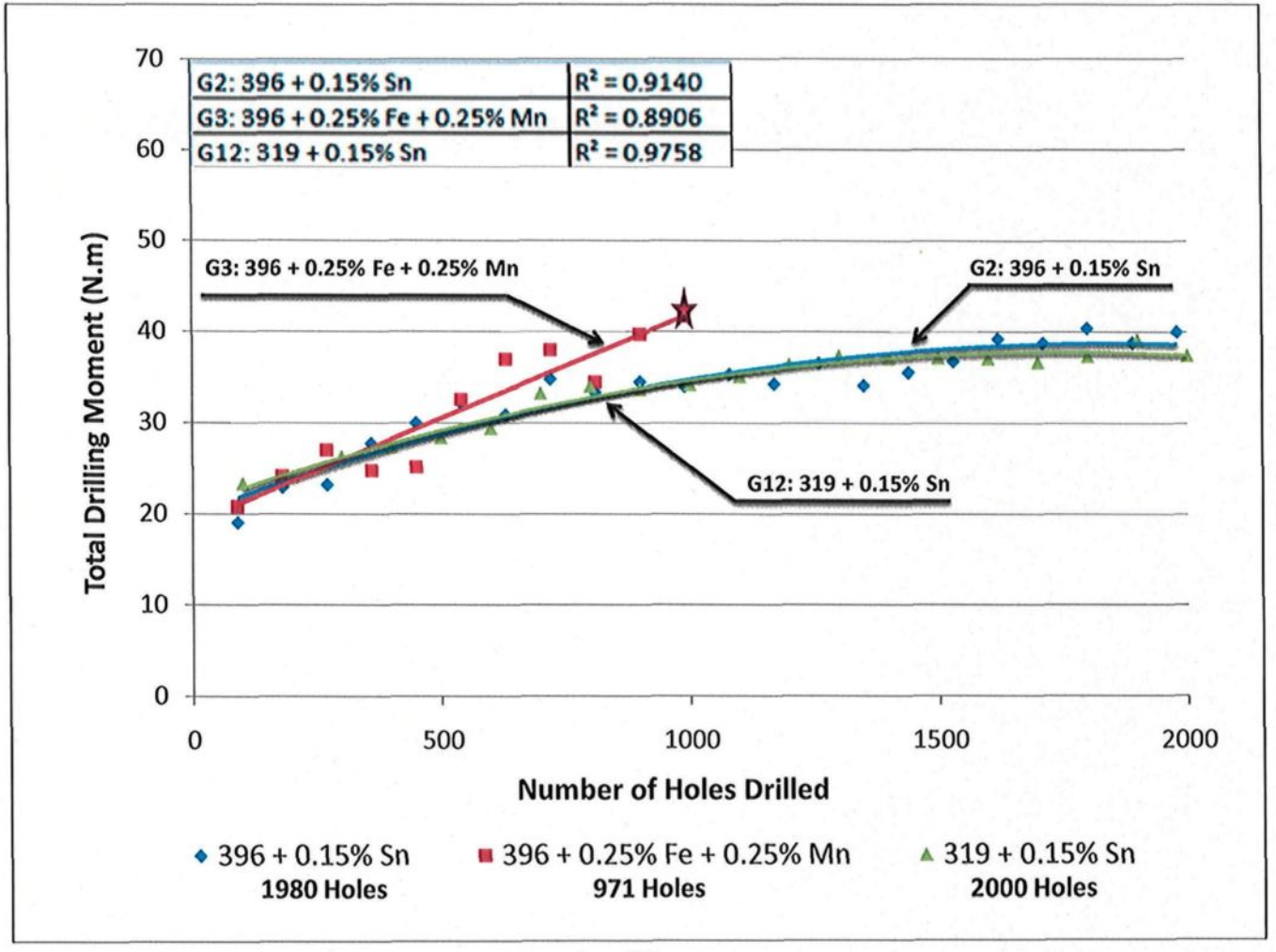


**(b)**

**Figure 4.7** Machinability of G2, G3, and G12 alloys in terms of (a) total drilling force, and (b) total drilling moment required for drilling 72 holes, using the solid carbide drill.

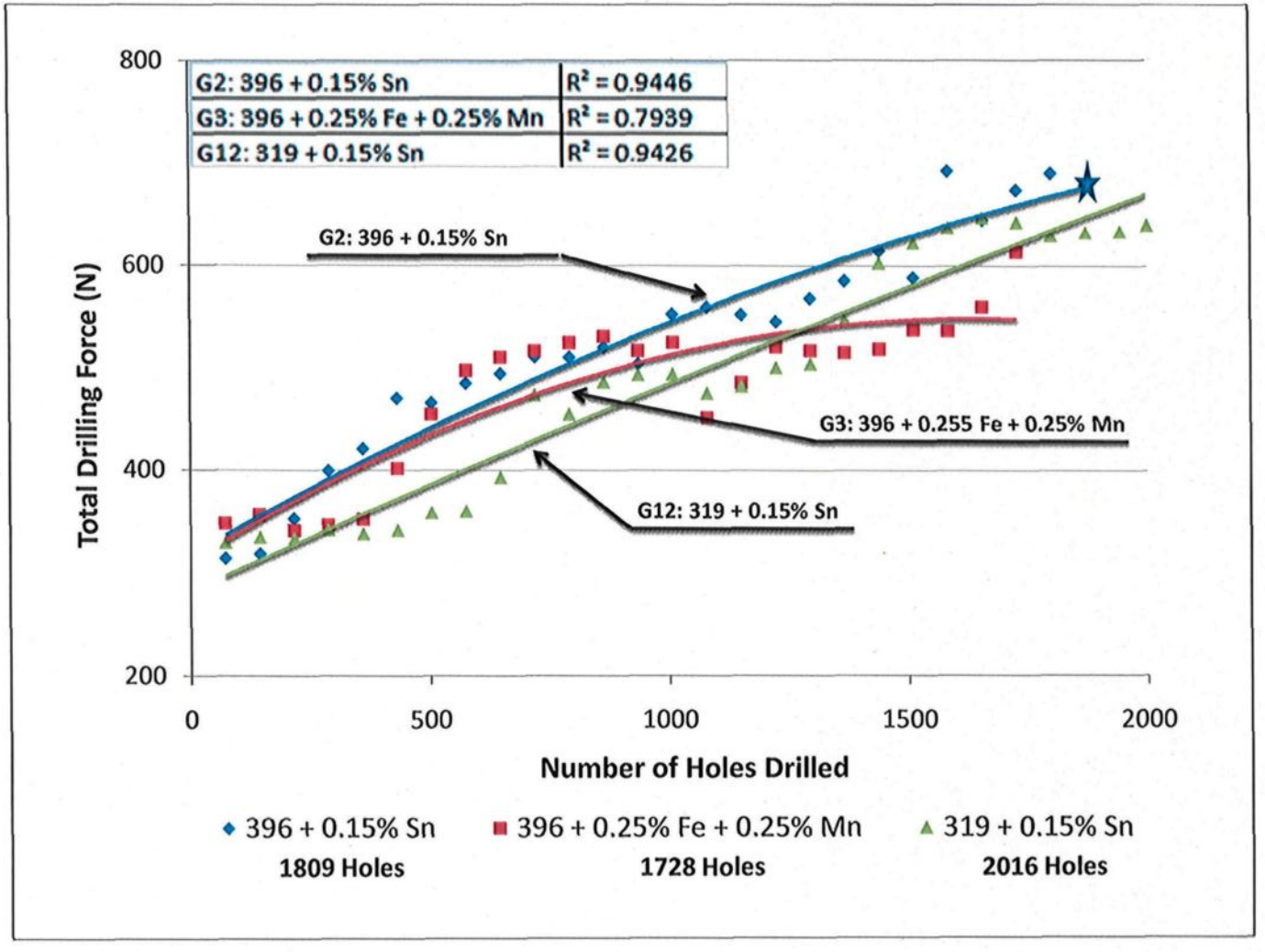
G2: 396 + 0.15% Sn | R² = 0.9446
G3: 396 + 0.25% Fe + 0.25% Mn | R² = 0.7939
G12: 319 + 0.15% Sn | R² = 0.9426
G2: 396 + 0.15% Sn
G3: 396 + 0.255 Fe + 0.25% Mn
G12: 319 + 0.15% Sn
Total Drilling Force (N)
800
600
400
200
0
500
1000
1500
2000
Number of Holes Drilled
396 + 0.15% Sn
1809 Holes
396 + 0.25% Fe + 0.25% Mn
1728 Holes
319 + 0.15% Sn
2016 Holes

**Figure 4.8(a)**

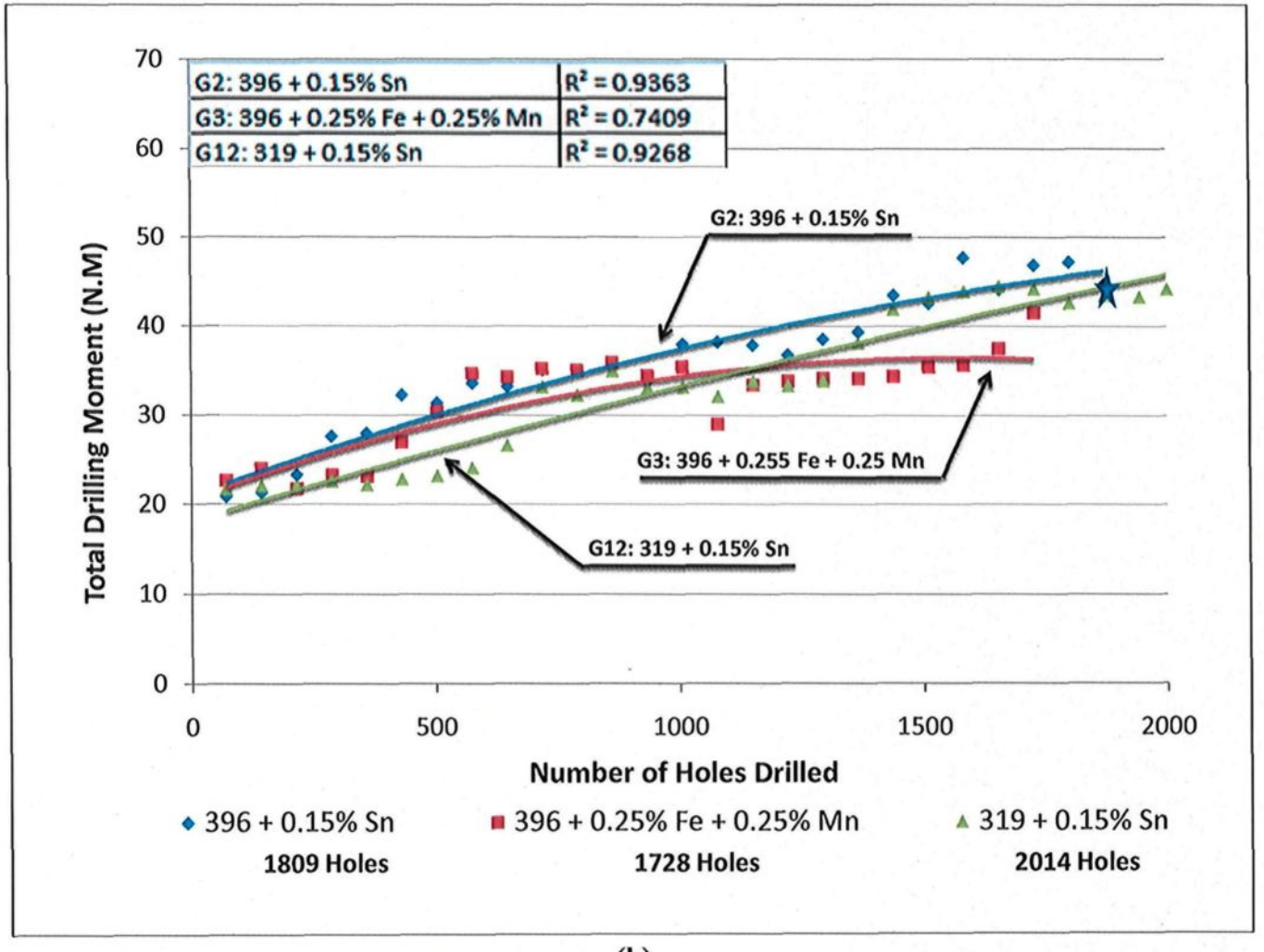


**(b)**

**Figure 4.8** Machinability of G2, G3, and G12 alloys in terms of (a) total drilling force, and (b) total drilling moment required for drilling 72 holes, using the special solid carbide drill.

Tool material selection and tool coating selection are the two primary techniques used by tool designers to reduce the occurrence of edge build-up. One rule of thumb for high-speed aluminum machining tooling designs is to maximize space for chip evacuation. This rule may be based on the fact that aluminum is a soft material and the feed rate is usually increased during the machining process, creating more and bigger chips.

Figure 4.9 (a) and (b), andFigure 4.10 (a) and (b) show the results of total drilling force and moment for the G2, G3 and G12 alloys obtained with the cobalt grade drill and the high precision solid carbide drill, respectively. These drills produced better results for the three alloys compared with the solid carbide and special solid carbide drills. The results of total drilling force and moment displayed in Figure 4.9 show that by using the cobalt grade drill with the G12 alloy (containing 7.5%Si and 0.15%Sn), it is possible to obtain the lowest values for total drilling force and moment; consequently homogeneous behavior with this drill and alloy may be observed.

The 396 alloys G2 and G3, containing higher silicon content of 10.8%Si, required greater cutting force and moment compared to the B319.2 alloy which contains only 7.5%Si. In addition, the G3 alloy showed many fluctuations in the cutting force/moment with the progress of drilling, due to the Fe-intermetallics present in the alloy. In terms of the number of holes drilled, however, the results shown in Figure 4.9 indicate that the silicon content had little effect on tool life. Johne[49] reported that the use of carbide tipped tools is gaining popularity within the automotive and aerospace industries. Moreover,

casting alloys which have a relatively high abrasive action are, for the most part, machined using carbide-tipped tools.

Drilling tests using the high precision solid carbide drill revealed that this drill gave the best total drilling force and moment when used with the three alloys. This result may be attributed to the higher hardness of the drill material compared to that of the workpiece material, *i.e.* aluminum. Moreover, the cutting geometry in this case is influenced by the cutting tool material and workpiece material, with regard to the desired surface finish quality and tolerance, as well as by the cutting speed, depth and feed rate used in the drilling process. Figure 4.10 (a) and (b) shows the results obtained from the drilling tests carried out for the three alloys using the high precision solid carbide drill.

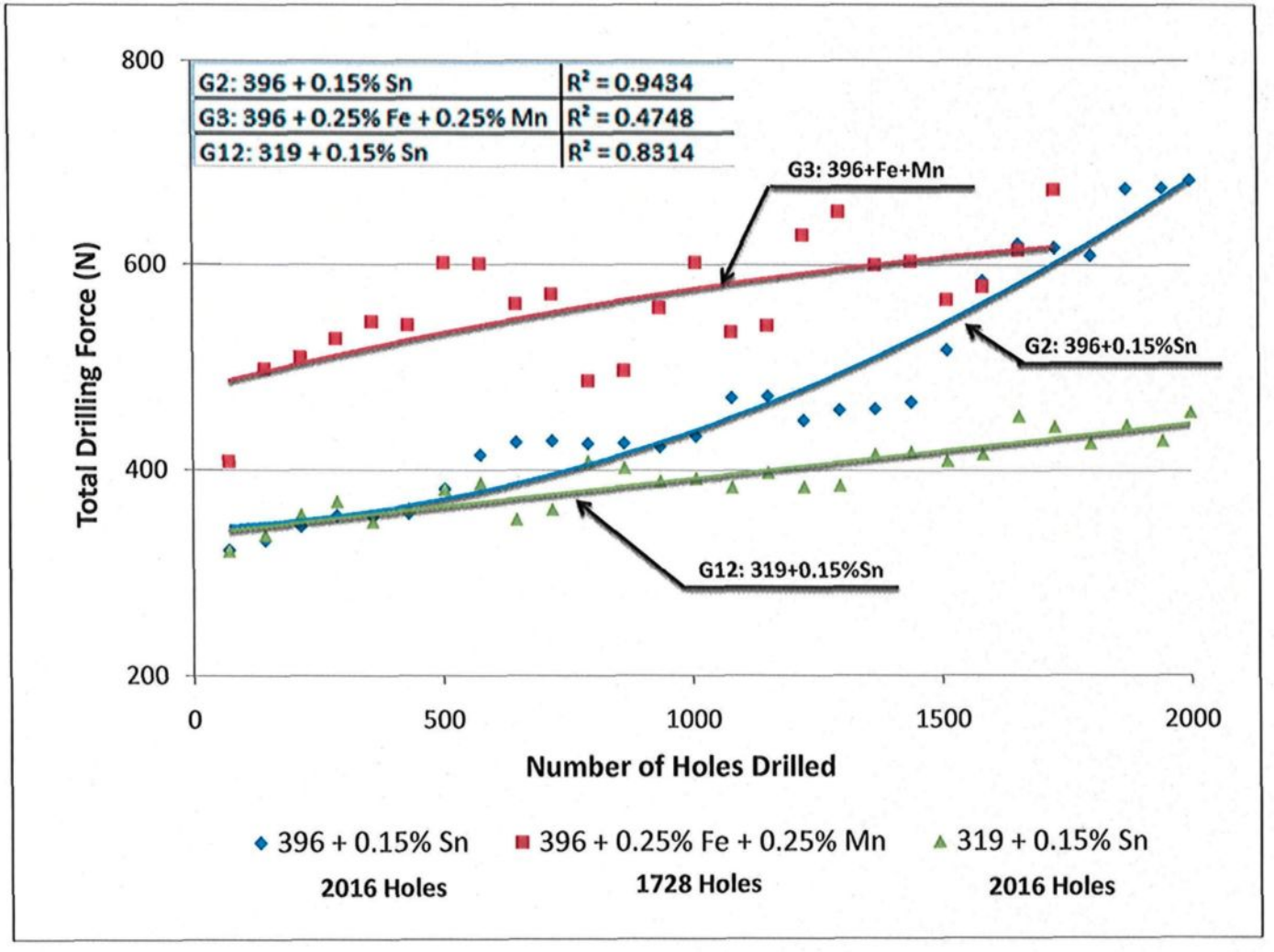
G2: 396 + 0.15% Sn
R² = 0.9434
G3: 396 + 0.25% Fe + 0.25% Mn
R² = 0.4748
G12: 319 + 0.15% Sn
R² = 0.8314
G3: 396+Fe+Mn
G2: 396+0.15%Sn
G12: 319+0.15%Sn
Total Drilling Force (N)
800
600
400
200
0
500
1000
1500
2000
Number of Holes Drilled
396 + 0.15% Sn
2016 Holes
396 + 0.25% Fe + 0.25% Mn
1728 Holes
319 + 0.15% Sn
2016 Holes

**Figure 4.9 (a)**

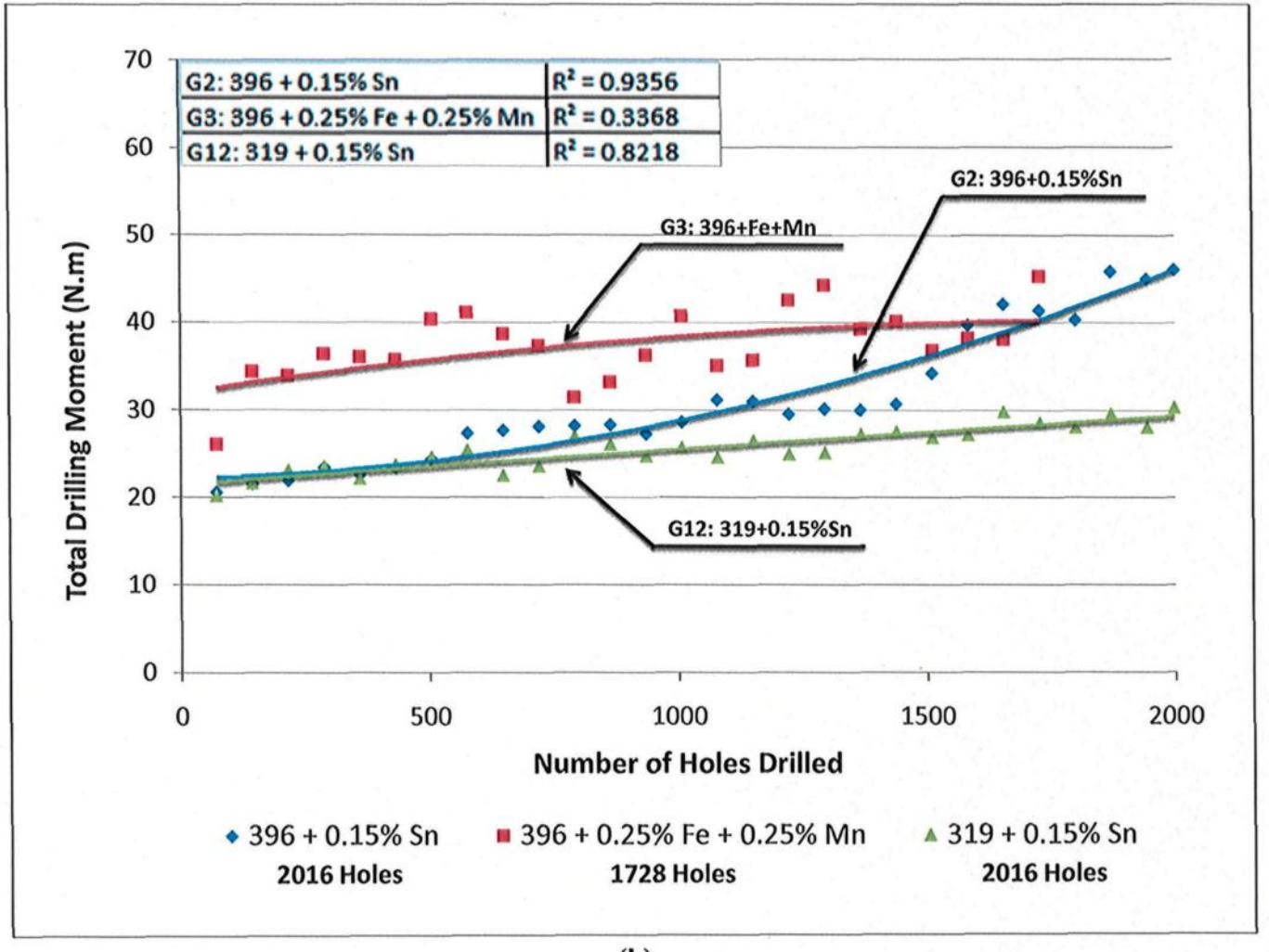


**(b)**

**Figure 4.9** Machinability of G2, G3, and G12 alloys in terms of (a) total drilling force, and (b) total drilling moment required for drilling 72 holes, using the cobalt grade drill.

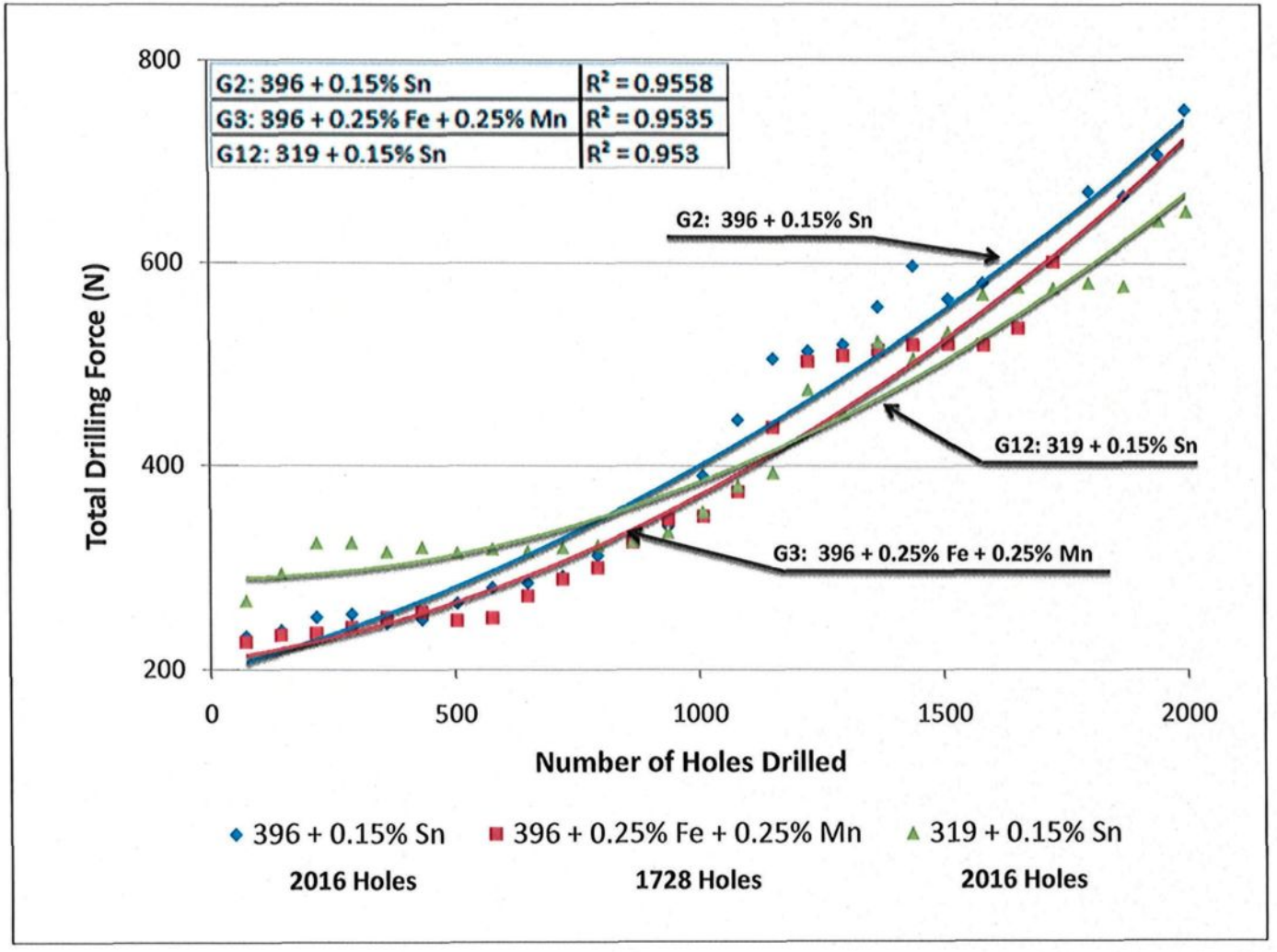
G2: 396 + 0.15% Sn | R² = 0.9558
G3: 396 + 0.25% Fe + 0.25% Mn | R² = 0.9535
G12: 319 + 0.15% Sn | R² = 0.953
G2: 396 + 0.15% Sn
G12: 319 + 0.15% Sn
G3: 396 + 0.25% Fe + 0.25% Mn
Total Drilling Force (N)
800
600
400
200
0
500
1000
1500
2000
Number of Holes Drilled
396 + 0.15% Sn
2016 Holes
396 + 0.25% Fe + 0.25% Mn
1728 Holes
319 + 0.15% Sn
2016 Holes

**Figure 4.10 (a)**

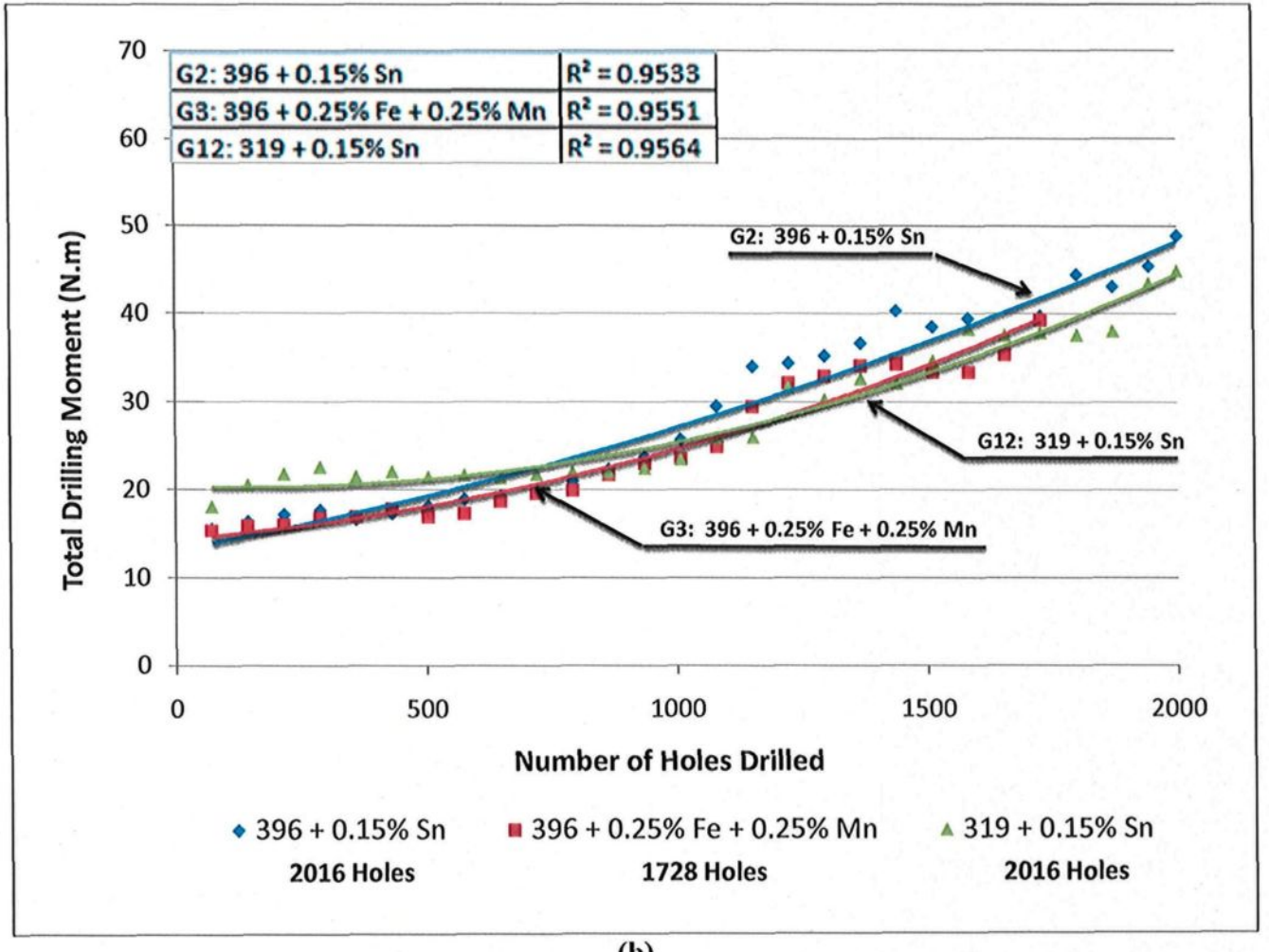


**(b)**

**Figure 4.10** Machinability of G2, G3, and G12 alloys in terms of (a) total drilling force, and (b) total drilling moment required for drilling 72 holes, using the high precision solid carbide drill.

### 4.3.3 Summary of the Evaluation of the Total Average Drilling Force and Moment

The differences in the machining behavior of 396 and B319.2 alloys may be attributed mainly to the differences in matrix hardness, as well as to differences in the microstructural constituents resulting from alloy chemistry, additions, and heat treatment. Matrix hardness (beneficial) and alloy abrasiveness (detrimental) seem to be the real issues controlling alloy machinability. In the present case, this was investigated for the G2, G3, and G12 alloys using two Al-Si alloys, 396 and B319.2 with different Si contents, and Sn, Fe, and Mn additions, tin for its free-cutting properties, and iron and manganese for producing Fe-intermetallics, namely $\alpha$-Fe, $\beta$-Fe, and sludge in the alloy structure. The histograms provided in Figure 4.11 and 4.12 display the results for total drilling force and moment for each alloy/drill combination.

As may be seen from the two figures, a higher Si content results in a higher cutting force and moment, as is the case for the G2 and G3 alloys containing 10.8%Si; in comparison, the G12 alloy with a Si content of 7.5% has a softer matrix, and hence requires smaller cutting forces and moments in general. In addition, in the case of the G3 alloy, the Fe-intermetallics, namely $\alpha$-Fe and sludge intermetallic phases, as well as their morphology will also influence the cutting forces and moments required in the drilling process. The purpose of heat treatment is to increase the hardness and reduce the edge build-up on the cutting tool. Hardness always affects the machinability of the alloys in the same way so that machinability consistently improves as the hardness increases, as shown in Table 4.3 in subsection 4.2.2 of this chapter.

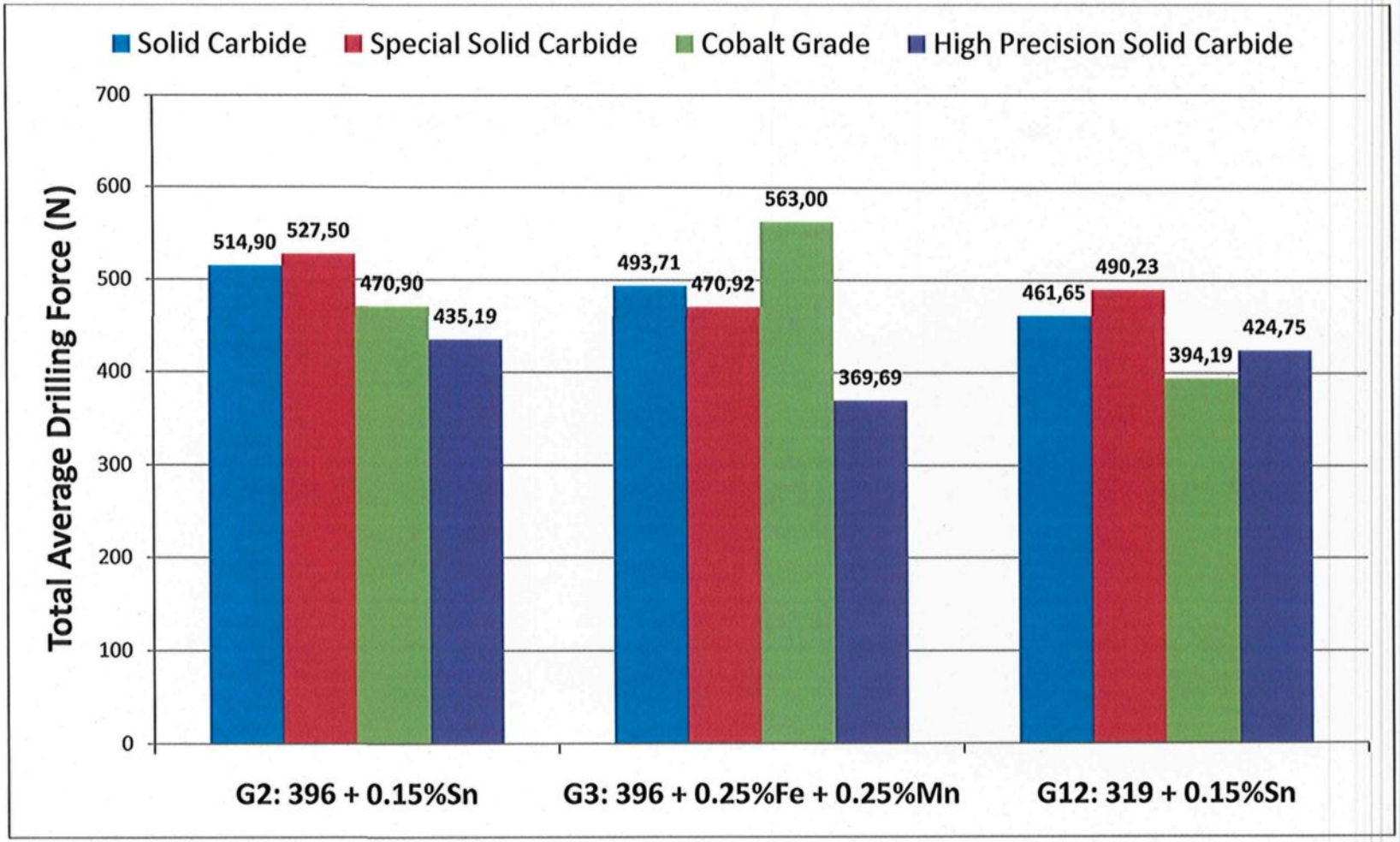


**Figure 4.11** Comparison of the total average drilling forces obtained for alloys G2, G3, and G12 using different drills.

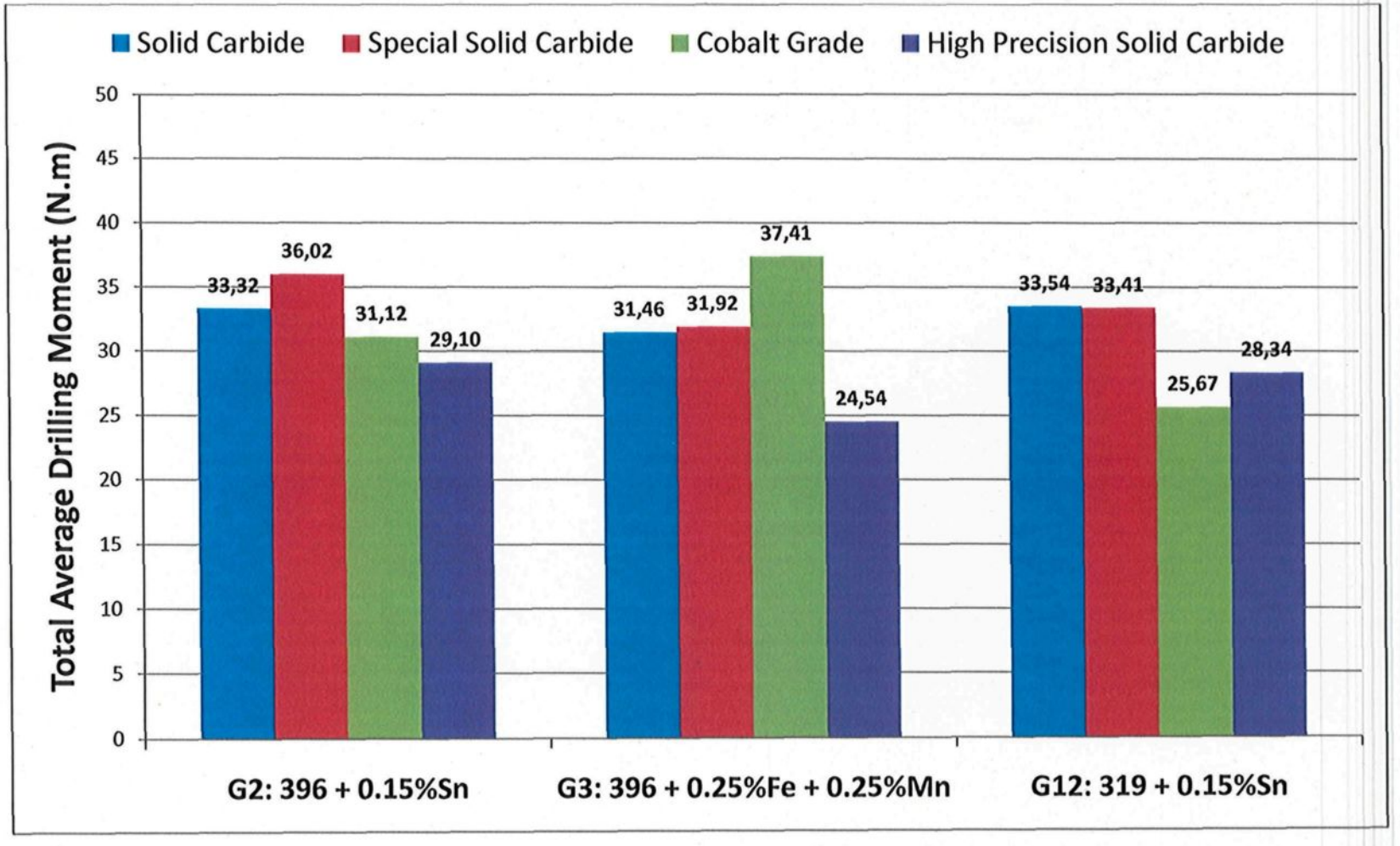


**Figure 4.12** Comparison of the total average drilling moments obtained for alloys G2, G3, and G12 using different drills.

Drill geometry, drill material, and the requirements of the tool holder remain as challenges to be met in utilizing advanced machines to the maximum of their capability. The drilling test results obtained using the high precision solid carbide drill lead to the conclusion that this drill is best suited for the 396 alloy, having obtained the lowest mean total drilling forces and moments for the G2 and G3 alloys during the tests. The results obtained may be attributed to the relevant geometry and properties such as those displayed by this drill which produces better results when used with G2 and G3 alloys, compared to the other three drills, namely, the solid carbide drill, the special solid carbide drill, and the cobalt grade drill.

The high precision solid carbide drill shows the most satisfactory behavior and results for the mean total drilling force and moment with the G2 alloy, followed by the cobalt grade drill, then the solid carbide drill, and lastly the special solid carbide drill. With regard to the results obtained for the G3 alloy, it was observed that the high precision solid carbide drill continues to produce the lowest values of the mean total drilling force and moment, 369.69N and 24.54N.m, respectively. In fact, these values are the lowest obtained among all the drilling tests carried out on the three alloys using the four drills.

From Figure 4.11 and 4.12, it may be seen that with regard to the G12 alloy, the cobalt grade drill reveals the most satisfactory behavior and obtained the lowest total drilling force and moment, with results of 394.19N and 25.67N.m, compared to the much higher values obtained when using the solid carbide, the special solid carbide, and the high

precision solid carbide drills. As will be shown in the next section, in terms of the number of holes drilled, the results indicated that the silicon content has little effect on tool life.

### 4.3.4 Tool Life

Long cutting tool life is one of the most important economic considerations in metal cutting, considering that tool wear degrades the surface finish and increases the tolerance on the workpiece machined; as well, the costs of machining and manufacturing are also increased, particularly in the case of aerospace and automotive components. Moreover, it is clear that any improvement in tool or work material which leads to an increase in tool life without causing unacceptable dips in production will be deemed beneficial. A cutting tool fails when it can no longer provide the required functions; these failures may occur through sudden catastrophic failure or through gradual wear.

Tool life is the most common criterion and important reason used to rate cutting tool performance and the machinability of materials. It may be measured in terms of the number of holes drilled under constant machining conditions for the alloy variations investigated in this study. This aspect is often the most important practical consideration when selecting cutting tools and cutting conditions. Tools which wear out or otherwise fail slowly have comparatively long service lives, resulting in reduced production costs and a more consistent dimensional and surface finish capability. The dominant variables governing tool life are the silicon content, the temperatures occurring at the contact surfaces of workpiece and tool, hard-spot or sludge inclusions, and non-metallic inclusions.[71] As Figure 4.11 and 4.12 demonstrate, the B319.2 alloy displayed lower cutting force and moment compared to

those obtained for the 396 alloy after additions of Sn, and Fe + Mn, regardless of heat treatment.

Figure 4.13 also provides the comparison between tool life in terms of number of holes drilled for each alloy used in this work. The addition of small amounts of Sn to the G2 and G12 alloys provide the desired drilling results in terms of number of holes drilled; for both alloys, the targeted number of holes, *i.e.* 2016 holes, could be achieved/drilled, with the exception of when using the special solid carbide drill, with which only 1809 holes could be drilled in the G2 alloy before drill breakdown occurred.

On the other hand, the drilling results obtained with the G3 alloy which contains sludge intermetallic particles, reveals that this alloy is more sensitive to tool wear than the G2 and G12 alloys. In this case, the maximum number of holes which may be drilled was found to be 1728, short of the target number by 288 holes, with the exception of the solid carbide drill which obtained only 971 drilled holes before breaking down.

From these results, it is clear that the sludge phase, which has a high hardness value, a high melting point, and high specific gravity compared to the matrix, is capable of causing damage to cutting tools. These observations are in good agreement with the work of Zedan,[73] who reported that the sludge phase is liable to cause rapid tool wear and to bring on all of the attendant problems accompanying a dull tool, as was confirmed by drill wear examination in the present study and shown in the photographs displayed in Figure 4.14 in the next section.

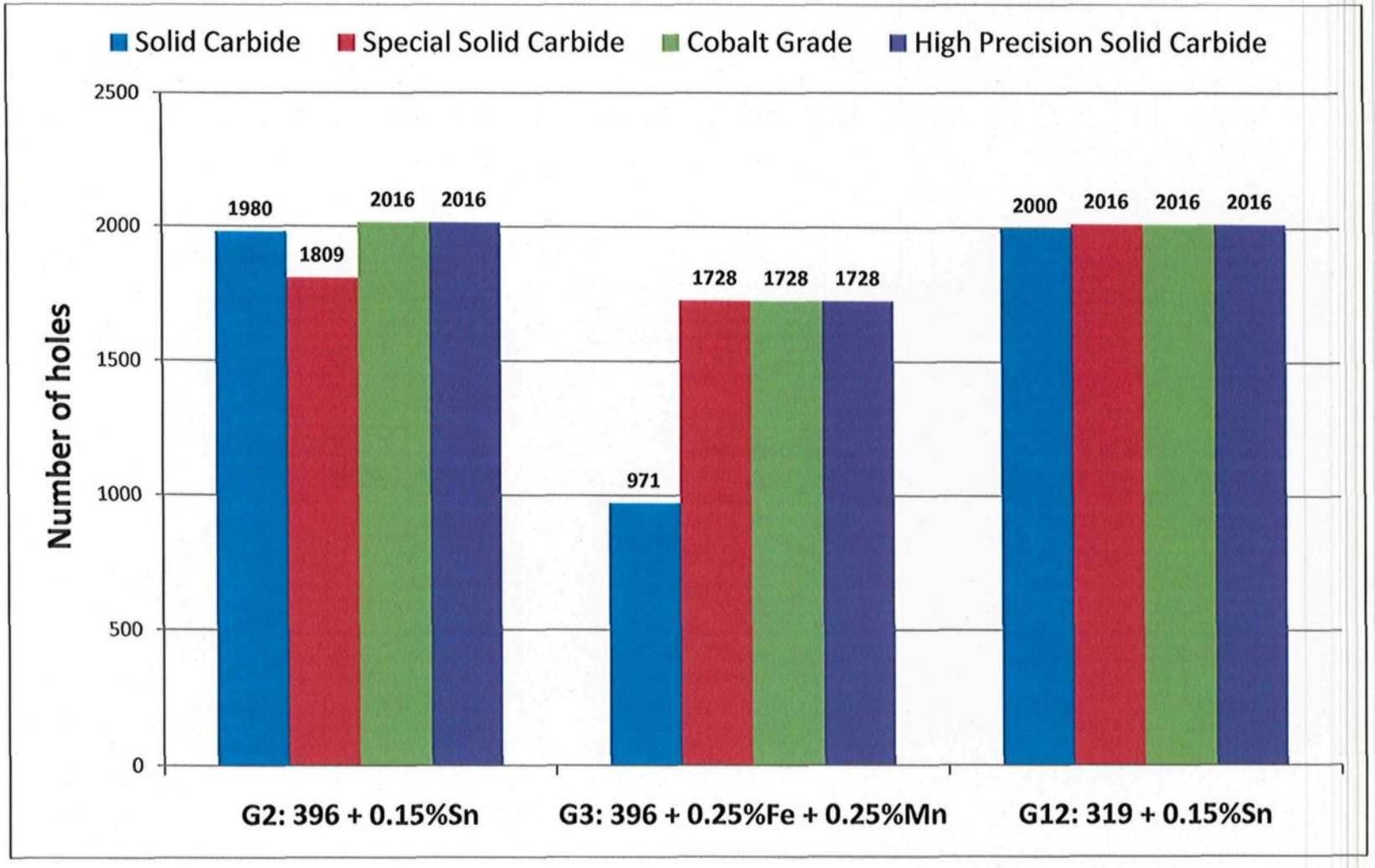


**Figure 4.13** Comparison of tool life in terms of number of holes drilled for G2, G3, and G12 alloys.

Table 4.4 shows the total number of holes drilled and the number of samples drilled from among all the alloys and drills used. The values marked with an asterisk in the table indicate that the drills broke before the end of the test. As Table 4.4 shows, the only drills which were affected were the special solid carbide drill when used with the G2 alloy, and the solid carbide drill when used with the G3 alloy, respectively.

**Table 4.4** Total number of holes drilled and total number of samples drilled for each alloy

| Drill | G2 396 + 0.15%Sn | | G3 396+ 0.25%Fe + 0.25%Mn | | G12 B319.2 + 0.15%Sn | |
|---|---|---|---|---|---|---|
| | N° of holes drilled | N° of samples drilled | N° of holes drilled | N° of samples drilled | N° of holes drilled | N° of samples drilled |
| **Solid Carbide** | 1980 | 13.75 | 971* | 6.74* | 2000 | 14 |
| **Special Solid Carbide** | 1809* | 12.56* | 1728 | 12 | 2016 | 14 |
| **Cobalt Grade** | 2016 | 14 | 1728 | 12 | 2016 | 14 |
| **High Precision Solid Carbide** | 2016 | 14 | 1728 | 12 | 2016 | 14 |

Note: The values marked with an asterisk indicate that in these cases, the drill broke before the end of the drilling test.

### 4.3.5 Built-Up Edge (BUE) Evolution and Drill Wear Characteristics

Built-up edge (BUE) is caused by the incidence of some strain-hardened workpiece material welding itself to the rake face and becoming a new cutting surface. As a result of increasing temperatures, small particles of metal adhere to the edge of the cutting tool causing build-up to result. In practice, the size and the shape of the built-up edge (BUE) vary greatly with the workpiece material and the prevailing cutting conditions.[74] For any material and cutting conditions the built-up edge seems to reach an equilibrium size and shape. Built-up edge should be capable of supporting the high compressive force and shear stresses imposed by the cutting process thereby preventing it from growing in height indefinitely.[4, 61] As the BUE grows in height and undergoes changes in shape, the stress system changes and parts of the built-up edge break away.[75] The presence of built-up edge is capable of inducing a number of effects including an alteration in tool geometry, which results in reducing the area of contact between the chip and the rake face.[76]

Heat build-up on the cutting tools is the biggest drawback to maintaining the machining characteristics of a material during machining operations. The accumulation of BUE results in the deterioration of chip size, tool life, surface-finish, and loss of dimensional control.[77] In the present study, the tendency of each alloy to adhere and build-up on the cutting edge of the tool was detected through a high magnification top-view of the projected area looking at the actual build-up on the drill; this was carried out using a toolmaker's TM-505 type microscope at a magnification of 30x. The presence of BUE

rapidly causes deterioration in the cutting ability of the tool. The drilling test results are summarized in Table 4.5, Table 4.6, and Table 4.7.

**Table 4.5** Effects of adding Sn to 396 alloy with regard to the width of built-up edge (BUE) during the drilling process

| G2: 396 + 0.15%Sn | | | | | | |
|---|---|---|---|---|---|---|
| **Drill** | **BUE width (mm) for different numbers of holes drilled** | | | | | |
| | **144** | **432** | **720** | **1440** | **2016** | **Average** |
| **Special Solid Carbide** | 0.051 | 0.064 | 0.064 | 0.076 | 0.127 | **0.076** |
| **Cobalt Grade** | 0.066 | 0.076 | 0.084 | 0.097 | 0.132 | **0.091** |
| **High Precision Solid Carbide** | 0.056 | 0.064 | 0.064 | 0.094 | 0.135 | **0.083** |

**Table 4.6** Effects of adding Fe and Mn to the 396 alloy with regard to the width of built-up edge (BUE) during the drilling process

| G3: 396 + 0.25%Fe + 0.25%Mn | | | | | | |
|---|---|---|---|---|---|---|
| **Drill** | **BUE width (mm) for different numbers of holes drilled** | | | | | |
| | **144** | **288** | **720** | **1152** | **1728** | **Average** |
| **Special Solid Carbide** | 0.076 | 0.076 | 0.091 | 0.102 | 0.122 | **0.093** |
| **Cobalt Grade** | 0.102 | 0.084 | 0.102 | 0.127 | 0.152 | **0.113** |
| **High Precision Solid Carbide** | 0.051 | 0.064 | 0.071 | 0.097 | 0.110 | **0.079** |

**Table 4.7** Effects of adding Sn to the B319.2 alloy with regard to the width of built-up edge (BUE) during the drilling process

| G12: B319.2 + 0.15%Sn | | | | | | |
|---|---|---|---|---|---|---|
| **Drill** | **BUE width (mm) for different numbers of holes drilled** | | | | | |
| | **144** | **432** | **720** | **1440** | **2016** | **Average** |
| **Special Solid Carbide** | 0.051 | 0.051 | 0.076 | 0.086 | 0.129 | **0.079** |
| **Cobalt Grade** | 0.081 | 0.097 | 0.089 | 0.107 | 0.124 | **0.098** |
| **High Precision Solid Carbide** | 0.046 | 0.066 | 0.094 | 0.102 | 0.132 | **0.088** |

It will be observed that, for all the alloys examined, there is no significant change to be observed in the width of the BUE with the progress of the drilling process. Figure 4.14, 4.15, and 4.16 show examples of edge build-up formation on the main cutting drill lip after drilling different numbers of holes in the G2, G3, and G12 alloy blocks using different drills. With respect to the measurements obtained for the G2, G3, and G12 alloys, the width of the built-up edge has no clear cut trend except for the detail that G3 contains sludge and is the predominant phase in this alloy.

Jorstad,[3, 4] reported that heavy elements, such as iron, manganese, and nickel have a negligible effect on microhardness and on the tool-edge build-up in 380 die casting alloys. The effects present with these heavy elements may be significant in the G3 alloy with additions of 0.25%Fe and 0.25%Mn, which would initially have been expected to reduce the build-up tendency through the abrasive action of hard intermetallic phases, but did not, however, measurably reduce the edge build-up width.

The drilling tests were carried out at high cutting speeds of around 11000 rpm and a high feed rate of about 1.117 m/min. Bao and Stevenson, [74] found that with higher rates of metal removal, *i.e.* at higher speeds or feed rates, BUE will no longer be detectable, since the transition from the built-up edge to the flow zone is strongly influenced by both speed and feed; also the flow zone occurs in the range of cutting conditions commonly encountered in industrial machining operations.

Observation of the optical images reveals that there are minimum changes in the width of BUE for different numbers of holes in the course of drilling for each alloy and drill. This observation may be attributed to the fact that the BUE deposit will gradually increase in size and, when it exceeds a critical size, will separate from the cutting face and adhere to the lower surface of the chip. It is thus assumed that when the deposit reaches this critical size, it will slide completely, or partly, off the cutting face under the action of a sufficiently strong lateral force, and then subsequently be eliminated with the chip itself. Immediately after the elimination of the existing deposit, a new deposit will begin to form; it will then proceed to grow gradually and will ultimately change or modify the tool geometry. Built-up edge (BUE) does not depend on either alloy composition or the drill materials; it does, however, depend to a great extent on the base alloy in use, namely, aluminum, in this case.

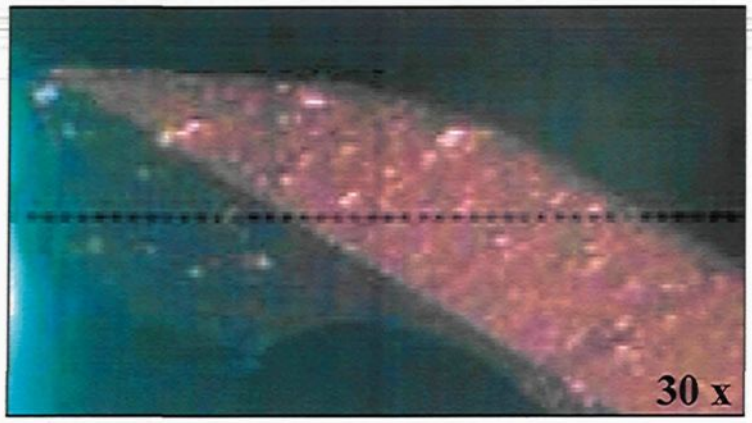


(a) Special Solid Carbide – New Drill

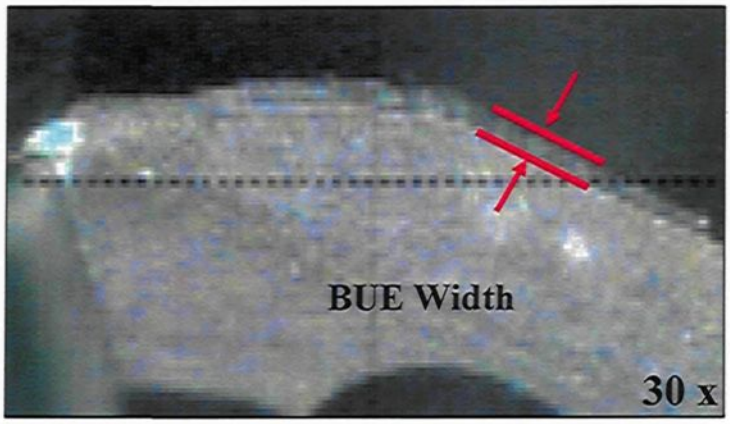


(b) G3 alloy (BUE after 144 holes) Special Solid Carbide Drill

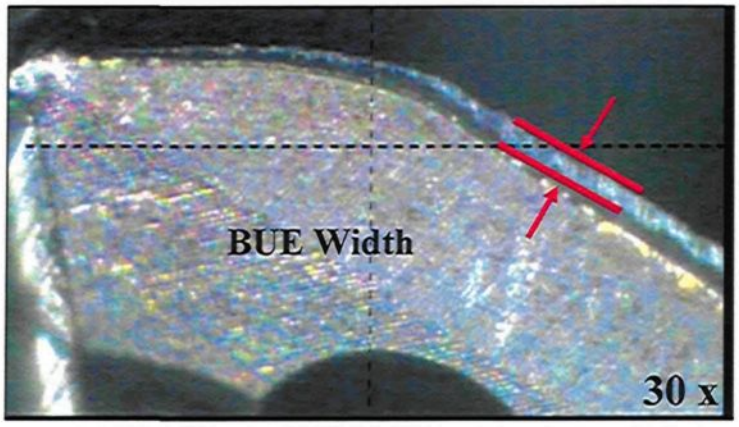


(c) G3 alloy (BUE after 2016 holes) Special Solid Carbide Drill

**Figure 4.14** Photographs showing the effects of Fe and Mn additions on edge build-up formation and wear of the cutting drill lip in the G3 alloy after different stages of drilling using the special solid carbide drill.

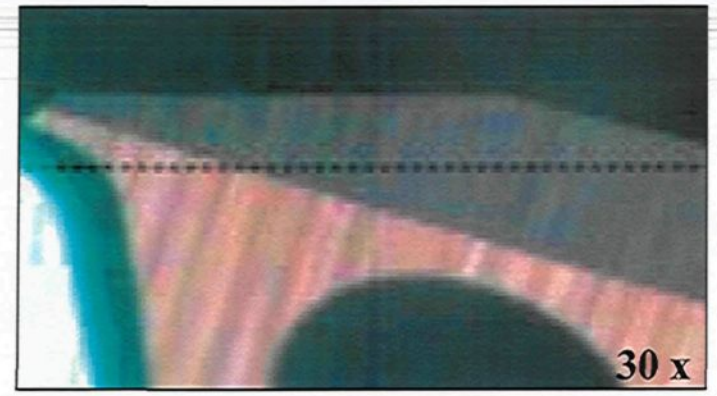


(a) Cobalt Grade – New Drill

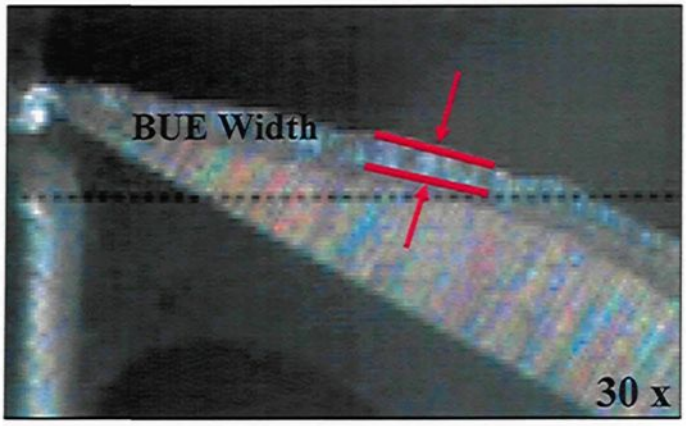


(b) G2 alloy (BUE after 144 holes) Cobalt Grade Drill

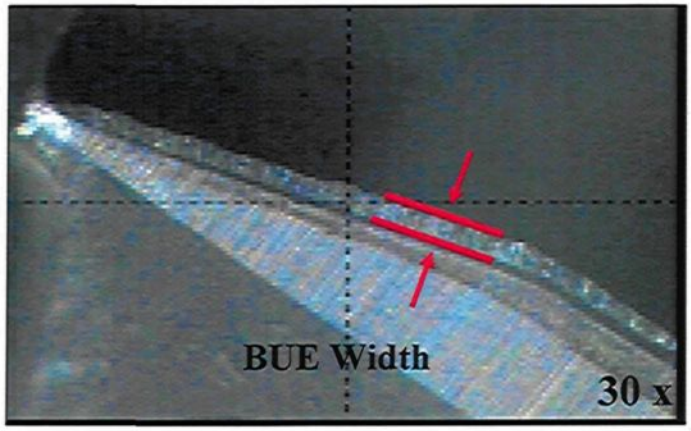


(c) G2 alloy (BUE after 2016 holes) Cobalt Grade Drill

**Figure 4.15** Photographs showing the effects of Sn addition on edge build-up formation and wear of the cutting drill lip in the G2 alloy after different stages of drilling using the cobalt grade drill.

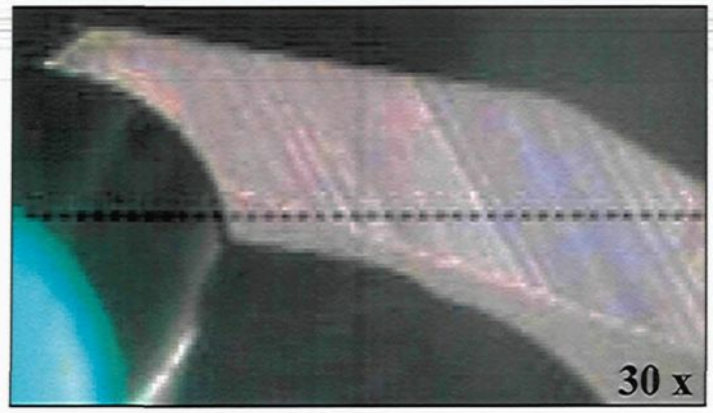


(a) High Precision Solid Carbide – New Drill

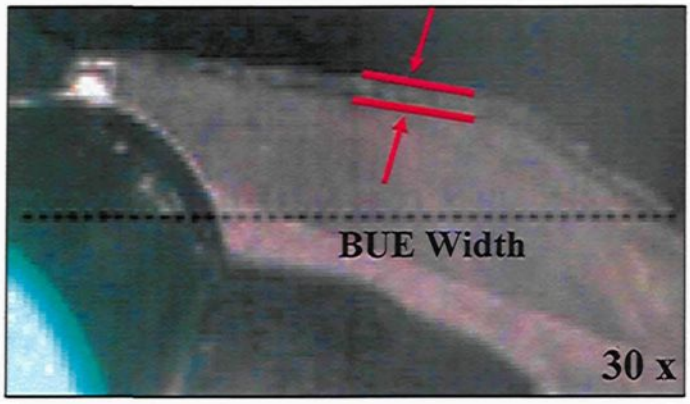


(b) G12 alloy (BUE after 144 holes) High Precision Solid Carbide

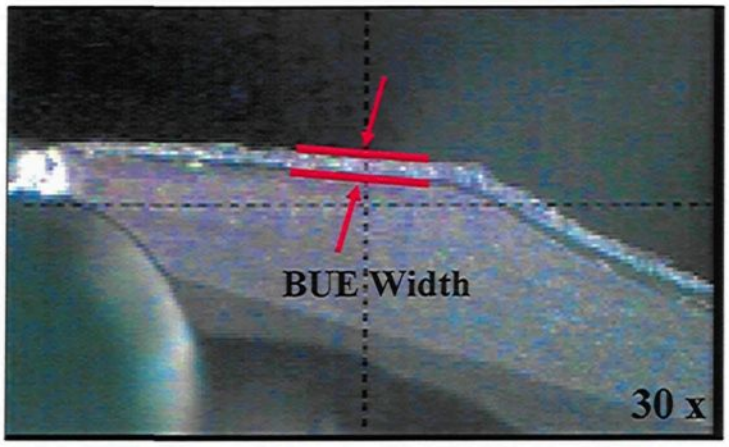


(c) G12 alloy (BUE after 1728 holes) High Precision Solid Carbide

**Figure 4.16** Photographs showing the effects of Sn addition on edge build-up formation and wear of the cutting drill lip in the G12 alloy after different stages of drilling using the high precision solid carbide drill.

### 4.3.6 Assessment of Hole Quality

In this study, no systematic measurements of flank wear on the cutting edge were considered, although it should be kept in mind that the determining factor in drill life is governed by the quality of the hole produced when using the Go/No Go gauge test; this test is, in particular, understood to mean the precision of dimensions and shape of the hole, as well as the surface quality at the side of the hole. The Go/No-Go test is taken as an assessment characteristic of the accuracy of hole dimension and shape. The reference diameter of the Go/No-Go gauge test, 6.5024 - 6.5278 mm, respectively, with acceptable tolerance of 0.39%, was used for the drilling test. The results relevant to this test are listed in Table 4.8 for all the alloy conditions investigated.

**Table 4.8** Go/No Go test results for hole dimension/shape accuracy

| Alloy code | Drilling Test | |
|---|---|---|
| | No. of holes | Go/No-Go 6.5024/6.5278 mm |
| G2 | 5841 | OK |
| G3 | 5184 | OK |
| G12 | 6084 | OK |

### 4.3.7 Chip Characterization

The main problems arising in the drilling of aluminum cast alloys include the adhesion, or welding, of the chip to the drill, and chip/flute clogging.[55] During the drilling process, the chip is formed within a closed space; hence it is quite difficult to observe the process of chip formation and the motion of the chip within the flute directly. Long chips

are usually not desirable because the chips, which subsequently have to be removed manually, may become tangled along the drill body. The qualitative inspection of drilling chips revealed that the form of the chips resulting from the 396 and B319.2 alloys closely approaches a fan-shaped form and is by far the predominant form of the chips formed, as shown in Figure 4.17. These observations are in good agreement with the work of Zedan,[73] who reported that these chips are formed when conical chips are unable to curl sufficiently to follow the flute, and they thus tend to fracture prior to one complete revolution of the drill; the fan shape is considered to be the ideal chip form for most drilling applications. It should be noted that free machinability is related to the formation of smaller chips. In the current study, chip size was not observed to be significantly different after the addition of free-machining elements.

The results also showed that the addition of iron and manganese, creating the G3: 396 + 0.25%Fe + 0.25%Mn alloy, produces no discernible effect on the chip configuration compared to the G2: 396 + 0.15%Sn, and the G12: B319.2 + 0.15%Sn alloys, as shown in Figure 4.17. Table 4.9 provides the difference in ductility between the 396 and B319.2 alloys. This table compares the tensile properties of the alloys under the same heat treatment conditions as those used for heat-treating their machinability test blocks. There is no clear demarcation between needle- and fan-shaped chips; it is the marked change in the radius of the chip about the lip axis which results in the needle shape. This radius change occurs when the edge build-up alters the geometry of the cutting surface of the drill.

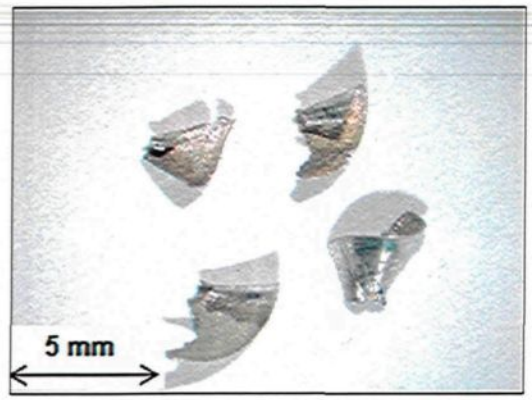


(a) G2: 720 holes – obtained using Special Solid Carbide Drill

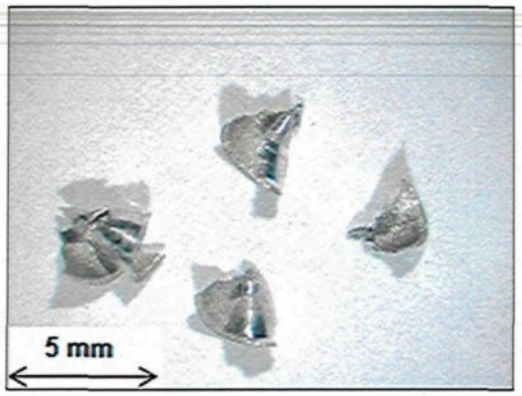


(b) G12: 720 holes – obtained using High Precision Solid Carbide Drill

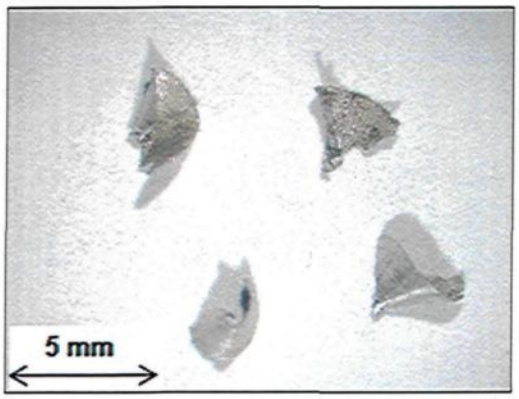


(c) G3: 1440 holes – obtained using Special Solid Carbide Drill

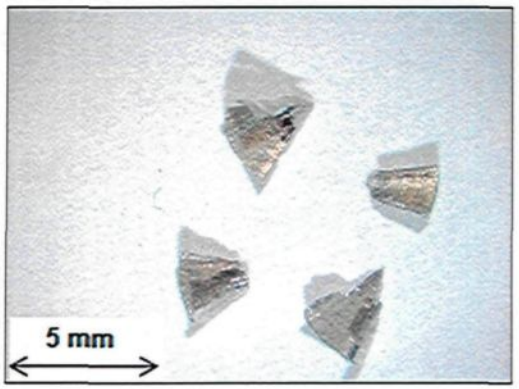


(d) G12: 1440 holes – obtained using Cobalt Grade Drill

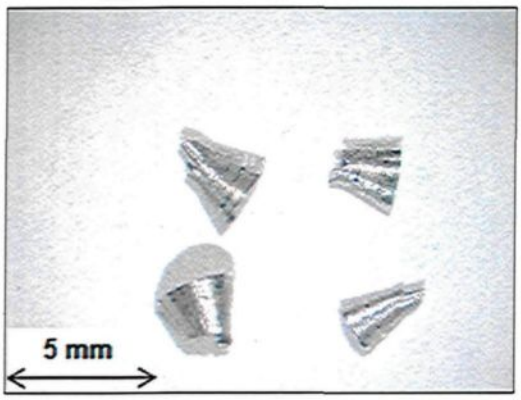


(e) G2: 2016 holes – obtained using Cobalt Grade Drill

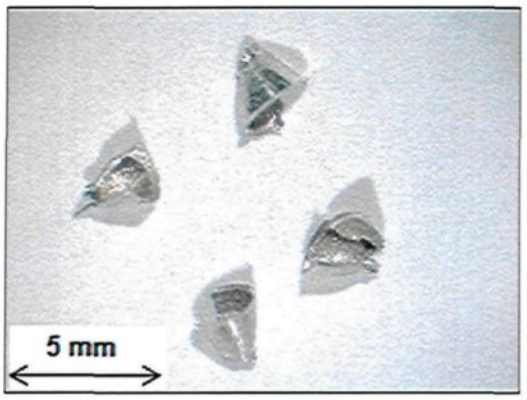


(f) G3: 2016 holes – obtained using High Precision Solid Carbide Drill

**Figure 4.17** Optical micrographs showing the different types of chips obtained for G2, G3, and G12 alloys after drilling the specified number of holes using various drills.

**Table 4.9** Tensile properties of the G2, G3, and G12 alloys [61]

| Alloy Code | YS (MPa) | UTS (MPa) | El (%) |
|---|---|---|---|
| **G2** | 351.65 ± 2.57 | 390.54 ± 5.73 | 1.02 ± 0.15 |
| **G3** | 326.84 ± 2.13 | 354.72 ± 4.86 | 0.84 ± 0.04 |
| **G12** | 392.83 ± 3.48 | 404.08 ± 3.75 | 0.77 ± 0.03 |

The difference in chip morphology may also be observed from the histogram provided in Figure 4.18 which evaluates chip breakability in terms of the number of chips-per-gram obtained from the drilling tests for the alloys investigated. For the G2 (396 + 0.15%Sn) alloy, for example, the cobalt grade drill achieves up to 56% better chip breakability than the high precision solid carbide drill, followed by the special solid carbide drill with a 34% better chip breakability than the solid carbide drill.

With respect to the G3 (396 + 0.25%Fe + 0.25%Mn) alloy, the chip breakability observed does not display any major difference in the number of chips-per-gram obtained using the special solid carbide drill and the cobalt grade drill, showing increases of 13% and 18%, respectively, compared to the high precision solid carbide drill which produced the lowest number of chips-per-gram. The data for G12 (B319.2 + 0.15%Sn) alloy shows that the cobalt grade drill continues to display excellent chip breakability, exhibiting an increase of 27% and 32%, respectively, in the number of chips-per-gram obtained, compared to the high precision solid carbide drill and the special solid carbide drill.

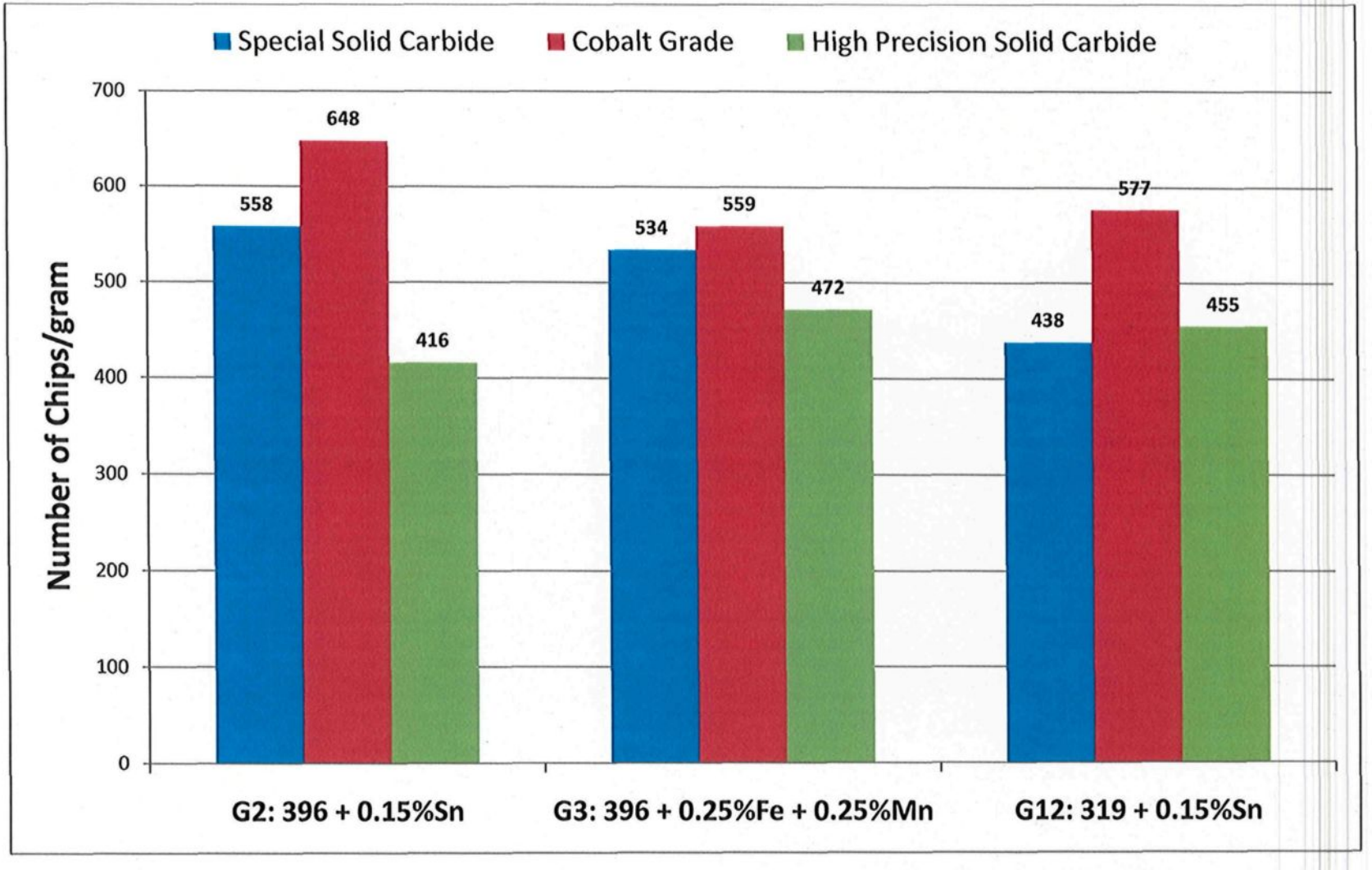


**Figure 4.18** Number of chips-per-gram produced using different drills for the alloys studied.

# CHAPTER 5

# CONCLUSIONS AND RECOMMENDATIONS

# CHAPTER 5

# CONCLUSIONS AND RECOMMENDATIONS

## 5.1 CONCLUSIONS

Drilling experiments were carried out on a Huron K2X 8 Five vertical machining center under fixed machining conditions to investigate the effects of drilling tool material and type on the machinability of 396 and B319.2 Al-Si casting alloys, namely G2: 396 + 0.15%Sn, G3: 396 + 0.25%Fe + 0.25%Mn, and G12: B319.2 + 0.15%Sn in the heat-treated condition. The machinability characteristics were studied in terms of the forces and moments as well as tool life, chip configuration, and built-up edge (BUE) evolution. From the analysis and discussion of the results presented in Chapter 4, the following may be concluded:

1. The results obtained from the drilling tests reveal that, for the 396 alloys, G2 and G3, the lowest total average drilling force and moment are obtained when using the high precision solid carbide drills; the cobalt grade drill, on the other hand, provides the lowest total average drilling force and moment for tests conducted on the B319.2 alloy, G12.

2. The results obtained from the drilling process reveal that the G2 and G3 alloys display a rapid increase in the total drilling force and moment as the number of holes drilled increases. This observation can be attributed to the higher Si content of these 396 alloys, namely 10.8%.
3. The differences in machining behavior observed between the 396 and B319.2 alloys may be ascribed mainly to the differences in matrix hardness and alloy chemistry obtained through additions, as well as to the differences produced by the silicon levels in the two alloy types (10.8% *vs.* 7.5%Si).
4. Drilling tests reveal that 396 alloys require greater cutting force and moment compared to the B319.2 alloy. In terms of the number of holes drilled, however, it was found that the silicon content has little effect on tool life.
5. The high precision solid carbide drill is recommended for alloys G2 and G3. This drill displays stable behavior when in operation, thereby obtaining the lowest total drilling force and total drilling moment, whereas for the G12 alloy the cobalt grade drill is recommended, since it is observed to obtain the lowest total drilling force and moment. These results may be attributed to the fact that the cutting tool material used in this study possesses a greater hardness than the workpiece material, namely, aluminum. In addition, the cutting tool geometry also influences the results obtained.
6. The addition of 0.15%Sn to the 396 and B319.2 alloys has a beneficial effect on the tool life of the four carbide drills, attributable to the precipitation of low melting-point $\beta$-Sn particles which provide a lubricating effect during the drilling process.

7. The presence of sludge in the G3 alloy, containing additions of 0.25%Fe and 0.25%Mn, leads to an extremely rapid increase in the total drilling force and moment; it also decreases tool life with the progress of the number of holes drilled, presenting more fluctuations in the drilling force and moment readings compared to those observed with the other alloys.
8. An examination of photographs of edge build-up on the tools indicates that there are minimal changes in the width of the BUE for different numbers of holes for each alloy and drill used in the course of the drilling process. This observation may be explained by the fact that the BUE deposit, which gradually increases in size, separates from the cutting face once it exceeds a critical size, and adheres to the lower surface of the chip, and is consequently removed along with the chip.
9. Built-up edge (BUE) does not depend on either alloy composition or the drill materials; it does, however, depend to a large extent on the base alloy being used, in this case, aluminum.
10. The addition of iron and manganese, which had originally been expected to reduce the tendency towards tool-edge build-up through the abrasive action of hard intermetallic phases, did not, in fact, reduce the built-up edge width.
11. A visual examination of the chips reveals that the fan shape is by far the predominant form during the drilling of the alloys studied. From the present study, as well as from the literature, this shape appears to be the ideal chip shape due to its compact size.

12. The addition of iron and manganese to the 396 alloy produces no discernible effect on the chip configuration.
13. Chip breakability, as observed when using the cobalt grade drill, was superior to that occurring with the use of the special solid carbide drill or the high precision solid carbide drill for the three alloys studied.

## 5.2 RECOMMENDATIONS FOR FUTURE WORK

1. Investigating the possibility of using different workpieces (material type and form), cutting tools (material type and geometry), and cutting medium (air or liquid) in diverse removal sequences (turning, drilling, tapping, milling, and sawing), under different cutting conditions (speed, feed, and depth of cut), all of which should be considered from the point of view of reducing machining costs and, hence, the overall production costs.
2. Carrying out heat treatment cycles for 396 and B319.2 alloys with preselected delay times between the quenching step (after solution treatment) and the aging treatment, with the intention of determining the effects produced by these times on the drilling process.
3. Investigating the use of drill materials other than the solid carbide tools used in the present study, with the aim of comparing tool material costs in order to reduce overall production costs.
4. Carrying out mathematical analyses of the experimental data in order to reduce the time required to determine the optimum drill and machining conditions in the production of automotive and aerospace components.

# REFERENCES

# REFERENCES


1. D. Raymond, F. Philip, "Manufacturing Feasibility of All-Aluminum Automotive Engines Via Application of High Silicon Aluminum Alloy," SAE International, 2000, Paper N°. 2000-01-0061.

2. M. Tadashi, "Advanced Near Dry Machining System," Chief Engineer, Machine Tool R&D Division, Horkos Corp, in 4th Annual NCMS Fall Workshop Series, Oct. 2000.

3. J.L. Jorstad, "Influence of Aluminum Casting Alloy Metallurgical Factors on Machinability," Society of Automotive Engineers, Warrendale, PA.15096, 1980, 15p.

4. J.L. Jorstad, "Machinability of 380 Alloy: Effect of Minor Elements and Impurities," *Transactions of the Society of Die Casting Engineers*, Paper No.G-T79-072, 1979.

5. M. Tash, "Effect of Metallurgical Parameters on the Machining Behaviour of 356 and 319 Alloys (Drilling and Tapping Study)," PhD, Thesis, Université du Québec à Chicoutimi, Canada, 2005.

6. J.E. Wyatt, G.J. Trmal, "Machinability: Employing a Drilling Experiment as a Teaching Tool," *Journal of Industrial Technology*, Vol. 22, 2006, pp. 1-12.

7. V.A. Tipnis, R.A. Joseph, "Testing For Machinability," *Influence of Metallurgy on Machinability*, ASM Materials/Metalworking Series No. 7, American Society for Metals, Materials Park, OH, 1973, pp. 11-30.

8. A.N. El-Azim, S.F. Moustafa, "Machinability of Aluminum-Silicon Alloy Castings Modified With Some Additions," *International Conference on Evolution of Advanced Materials*, 31 May-2 June, 1989, Milan, Italy.

9. E.M. Huseyin, O. Cuneyt, "Drill Wear Monitoring Using Cutting Force Signals," *Mechatronics*, Vol. 14, 2004, pp 533-548.

10. S.A. Jalali, W.J. Kolarik, "Tool Life and Machinability Models for Drilling Steels," *International Journal of Machine Tools & Manufacture*, Vol. 31(3), 1991, pp 273-282.

11. J.E. Wyatt, J.T. Berry, "A new technique for the determination of superficial residual stresses associated with machining and other manufacturing processes," *Journal of Materials Processing Technology*, Vol. 171, 2006, pp. 132-140.

12. H.A. Kishawy, M. Dumitrescu, M.A. Elbestawi, "Effect of Coolant Strategy on Tool Performance, Chip Morphology and Surface Quality during High-Speed Machining of A356 Aluminum Alloy," *International Journal of Machine Tools & Manufacture,* Vol. 45, 2005, pp. 219-227.

13. T. Cselle, "New Directions in Drilling," *Manufacturing Engineering*, Vol. 115(2), 1995, pp. 77-80.

14. E. Kannatey-Asibu, "A Transport Diffusion Equation in Metal Cutting and its Application to Analysis of the Rate of Flank Wear," *Journal of Engineering for Industry,* Vol. 107(1), 1985, pp. 81-89.

15. R. Komanduri, J. McGee, R.A. Thompson, J.P. Covey, F.J. Truncale, V.A. Tipnis, R.M. Stach, R.I. King, "On a methodology for establishing the machine tool system requirements for high-speed/high throughput machining," *Journal of Engineering for Industry*, Vol. 107(4), 1985, pp. 316-324.

16. E.M. Trent, P.K. Wright, *Metal Cutting,* 4th Edition, Butterworth's-Heinemann, London, 2000, pp. 149-166.

17. I.J. Polmear, *Light Alloys: Metallurgy of the Light Metals*, 3rd Edition, Hodder & Arnold, London, 1995.

18. D. Altenpohl, *Aluminum Viewed from Within: An Introduction into the Metallurgy of Aluminum Fabrication*, 1st. Edition, Aluminium-Verlag, Dusseldorf, 1982.

19. A. Sverdlin, "Properties of Pure Aluminum," in *Handbook of Aluminum Volume 1 - Physical Metallurgy and Processes*, Marcel Dekker, Inc., New York, 2003, pp. 33-81.

20. G.E. Dieter, *Mechanical Metallurgy*, SI Metric Edition, McGraw-Hill, London, 1988.

21. R. Colás, E. Velasco, S. Valtierra, "Castings," in *Handbook of Aluminum Volume 1 - Physical Metallurgy and Processes*, Marcel Dekker, Inc., New York, 2003, pp. 591-642.

22. D.L. Zalensas, *Aluminum Casting Technology*, 2nd Edition, American Foundrymen's Society, Inc., Des Plaines, IL, 1993.

23. L. Katgerman, D. Eskin, "Hardening, Annealing and Aging," in *Handbook of Aluminum Volume 1 - Physical Metallurgy and Processes*, Marcel Dekker, Inc., New York, 2003, pp. 259-304.

24. M.A. Meyers, K.K. Chawla, *Mechanical Metallurgy: Principles and Applications*, Prentice-Hall Inc., New York, 1984.

25. J. Gruzleski, B. Closset, *The Treatment of Liquid Aluminum-Silicon Alloys*, American Foundrymen's Society Inc., Des Plaines, IL, 1990.

26. O. Madelaine-Dupuich, J. Stolarz, "Fatigue of Eutectic Al-Si Alloys," *Materials Science Forum*, Vols 217-222, 1996, pp. 1343-1348.

27. A.M. Samuel, F.H. Samuel, "Modification of Iron Intermetallics by Magnesium and Strontium in Al-Si Alloys," *International Journal of Cast Metals Research*, Vol. 10, 1977, pp. 147-157.

28. T. Tanaka, T. Akasawa, "Machinability of Hypereutectic Silicon-Aluminum Alloys," *ASM International-Journal of Materials Engineering and Performance*, Vol. 8(4), 1999, pp. 463-468.

29. T. Murat, J. Staley, "Physical Metallurgy and the Effect of Alloying Additions in Aluminum Alloys," in *Handbook of Aluminum Volume 1 - Physical Metallurgy and Processes,* Marcel Dekker, Inc, New York, 2003, pp. 81-210.

30. American Society for Metals, "Properties of Cast Aluminum Alloys," in *ASM Handbook, Vol. 2: "Properties and Selection: Nonferrous Alloys and Special-Purpose Materials,"* ASM International, Materials Park, OH, 1991.

31. Robert Ian Mackay, "Quantification of Iron in Al-Si Foundry Alloys via Thermal Analysis," Master's Thesis, McGill University Montreal, Quebec, Canada, 1996.

32. A. Mohamed, "Effet des additifs sur la microstructure et les propriétés mécaniques des alliages d'aluminium-silicium," PhD Thesis, Université du Québec à Chicoutimi, Canada, 2008.

33. R. Howard, N. Bogh, D.S. MacKenzie, "Heat Treating Processes and Equipment," in *Handbook of Aluminum Volume 1 - Physical Metallurgy and Processes*, Marcel Dekker, Inc., New York, 2003.

34. D. Mukhopadhyay, "Structural Evolution in Mechanically Alloyed Al-Fe Powder Mixtures," TMS Outstanding Student Paper Contest Winner-1994 Graduate Division, http://www.tms.org/Students/Winners/Mukhopadhyay/Mukhopadhyay.html

35. S.G. Shabestari, "The Effect of Iron and Manganese on the Formation of Intermetallic Compounds in Aluminum-Silicon Alloys," *Materials Science and Engineering A,* Vol. 383, 2004, pp. 289-298.

36. S.G. Shabestari, M. Mahmudi, M. Emani, J. Campbell, "Effect of Mn and Sr on intermetallics in Fe-rich eutectic Al-Si alloy," *International Jornal of Cast Metals Research*, Vol. 15, 2002, pp. 17-24.

37. J.L Jorstad, "Understanding "Sludge," *Die Casting Engineer*, Nov-Dec 1986, pp. 30-36.

38. D.L. Colwell, R.J. Kissling, "Die and Permanent Mold Casting Aluminum Alloy Minor Elements," *AFS Transactions*, Vol. 69, 1961, pp. 610-615.

39. J.N. Pratt, G.V. Raynor, "The Intermetallic Compounds in the Alloys of Aluminum and Silicon with Cr, Mn, Fe, Co, and Ni," *Journal of the Institute of Metals*, Vol. 79, 1951, pp. 211-232.

40. J. Gobrecht, "Ségrégation par Gravite du Fer, du Manganèse et du Chrome dans les Alliages Al-Si de Fonderie," *Fonderie,* Vol. 367, 1977, pp. 171-173.

41. G. Pucella, A.M. Samuel, F.H. Samuel, H.W. Doty, S. Valtierra, "Sludge Formation in Sr-Modified Al-11.5wt%Si Diecasting Alloys," *AFS Transactions*, Vol. 107, 1999, pp. 117-125.

42. S. Koch, H. Antrekowitsch, "Free-Cutting Aluminum Alloys with Tin as Substitution for Lead. *BHM Berg- und Hüttenmännische Monatshefte*, Vol. 153(7), 2008, pp. 278-281.

43. A. Smolej, B. Breskvar, M. Soković, V. Dragojević, E. Slaček, "Properties of Aluminum Free-Cutting Alloys with Tin, Part I," *Aluminum,* Vol. 78, 2002, pp. 284-288.

44. Kyung-Hyun, Kim, In-Sang Chung, "Effect of Pb and Bi Element on the Cutting Characteristics in Al-Cu Alloys," *Journal of the Korean Institute of Metals*, Vol. 28(3), 1990, pp. 244-251.

45. L.T. Thai, "The Effects of Bismuth, Strontium and Antimony Additions on the Microstructure and Mechanical Properties of A356 Aluminum Casting Alloy," M.Sc. Thesis, Technological University of Malaysia, 2006.

46. Young Sek Yang, "Free-Machinable Eutectic Al-Si Alloy," U.S. Patent, No. 6511633, 28 January 2003.

47. M.C. Flemings, *Solidification Processing*, McGraw-Hill, New York, 1974.

48. American Society for Metals, "Heat Treating of Aluminum Alloys," in *ASM Handbook, Vol. 4: "Heat Treating,"* ASM International, Materials Park, OH, 1991.

49. D.A. Porter, K.E. Easterling, *Phase Transformations in Metals and Alloys*, 2nd Edition, Chapman and Hall, 1992.

50. G.T. Smith, "Drilling and Associated Technologies," in *Cutting Tool Technology: Industrial Handbook, Springer*, London, 2008, pp. 33-142.

51. http://www.toolingandproduction.com, G. Schneider, *Cutting Tool Applications*, 2002.

52. TALAT Lecture 3100: "Machining of Products," prepared by P. Johne, Aluminium-Zentrale e.V., Düsseldorf, European Aluminum Association, Brussels, 1994.

53. D.A. Stephenson, J.S. Agapiou, *Metal Cutting Theory and Practice*, 2nd Edition, Taylor and Francis Group, Boca Raton, FL, 2006.

54. K. Nakayama, M. Ogawa, "Basic Rules on the Form of Chip in Metal Cutting," *CIRP Annals*, Vol. 27(1), 1978, pp. 17-21.

55. S.A. Batzer, D.M. Hann, P.D. Rao, W.W. Olson, J.W. Sutherland, "Chip Morphology and Hole Surface Texture in the Drilling of Cast Aluminum Alloys," *Journal of Materials Processing Technology*, Vol. 79, 1998, pp. 72-78.

56. C.H. Kahng, W.C. Koegler, "A Study of Chip Breaking during Twist Drilling," *NAMRC/SME* Technical Paper, MR76-267, 1977, pp. 8-12.

57. C.J. Oxford, "On the Drilling of Metals: 1-Basic Mechanics of the Process," *Transactions of ASME, Journal of Engineering for Industry*, Vol. 77, 1955, pp. 103-114.

58. http://its.fvtc.edu/machshop1/coolant/cutfluids.htm, FVTC - Machine Tool Technician, Cutting Fluid Types and Uses.

59. *Drill Nomenclature, Metal Cutting Tool Handbook* published by the Metal Cutting Tool Institute, N.Y., 2004.

http://www.mfg.mtu.edu/cyberman/machining/trad/drilling/nomen.html.

60. D.A. Stephenson, J.S. Agapiou, *Metal Cutting Theory and Practice*, 2nd Edition, Taylor and Francis Group, Boca Raton, FL, 2006.

61. Y. Zedan, "Machinability Aspects of Heat-Treated Al-(6-11%)Si Cast Alloys: Role of Intermetallics and Free-Cutting Elements," PhD, Thesis, Université du Québec à Chicoutimi, Canada, 2010.

62. M.A. Moustafa., F.H. Samuel, H.W. Doty, "Effect of Solution Heat Treatment and Additives on the Hardness, Tensile Properties and Fracture Behaviour of Al-Si (A413.1) Automotive Alloys," *Journal of Materials Science*, Vol. 38, 2003, pp. 4523-4534.

63. A.T. Joenoes, J.E. Gruzleski "Mg Effects on the Microstructure of Unmodified and Modified Al-Si Alloys," *International Journal of Cast Metals Research*, Vol. 4(2), 1991, pp. 62-71.

64. M.A. Moustafa, C. Lepage, F.H. Samuel, H.W. Doty, "Metallographic Observations on Phase Precipitation in Strontium-Modified Al-11.7%Si Alloys: Role of Alloying Elements," *International Journal of Cast Metals Research*, Vol. 15, 2003, pp. 609-626.

65. F. Paray, B. Kulunk, J.E. Gruzleski, "Impact Properties of Ai-Si Foundry Alloys," *International Journal of Cast Metals Research*, Vol. 13, 2000, pp. 17-37.

66. F.H. Samuel, A.M. Samuel, H. Liu, "Effect of Magnesium Content on the Aging Behaviour of Water-Chilled Al-Si-Cu-Mg-Fe-Mn (380) Alloy Castings," *Journal of Materials Science*, Vol. 30, 1995, pp. 1-10.

67. A. Smolej, B. Breskvar, M. Soković, V. Dragojević, E. Slaček, "Properties of Aluminum Free-Cutting Alloys with Tin, Part II," *Aluminum*, Vol 78, 2002, pp. 388-391.

68. S. Subhasish, "Free-Machining Aluminum Alloy and Method of Use," U.S. Patent, No. 5,725,694, 1998, Granted.

69. C.J Ting, "Tool Wear Monitoring in Drilling Using Force Signals," *Wear*, Vol. 180, 1995, pp. 53-60.

70. W. Bonsack, "Iron - The Problematic Factor in Quality of Aluminum Alloy Die Castings," *AFS Transactions*, Vol.69, 1961, pp. 712-720.

71. D.L. Colwell, O. Tichy, "Machinability of Aluminum Die Castings," *AFS Transactions*, Vol. 64, 1956, pp. 236-241.

72. *ASM Metals Handbook, Vol. 16: Machining*, American Society for Metals, Materials, Park, OH, 1990.

73. Y. Zedan, F.H. Samuel, A.M. Samuel, H.W. Doty, "Effects of Fe Intermetallics on the Machinability of Heat-Treated Al-(7-11)%Si Alloys," *Journal of Materials Processing Technology,* Vol. 210, 2010, pp. 245-257.

74. H. Bao, M.G. Stevenson, "An Investigation of Built-Up Edge Formation in the Machining of Aluminum," *International Journal of Machine Tool Design and Research,* Vol. 16, 1976, pp. 165-178.

75. E.M. Trent, "Metal Cutting and the Tribology of Seizure: II - Movement of Work Material over the Tool in Metal Cutting," *Wear*, Vol. 128, 1988, pp 47-64.

76. E.M. Trent, "Metal Cutting and the Tribology of Seizure: I - Seizure in Metal Cutting," *Wear*, Vol.128, 1988, pp 29-45.

77. M. Tash, F.H. Samuel, F. Mucciardi, H.W. Doty, S. Valtierra, "Effect of Metallurgical Parameters on the Machinability of Heat-Treated 356 and 319 Aluminum Alloys," *Materials Science and Engineering A*, Vol. 434, 2006, pp 207-217.